ЛУЦЬКИЙ
НАЦІОНАЛЬНИЙ
ТЕХНІЧНИЙ
УНІВЕРСИТЕТ

ТОВАРОЗНАВЧИЙ ВІСНИК

Том 19, № 1

Заснований у 2009 році
Видається два рази на рік

Луцьк
2026

ISSN 2310-5283
e-ISSN 3041-1432

DOI: 10.62763/cb/1.2026

Видавець:
Луцький національний технічний університет

Рекомендовано до друку та поширення
через мережу Інтернет Вченою радою
Луцького національного технічного університету
(протокол № 12 від 28 травня 2026 р.)

**Свідоцтво про державну реєстрацію
друкованого засобу масової інформації:**
Національна рада України з питань телебачення та радіомовлення (Рішення № 40 від 11.01.2024).
Ідентифікатор медіа – R30-02530.

Науковий журнал включено до категорії «Б» Переліку наукових фахових видань України, у яких можуть публікуватися результати дисертаційних робіт на здобуття наукових ступенів доктора та кандидата наук зі спеціальностей: 076 – Підприємництво та торгівля; 132 – Матеріалознавство; 181 – Харчові технології; 182 – Технології легкої промисловості (наказ МОН України № 886 від 02.07.2020 р.)

**Журнал представлено у міжнародних наукометричних базах даних,
репозитаріях та пошукових системах**: Google Scholar, Crossref,
Національна бібліотека України імені В. І. Вернадського, Dimensions, UC Santa Barbara Library,
University of Oslo Library, OUCI (Open Ukrainian Citation Index), Ulrich's Periodicals Directory, Sherpa/Romeo,
ScienceOpen, Litmaps, J-Gate, WorldCat

Контактна адреса:
Луцький національний технічний університет
43018, вул. Львівська, 75, м. Луцьк, Україна
E-mail: info@c-bulletin.com.ua
https://c-bulletin.com.ua/uk

LUTSK
NATIONAL
TECHNICAL
UNIVERSITY

COMMODITY BULLETIN

Volume 19, No. 1

Year of foundation: 2009
Frequency: 2 issues per year

Lutsk
2026

ISSN 2310-5283
e-ISSN 3041-1432

DOI: 10.62763/cb/1.2026

Publisher:
Lutsk National Technical University

Recommended for printing and distribution
via the Internet by the Academic Council
of Lutsk National Technical University
(Minutes 12 of May 28, 2026)

Certificate of state registration of the print media:
National Council of Ukraine on Television and Radio Broadcasting (Decision No. 40 of 11.01.2024).
Media identifier – R30-02530.

The scientific journal is included in category "B" of the List of scientific specialised publications of Ukraine,
in which can be published the results of dissertations for obtaining the scientific degrees of doctor and candidate of sciences in specialties: 0416 – Wholesale and retail sales;
0788 – Interdisciplinary programmes and qualifications involving engineering, manifacturing and construction;
0721 – Food processing; 0723 – Textiles (clothes, footwear and leather)
(Order of the Ministry of Education and Science of Ukraine No. 886 of 02.07.2020)

The journal is presented international scientometric databases, repositories and scientific systems: Google Scholar, Crossref, Vernadsky National Library of Ukraine, Dimensions, UC Santa Barbara Library, University of Oslo Library, OUCI (Open Ukrainian Citation Index), Ulrich's Periodicals Directory, Sherpa/Romeo, ScienceOpen, Litmaps, J-Gate, WorldCat

Address for contacts:
Lutsk National Technical University
43018, 75 Lvivska Str., Lutsk, Ukraine
E-mail: info@c-bulletin.com.ua
https://c-bulletin.com.ua/en

ТОВАРОЗНАВЧИЙ ВІСНИК
Journal homepage: https://c-bulletin.com.ua/en
Том 19, № 1, 2026

Редакційна колегія

COMMODITY BULLETIN
Journal homepage: https://c-bulletin.com.ua/en
Vol. 19, No. 1, 2026

Editorial Board

ЗМІСТ

Content

COMMODITY BULLETIN
Journal homepage: https://c-bulletin.com.ua/en
DOI: 10.62763/cb/1.2026.09

Article's History: Received: 03.02.2026 Revised: 01.05.2026 Accepted: 28.05.2026 Published: 29.05.2026

ISSN 2310-5283; e-ISSN 3041-1432 Vol. 19, No. 1, 2026, 9-16

UDC 620.22:621.7(075.8)

Factors influencing the formation plasma electrolytic oxidation coatings synthesised on a titanium and zirconium alloys

Nataliia Imbirovych*
Doctor of Technical Sciences, Associate Professor
Lutsk National Technical University
43018, 75 Lvivska Str., Lutsk, Ukraine
https://orcid.org/0000-0001-8276-6349

Yurii Feshchuk
PhD in Technical Sciences Associate Professor
Lutsk National Technical University
43018, 75 Lvivska Str., Lutsk, Ukraine
https://orcid.org/0000-0001-6259-1916

Abstract. The research presented in this article is relevant due to the need to improve prediction and control of oxide-ceramic coating formation on titanium and zirconium alloys used in aggressive and high-load environments. The aim was to investigate electrophysical regularities of coating formation during plasma electrolytic oxidation of titanium and zirconium alloys and the influence of electrolyte composition and current density on synthesis voltage. Methods included galvanostatic anodic and anodic-cathodic modes, time-resolved voltage and current recording, comparison of electrolytes expressed in grams per liter, and analysis of current-voltage dependences during coating synthesis. It was established that coating formation on zirconium alloy proceeded in two stages and was unstable at low electrolyte concentrations, while increased potassium hydroxide and liquid glass improved stability and uniformity. Titanium alloy demonstrated a more uniform synthesis process with lower voltage levels than zirconium alloy due to higher conductivity and more stable coating growth behaviour. Decreasing current density reduced anodic and cathodic voltage components, while additives such as chromium oxide, glycerin and hydrogen peroxide influenced stability and magnitude of synthesis voltage. Optimal conditions were identified at balanced current density ratios and moderate electrolyte concentrations, ensuring stable discharge behaviour and improved coating quality. Results can be used by materials engineers to optimise plasma electrolytic oxidation regimes for producing corrosion-resistant and mechanically stable coatings

Keywords: electrophysical parameters; synthesis voltage; current density; electrolyte; cathode; anode

Introduction

In technology, many types of metal functional elements prematurely lose their operability, especially if they operate in aggressive environments or under conditions of cavitation-erosion wear. Practically the only way to increase the reliability and durability of elements and devices is to strengthen their surface by applying corrosion and abrasion-resistant coatings. The development of new environmentally friendly technologies for applying protective coatings is certainly one of the important problems of materials science.

Scientists are constantly improving existing methods of surface hardening of metals in order to create new effective surfaces with increased performance characteristics. Thus K. Sarakinos *et al.* (2010) in their work

Suggested Citation:
Imbirovych, N., & Feshchuk, Yu. (2026). Factors influencing the formation plasma electrolytic oxidation coatings synthesised on a titanium and zirconium alloys. *Commodity Bulletin*, 19(1), 9-16 . doi: 10.62763/cb/1.2026.09.

*Corresponding author (n.imbirovych@lntu.edu.ua)

investigated a new method such as HIPIMS (high-power pulsed magnetron sputtering). The proposed method allows generating an ultra-dense plasma with unique properties, such as a high degree of ionisation of sputtered atoms and non-standard transfer of ionised particles relative to the target. However, this method allows creating coatings of small thickness, requires high accuracy to the surface and places high demands on its pre-treatment. Plasma electrolytic treatment belongs to relatively new methods of surface treatment of metals and allows the formation of multifunctional coatings with a wide range of properties. The development of new environmentally friendly technologies for applying highly effective and reliable coatings to protect and strengthen metal products is currently one of the most urgent tasks of modern science and technology due to the increasing severity of operating conditions. Scientists H. Bai *et al.* (2021), Y.X. Ou *et al.* (2023) have proven that coatings effectively improve the performance properties of metals. In their work, they investigate synthesised coatings on titanium alloys, which are modified with nanoparticles by introducing them into the electrolyte, and show that plasma electrolytic oxidation (PEO) is an effective method of modifying the surface of titanium alloys to improve corrosion properties, the effect of such modification on the roughness, adhesion, and thickness of the coatings.

Titanium and its alloys are of great interest for advanced engineering applications through to their excellent properties, such as a join high strength-to-weight ratio, corrosion resistance, biocompatibility, and others. The authors P. Canepa *et al.* (2020), with the aim of increasing the biocompatibility of titanium alloys, saturated their coatings with calcium and phosphorus. X. Han *et al.* (2023) in their work explain that surface modification is an important and determining factor for improving the biocompatibility of implants. They consider various surface modification methods that allow to increase the porosity of the surface. The main attention is paid to some of the most promising methods for modifying the surface of titanium implants: mechanical methods, such as acid etching and grinding, as well as coatings, such as hydrogen peroxide treatment using fluoride and chloride ions, hydroxyapatite, nitride, metal oxides and silver. Experimentally, it has been shown that these methods increase the biocompatible properties of titanium implants. Researchers X. Li *et al.* (2025) used a cost-effective mesh-shaped powder metallurgy method to produce a titanium-based alloy with high corrosion resistance. The titanium alloy Ti–24Nb–4Zr–8Sn (Ti2448) they developed has a low Young's modulus and high corrosion resistance, which is 3.5 times higher than that of the Ti–6Al–4V (Ti64) alloy, which is widely used in implantology and is characterised by high biocompatibility. In their work, E.S. Krishna *et al.* (2021) emphasise the importance of using titanium alloys in implantology due to their high biocompatible properties and describe the main directions in implantology where titanium alloys are used. These include total joint replacement, dental and maxillofacial implants. Composites exhibit hybrid properties and offer more flexibility to choose different composition to achieve desired properties in the end product. They emphasise in their work that adding ceramic additives to a composite titanium alloy can significantly increase its biocompatible properties and reduce the risks of rejection of such implants.

However, titanium is a highly chemically reactive element, and its corrosion resistance in various environments is ensured only by a thin natural oxide layer, which can be damaged under mechanical loading. As a result, the unprotected substrate is exposed to a corrosive/erosive environment, making it highly susceptible to premature failure. These properties of natural titanium oxide films have attracted the attention of scientists to the idea of applying protective coatings to the surface of such alloys. For example, A. Fattah-alhosseini & M. Molayei (2023) in their work investigated the properties of PEO coatings on a titanium alloy with a preliminary azure surface treatment. The authors investigated that such treatment leads to an improvement in the anti-corrosion, wear-resistant and biocompatible properties of titanium alloys. K. Kombayev *et al.* (2025) used the method of microplasma sputtering of tantalum coatings on a titanium alloy such as Grade 5. They found that the coatings created by this method allow the formation of coatings with high hardness, which is twice the hardness of the base, and has a fairly high thickness, which is 250 μm. Chemical vapor deposition (CVD) is also used to improve the characteristics of various metal surfaces, including titanium alloys. M. Molaei & A. Fattah-alhosseini *et al.* (2024) investigated the results of modifying plasma-electrolytic coatings on titanium alloy with ZrO_2 nanoparticles. The results of the conducted studies revealed improved corrosion and wear-resistant properties of the synthesised coatings. The authors found that the nanoparticles were included in the coating on the surface or in the pores. It was found that a higher content of zirconium oxide nanoparticles in the amount of 5 g/l improves the wear resistance of the coatings by 8%.

Zirconium and its alloys that have superior properties including biocompatibility, good corrosion resistance, chemical stability, high fracture toughness, high flexural strength and lower cytotoxicity are one of the best choices for dental and orthopedic implant materials. The authors N. Attarzadeh & C.V. Ramana (2021), investigated the growth processes of coatings and identified methods for controlling the properties of the surface layer. It was found that PEO coatings are formed in two stages, which the authors divided into pre-spark and spark regions. A. Fattah-alhosseini *et al.* (2021) in their article conducted a detailed review of clinical

and research conditions dedicated to zirconium alloys and PEO coatings based on them. Comparative analysis of the wetting angle, by which osseointegration is assessed, showed that zirconium alloys with PEO coatings are characterised by a lower wetting angle, which leads to the elimination of the possibility of capsule formation around the implant with such a coating and is positive for its rapid engraftment in the in vivo environment. The authors M. Molaei *et al.* (2021) found that the treatment of the synthesised coating containing ZrO_2 with UV radiation leads to an increase in biocompatibility. The implant coated with ZrO_2 together with bone is characterised by higher strength and higher ability to rapidly form new bone within 12 weeks due to the content of Ca-P compounds and porous structure. The authors note that the coatings have a high antibacterial effect.

However, it should be noted that the natural oxide films that are created on the surface of the valve metals under consideration are not characterised by a high thickness, which is several nanometers. In the works of D. Chopra *et al.* (2022) the problem of artificial modification of the surface of such alloys in order to create high-temperature ceramics, which are also distinguished by high mechanical properties, is presented. One of the promising and innovative methods for modifying the surface of valve metals has recently been considered the PEO method. In this work, a PEO method is developed to improve the surface properties of Ti and Zr alloys. Surfaces modified with PEO have the appearance of ceramic coatings, which are characterised by good functional properties, such as bioactivity or photocatalytic behaviour. In the works of N.Yu. Imbirovych *et al.* (2023), Z. Li *et al.* (2021) and other authors note the high corrosion-resistant and mechanical properties of the obtained coatings. The authors note that oxidation technologies improve the natural oxide layer formed on the surface of Ti and Zr. In general, the oxide layer on a titanium alloy consists of titanium dioxide, including anatase, rutile. Rutile is the most stable form of titanium dioxide. A coating is synthesised on a zirconium alloy, the basis of which consists of zirconium dioxide. The composition of the coating synthesised on the surfaces also includes electrolyte components, which also affect their properties.

A large number of publications on PEO in recent years demonstrate the relevance of this coating method and the constant progress of research both in the theoretical understanding of processes and in improving the technological foundations of coating formation. To date, many issues in this area remain unresolved, such as the influence of the material composition on the synthesis mechanism and properties of the obtained coatings, as well as the influence of the electrolyte composition, current density and synthesis time on the formation of coatings obtained by the plasma-electrolytic oxidation method. The resolution of these issues will accelerate the practical implementation of this technology to solve specific engineering problems.

Therefore, the task of this work was to establish the stages of the synthesis process of plasma-electrolytic coatings on zirconium and titanium alloys, to identify the main dependencies of the influence of the electrolyte composition on the change in the synthesis voltage and to establish the time parameters of the initial sparking stage, which is characterised by a rapid increase in voltage, which is explained by the breakdown of the natural protective barrier film on metals.

Materials and Methods

The development of anodising technology and research of anodic coating were carried out on plate samples made of zirconium and titanium alloys Zr-2.5%Nb and Grade 5 respectively. The studies presented in this work were conducted using the well-known method of recording voltage changes in the process of coating synthesis over time. Researchers such as M. Aliofkhazraei *et al.* (2021), K. Hurle *et al.* (2021), K. Kombayev *et al.* (2024) investigated the energy parameters of the coating process on zirconium and titanium alloys.

The formation of the anodic-spark coating was carried out in galvanostatic mode (anode and anode-cathode). The power supply provided an increase in the voltage amplitude for the anodic half-period to 800 V, and for the cathode to 400 V at the average values of the anodic (I_a) and cathodic (I_k) currents recorded in a certain process. The cathode was a stainless steel bath. The current density was 10-30 A/dm^2, and the ratio of the cathodic and anode currents varied in the range from 1 to 1.5. Using voltmeters and ammeters, the time dependence of the amplitude values of the anodic (U_a) and cathodic ($U_к$) voltages and current values was recorded.

PEO was carried out in different electrolytes, the composition of which was (g/l): KOH – 3; 2; 5; 10; liquid glass – 2; 5; 15; GrO_3 – 0.1; glycerin – 18; 10; H_2O_2 – 10. The electrolyte in which the coating was synthesised was mixed with air, which was supplied to the electrolyte bath. When studying the influence of the electrolyte composition, the latter was changed according to the experimental conditions. After the process was completed, the samples were washed with running and distilled water, dried and analysed. The Faraday section is an integral part of the process at the pre-spark stage, and its duration depends on the method of implementation of the process and the speed of voltage rise to the spark potential.

Results and Discussion

The electrical parameters of the synthesis of the oxide ceramic coating (OCC) are selected mainly experimentally, without proper theoretical justification. However, it is the current density and voltage that determine the nature and intensity of the discharges and the temperature conditions on the alloy surface, and affect the

functional characteristics of the formed coating. The formation of the OCC on a zirconium alloy occurs in two stages: in the first seconds, the anode voltage U_a increases by approximately 5...10 V (Fig. 1a, stage I), here the formation of the primary oxide film occurs by an electrochemical mechanism. The only reaction at the anode under a voltage of up to 100 V is the anodic growth of the oxide. In this case, the overvoltage of oxide formation is less than the decomposition voltage of the electrolyte. When it is reached, electrons are injected into the oxide layer, and oxygen begins to be released at the anode. Thus, the second stage of the formation of the spark discharge channel in the "metal - oxide - electrolyte" system begins. With a further increase in the voltage in the process of coating synthesis, a breakdown by electrons of this channel occurs.

During the synthesis of anodic-spark coating on zirconium alloy in galvanostatic mode, a slight increase in the anodic U_a and cathodic U_k voltages is observed with increasing KOH and liquid glass concentrations in the electrolyte (Fig. 1a, b). With increasing KOH and liquid glass concentrations (Fig. 1b, stage II), as well as in a more concentrated electrolyte (Fig. 1c, d, stage II), the coating formation process stabilises and proceeds evenly. Only with the addition of 10 g/l H_2O_2 at the coating formation stage does the voltage begin to gradually decrease (Fig. 1e, f, section II).

Reducing the current density lowers the anodic component of the synthesis voltage. The coating synthesised in an electrolyte of 3 g/l KOH + 2 g/l liquid glass at a current ratio of 20/20 A/dm^2 has an anodic voltage of 160...140 V (Fig. 1a, curve 1). If the current ratio is slightly reduced to 10/15 A/dm^2, the synthesis voltage decreases by 10...12 V (Fig. 1e, curve 2). At I_a/I_k = 10/10 A/dm^2, it is even lower by 8 V (Fig. 1a, curve 3), and the difference between curves 1 and 3 is 20...28 V.

For a higher concentration of KOH and insufficient glass up to 10 g/l and 15 g/l, respectively, the component anode voltages have values higher by 5...10 V. Adding even a small amount of GrO_3 (0,1 g/l) to such an electrolyte significantly reduces the formation of voltage at the anode. Under such conditions, it is 15...20 V lower (Fig. 1e, curves 1, 2). Increasing the electrolyte concentration by adding 10 g/l of glycerin to the already existing one has practically no effect on its value (Fig. 1d, curves 1, 2, 3). When adding 10 g/l of H_2O_2 to such an electrolyte, the process of coating formation does not proceed evenly (Fig. 1e, curve 1), the anode voltage is 140 V and drops to 125 V.

At a current ratio of I_a/I_c = 1, it is lower by 5 V. A higher glycerin content (18 g/l) increases the anodic and cathodic voltage components by approximately 10 V, and also stabilises the synthesis process on a zirconium alloy (Fig. 1f). Thus, the electrophysical parameters of the synthesis process of OCC on zirconium alloy depend on the composition of the electrolyte and the ratio of the anodic to cathodic current density. Thus, in the least concentrated electrolyte, which contains alkali and liquid glass, the synthesis proceeds unevenly, which affects the quality of the coating. Such a coating does not completely cover the metal surface, and therefore is not of high quality. Further increase in the electrolyte concentration by increasing the content of the main composition of KOH and liquid glass and introducing additional chromium oxide and glycerin stabilises the synthesis process, and from the assessment of the quality of the appearance, such a coating is of high quality. The introduction of hydrogen peroxide into the electrolyte slightly changes the voltage-current dependence.

In such an electrolyte, during the oxidation process, the anodic component of the voltage decreases with the synthesis time, which is reflected in the microhardness of the coating. Such a coating has better microhardness and greater thickness. The ratio of currents does not change the nature of the current-voltage dependences, i.e. it does not affect the stability of the synthesis process. A decrease in currents lowers the anodic and cathodic components of the voltage. And this, in turn, affects the properties of the coatings. The most favorable conditions for the formation of the oxide are formed at the ratio of current densities I_a/I_k = 1,5 and at a relatively low electrolyte concentration of 10 g/l KOH+15 g/l liquid glass. The time dependences of the current-voltage characteristics during the synthesis in different electrolytes of oxide-ceramic coatings on a titanium alloy are shown in Figure 2.

The study of the synthesis voltage of the coating was carried out in the system titanium alloy - alkaline electrolyte with the addition of liquid glass with electrolyte components of different concentrations. As in zirconium alloys, in the first 3-5 minutes, when spark discharges are formed, the components of the anode and cathode voltages increase by 5...10 V. The increase in voltage is observed in all studied systems with the same regularity, which depends on the concentration of KOH and liquid glass (Fig. 2a, b). After the plasma is formed, the character of the curve changes and it slightly decreases. In the galvanostatic mode, in the section A - B of stable formation of the oxide coating, the dependence of the voltage on the synthesis time in the given range is rectilinear. With increasing current, the voltage at the anode increases. In this case, the increase in voltage is accompanied by a decrease in the electrolyte concentration, which, obviously, is accompanied by a possible localisation of current carriers on the molecules of liquid glass (since the latter are also electron donors) and a decrease in their mobility.

Thus, in an electrolyte of lower concentration at a current density of 20/20 A/dm^2 the anodic component of the voltage is 150...140 V (Fig. 2a, curve 1), and at Ia/Ic=5/10 A/dm^2 it drops to 100...110 V (curve 4). When forming oxide in an electrolyte of composition 10 g/l KOH + 15 g/l liquid glass at a current density of 5/10 A/dm^2 (Fig. 2b), the anodic voltage reaches 88...102 V.

With the same ratio of currents, but in an electrolyte less concentrated at the anode, the oxide is formed at a voltage 12...18 V lower than in a more concentrated one. The same situation is true for other modes.

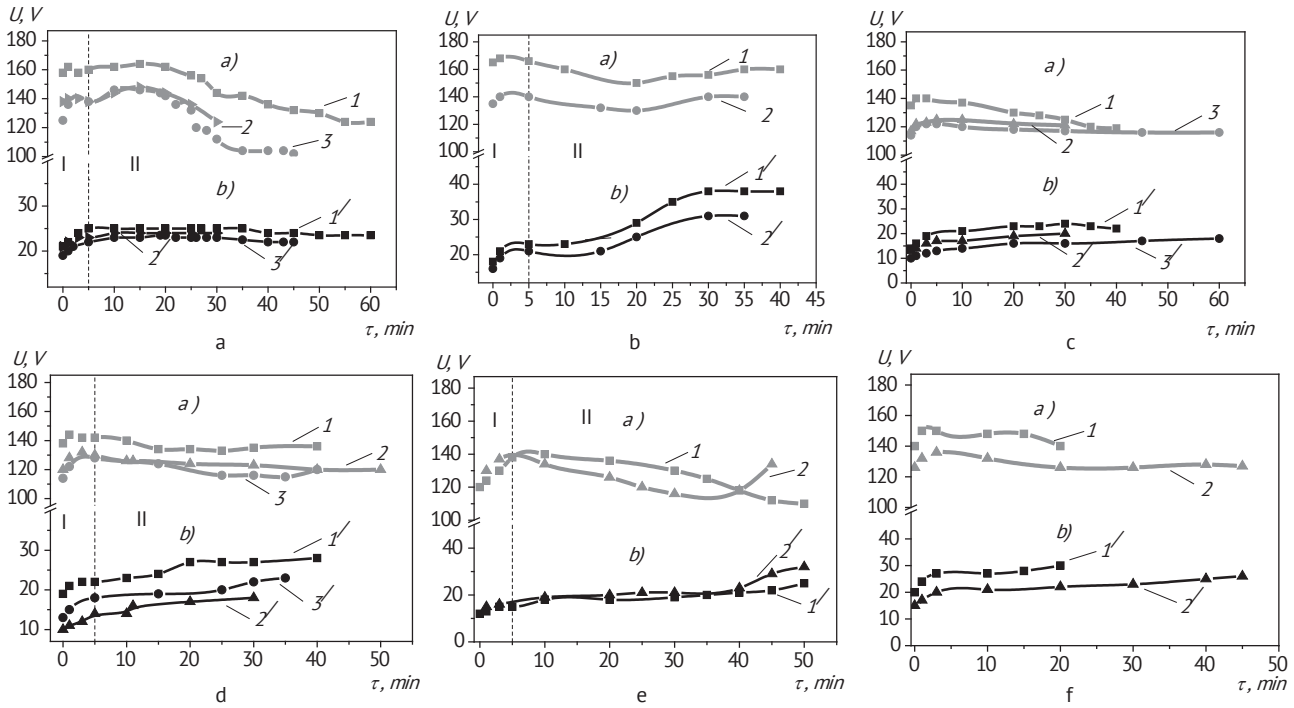

Figure 1. *Dependence of anodic (a) and cathodic (b) voltages on synthesis time on zirconium alloy electrodes in an electrolytes*

Note: *a – 3 g/l KOH+2 g/l liquid glass at different current densities: 1, 1′ – 20/20 A/dm², 2, 2′ – 10/15 A/dm², 3, 3′ – 10/10 A/dm²; b – 10 g/l KOH + 15 g/l liquid glass + 0,1 g/l GrO_3 at different current densities: 1, 1′ – 20/20 A/dm², 2, 2′ – 10/15 A/dm², 3, 3′ – 10/10 A/dm²; c – 10 g/l KOH+15 g/l liquid glass + 0,1 g/l GrO_3 + 10 g/l glycerin at different current densities: 1, 1′ – 20/30 A dm², 2, 2′ – 10/15 A/dm², 3, 3′ – 10/10 A/dm²; d – 10 g/l KOH+15 g/l liquid glass + 0,1 g/l GrO_3 + 10 g/l glycerin + 10 H_2O_2 at different current densities: 1, 1′ – 10/15 A/dm², 2, 2′ – 10/10 A/dm²; e – 10 g/l KOH + 15 g/l liquid glass + 0,1 g/l GrO_3 + 18 g/l glycerin + 10 H_2O_2 at different current densities: 1, 1′ –20/30A/dm², 2, 2′ –10/15 A/dm²*

Source: *developed by the authors*

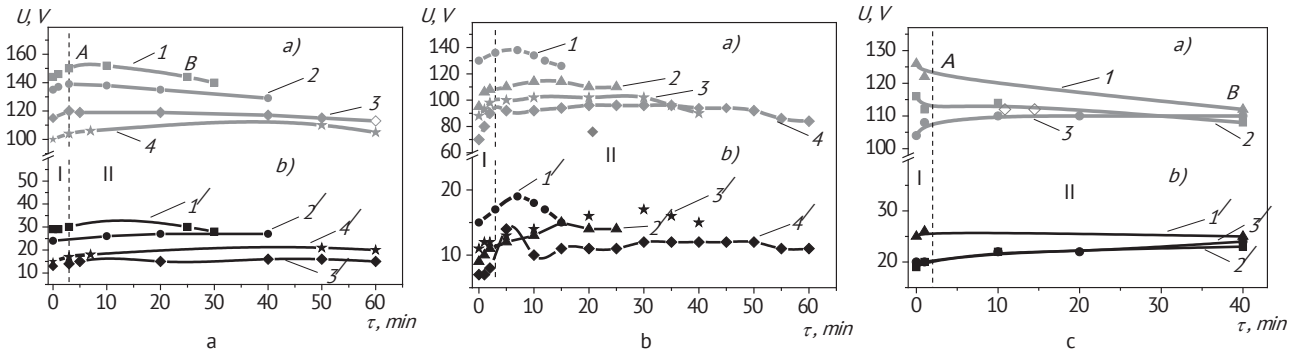

Figure 2. *Voltage curves depending on the synthesis time of oxide-ceramic coatings on titanium alloys in different electrolytes*

Note: *a – 5 g/l KOH+5 g/l liquid glass; b – 10 g/l KOH+15 g/l liquid glass; c – 5 g/l KOH + 5 g/l liquid glass+KF*

Source: *developed by the authors*

The introduction of 0.1 g/l of KF into the electrolyte lowers the anodic component of the voltage compared to the least concentrated electrolyte by 19...22 V. Further doping of the electrolyte with 0,2 and 0,5 g/l of KF, as expected, lowers the voltages at which the oxide is formed (Fig. 2c). It is known that the current density has a significant effect on the voltage of the synthesis of the anodic coating. As expected, an increase in the current density during anodic spark oxidation leads to an increase in the voltage (Fig. 2). This pattern is

observed at all electrolyte concentrations. Thus, at an electrolyte concentration of KOH 5 g/l and liquid glass 5 g/l, an increase in current density leads to an increase in voltage by 10...15 V. In an electrolyte with a higher concentration of its components, the voltage with an increase in current density also increases by 10...15 V.

Therefore, the OCC on a titanium alloy is synthesised more evenly compared to its synthesis on a zirconium alloy. Obviously, this is due to the conductivity of the electrolyte. Coatings synthesised on a titanium alloy have a much smaller thickness than on a zirconium alloy, so their conductivity increases, and the synthesis process proceeds evenly. The most favorable conditions for the formation of a coating on a titanium alloy are created when using low electrolyte concentrations.

The results presented in this work make it possible to establish several stages of the formation of the oxide coating on titanium and zirconium alloys. Thus, according to the results of the studies, it was found that the increase in current is accompanied by the breakdown of the oxide natural film. The results of the studies are investigated with data obtained by such scientists as M. Aliofkhazraei *et al*. (2021). The voltage value in the process of coating synthesis (second stage of synthesis) on the surface of the titanium alloy under different operating modes is within 90 ... 150 V. According to the comparative analysis of the synthesis of PEO coatings in electrolytes of different composition, it is noted that in the electrolyte with a higher concentration of components, the synthesis voltage decreases, which is also consistent with the results of studies of the electrophysical parameters of the PEO process by M. Aliofkhazraei *et al*. (2021).

The value of the voltage at the anode during the synthesis of zirconium alloy differs from the values obtained by V. Aubakirova *et al*. (2022) and is lower in this work. However, it is noted that the composition of the electrolyte is decisive for establishing energy dependencies. In the work of V. Aubakirova *et al*. (2022) more complexly alloyed electrolytes were used, and therefore the system requires more energy to introduce the components of the electrolyte composition into the oxide coating. It should also be noted that the different reactivity of each of the components changes the value of the synthesis voltage, however, the dependence between voltage and time is consistent with other works of researchers.

Conclusions

Studies of the current-voltage dependences during the synthesis of OCC on zirconium and titanium alloys showed that the synthesis process on a titanium alloy proceeds more evenly compared to its synthesis on a zirconium alloy. According to the electrophysical parameters, it was established that the stability of the formation of OCC on a zirconium alloy depends on the composition of the electrolyte, and an increase in the concentration of electrolyte components from 3 g/l KOH and 2 g/l of liquid glass to 10 g/l of alkali and 15 g/l of liquid glass stabilises the process of coating formation, which has a positive effect on its quality, and the introduction of chromium oxide, glycerin and hydrogen peroxide into the electrolyte reduces the components of the anodic and cathodic voltages.

When synthesising OCC on a titanium alloy, increasing the content of electrolyte components from 5 g/l KOH and 5 g/l liquid glass to 10 g/l KOH and 15 g/l liquid glass also leads to a decrease in the components of the anodic and cathodic voltages, and it was also found that a decrease in the anodic and cathodic currents reduces the components of the anodic and cathodic voltages at which the coating is formed. The following works will be related to the correlation dependencies between the parameters of the synthesis process and the properties of the obtained coatings. This will make it possible to establish the optimal coating application modes. Conceptually, it can be established that the electrophysical parameters of the process of plasma electrolytic synthesis of oxide-ceramic layers significantly depend on both the composition of the electrolyte and the processing modes and the nature of the base material. Increasing the concentration of electrolyte components helps stabilise the process of coating formation, reduce the anodic and cathodic voltages and create more favorable conditions for the formation of high-quality oxide layers. At the same time, titanium alloys are characterised by a more uniform course of the synthesis process compared to zirconium ones, which indicates a higher stability of the formation of coatings on their surface. Future research should focus on establishing quantitative correlation models between electrophysical synthesis parameters and the functional properties of oxide-ceramic coatings, as well as optimising electrolyte composition and processing regimes to achieve controlled, stable, and reproducible coating formation on titanium and zirconium alloy substrates.

Acknowledgements

None.

Funding

None.

Conflict of Interest

None.

References

[1] Aliofkhazraei, M., *et al*. (2021). Review of plasma electrolytic oxidation of titanium substrates: Mechanism, properties, applications and limitations. *Applied Surface Science Advances*, 5, article number 100121. doi: 10.1016/j.apsadv.2021.100121.

[2] Attarzadeh, N., & Ramana, C.V. (2021). Plasma Electrolytic Oxidation ceramic coatings on zirconium (Zr) and Zr-alloys: Part-II: Properties and applications. *Coatings*, 11, article number 620. doi: 10.3390/coatings11060620.
[3] Aubakirova, V., Farrakhov, R., Astanin, V., Sharipov, A., Gorbatkov, M., & Parfenov, E. (2022). Plasma electrolytic oxidation of Zr-1%Nb alloy: Effect of sodium silicate and boric acid addition to calcium acetate-based electrolyte. *Materials*, 15(6), article number 2003. doi: 10.3390/ma15062003.
[4] Bai, H., Zhong, L., Kang, L., Liu, J., Zhuang, W., Lv, Z., & Xu, Y. (2021). A review on wear-resistant coating with high hardness and high toughness on the surface of titanium alloy. *Journal of Alloys and Compounds*, 882, article number 160645. doi: 10.1016/j.jallcom.2021.160645.
[5] Canepa, P., Firpo, G., Mattera, L., Canepa, M., & Cavalleri, O. (2020). Calcium and phosphorous enrichment of porous niobium and titanium oxides for biomaterial applications. *Surface and Coatings Technology*, 389, article number 125634. doi: 10.1016/j.surfcoat.2020.125634.
[6] Chopra, D., Jayasree, A., Guo, T., Gulati, K., & Ivanovski, S. (2022). Advancing dental implants: Bioactive and therapeutic modifications of zirconia. *Bioactive Materials*, 13, 161-178. doi: 10.1016/j.bioactmat.2021.10.010.
[7] Fattah-alhosseini, A., & Molaei, M. (2023). A review of functionalizing plasma electrolytic oxidation (PEO) coatings on titanium substrates with laser surface treatments. *Applied Surface Science Advances*, 18, article number 100506. doi: 10.1016/j.apsadv.2023.100506.
[8] Fattah-alhosseini, A., Chaharmahali, R., Keshavarz, M.K., & Babaei, K. (2021). Surface characterization of bioceramic coatings on Zr and its alloys using plasma electrolytic oxidation (PEO): A review. *Surfaces and Interfaces*, 25, article number 101283. doi: 10.1016/j.surfin.2021.101283.
[9] Han, X., Ma, J., Tian, A., Wang, Y., Li, Y., Dong, B., Tong, X., & Ma, X. (2023). Surface modification techniques of titanium and titanium alloys for biomedical orthopaedics applications: A review. *Colloids Surf B Biointerfaces*, 227, article number 113339. doi: 10.1016/j.colsurfb.2023.113339.
[10] Hurle, K., Oliveira, J.M., Reis, R.L., Pina, S., & Goetz-Neunhoeffer, F. (2021). Ion-doped brushite cements for bone regeneration. *Acta Biomaterialia*, 123, 51-71, doi: 10.1016/j.actbio.2021.01.004.
[11] Imbirovych, N., Boyarska, I., Povstyanoy, O., Kurdzydlowski, K., Homon, S., & Kulakovskyi, L. (2023) Modification of oxide coatings synthesised on zirconium alloy by the method of plasma electrolytic oxidation. *AIP Conference Proceedings*, 2949(1), article number 020011. doi: 10.1063/5.0165655.
[12] Kombayev, K., Khoshnaw, F., Kozhakhmetov, Y., Tleuzhanova, G., Azamatov, B., & Tabiyeva, Y. (2025). Microplasma sprayed tantalum coatings on Ti Grade 5 extra-low interstitials: Investigation of thickness and porosity control. *Coatings*, 15, article number 464. doi: 10.3390/coatings15040464.
[13] Kombayev, K., Khoshnaw, F., Uazyrkhanova, G., & Moldabayeva, G. (2024). Experimental and mathematical modelling investigation of Plasma Electrolytic Oxidation (PEO) for surface hardening of 20ch steel. *Materials*, 17(24), article number 6043. doi: 10.3390/ma17246043.
[14] Krishna, E.S., Suresh, G., Ratna Sunil, B., & Dumpala, R. (2021). Bioactive titanium composites for bone implant applications. *IOP Conference Series: Materials Science and Engineering*, 1185, article number 012032. doi: 10.1088/1757-899X/1185/1/012032.
[15] Li, X., Tang, J., Ju, J., Gan, J., Zhang, J., Yan, M., Yu, P., Ke, H., Wang, W., & Yang, T. (2025). Superior corrosion resistance and good biocompatibility of Ti–24Nb–4Zr–8Sn alloy fabricated by a cost-effective, net-shape powder metallurgy method. *Materials Futures*, 0354401. doi: 10.1088/2752-5724/adf080.
[16] Li, Z., Cai, Z., Cui, X.J., Liu, R., Yang, Z., & Zhu, M. (2021). Influence of nanoparticle additions on structure and fretting corrosion behavior of micro-arc oxidation coatings on zirconium alloy. *Surface and Coatings Technology*, 410, article number 126949. doi: 10.1016/j.surfcoat.2021.126949.
[17] Molaei, M., Attarzadeh, N., & Fattah-Alhosseini, A. (2021). Tailoring the biological response of zirconium implants using zirconia bioceramic coatings: A systematic review. *Journal of Trace Elements in Medicine and Biology*, 66, article number 126756. doi: 10.1016/j.jtemb.2021.126756.
[18] Molaei, M., Fattah-alhosseini, A., Nouri, M., & Kaseem, M. (2024). Assessing the wear properties of plasma electrolytic oxidation TiO_2 coatings incorporated ZrO_2 nanoparticles on Cp-Ti in simulated body fluid. *Applied Surface Science Advances*, 19, article number 100563. doi: 10.1016/j.apsadv.2023.100563.
[19] Ou, Y.X., Wang, H.Q., Ouyang, X., Zhao, Y.Y., Zhou, Q., Luo, C.W., Hua, Q.S., Ouyang, X.P., & Zhang, S. (2023). Recent advances and strategies for high-performance coatings. *Progress in Materials Science*, 136, article number 101125. doi: 10.1016/j.pmatsci.2023.101125.
[20] Sarakinos, K., Alami, J., & Konstantinidis, S. (2010). High power pulsed magnetron sputtering: A review on scientific and engineering state of the art. *Surface and Coatings Technology*, 204(11), 1661-1684. doi: 10.1016/j.surfcoat.2009.11.013.

Фактори, що впливають на формування плазмо-електролітних оксидних покриттів, синтезованих на титанових та цирконієвих сплавах

Наталія Імбірович
Доктор технічних наук, професор
Луцький національний технічний університет
43018, вул. Львівська, 75, м. Луцьк, Україна
https://orcid.org/0000-0001-8276-6349

Юрій Фещук
Кандидат технічних наук, доцент
Луцький національний технічний університет
43018, вул. Львівська, 75, м. Луцьк, Україна
https://orcid.org/0000-0001-6259-1916

Анотація. Дослідження, представлене в цій статті, є актуальним через необхідність підвищення керованості та прогнозування процесів формування оксидно-керамічних покриттів на титанових і цирконієвих сплавах, що застосовуються в агресивних умовах експлуатації та високонавантажених конструкціях. Метою роботи було дослідження електрофізичних закономірностей формування покриттів під час плазмово-електролітичного оксидування титанових і цирконієвих сплавів та визначення впливу складу електроліту і густини струму на синтезну напругу. У роботі використано гальваностатичні анодно- та анодно-катодно режими, часову реєстрацію напруги і струму, порівняльний аналіз складу електролітів у грамах на літр та оцінювання вольт-амперних залежностей під час синтезу покриттів. Встановлено, що формування покриттів на цирконієвому сплаві відбувалося у два етапи та було нестабільним за низьких концентрацій електроліту, тоді як підвищення вмісту гідроксиду калію і рідкого скла забезпечувало стабілізацію процесу та рівномірність покриття. Показано, що титановий сплав забезпечував більш рівномірний перебіг синтезу та нижчі рівні напруги порівняно з цирконієвим завдяки вищій провідності та стабільнішому росту оксидного шару. Виявлено, що зменшення густини струму знижувало анодну та катодну складові напруги, а добавки до електроліту, такі як оксид хрому, гліцерин і пероксид водню, впливали на стабільність і величину синтезної напруги. Визначено оптимальні умови формування покриттів за збалансованих співвідношень густини струму та середніх концентрацій електроліту, що забезпечувало стабільний режим розрядів і покращення якості покриття. Отримані результати можуть бути використані інженерами-матеріалознавцями для оптимізації режимів плазмово-електролітичного оксидування з метою отримання корозійностійких та механічно стабільних захисних покриттів

Ключові слова: електрофізичні параметри; напруга синтезу; густина струму; електроліт; катод; анод

COMMODITY BULLETIN
Journal homepage: https://c-bulletin.com.ua/en
DOI: 10.62763/cb/1.2026.17

Article's History: Received: 29.12.2025 Revised: 30.03.2026 Accepted: 28.05.2026 Published: 29.05.2026

ISSN 2310-5283; e-ISSN 3041-1432 Vol. 19, No. 1, 2026, 17-28

UDC 620.2:621.395.721.5

Comparative commodity evaluation of smartphones across different price segments

Fisnik Brovina*
Doctor of Management Sciences, Associate Professor
Sports University of Tirana
1001, Muhamed Gjollesha Str., Tirana, Albania
https://orcid.org/0000-0002-4347-5538

Abstract. The aim of the study was to make a comparative evaluation of smartphones of different price segments – in terms of their technical, operational, economic and informational characteristics. The research methodology was based upon a type of comparative commodity analysis, establishing evaluation criteria and employing both a weighted scoring approach and verification of correspondence between official specifications and manufacturer technical details. Four smartphone models representing the budget, mid-range, premium, and flagship price segments were selected for the analysis. The comparative assessment showed that the Samsung Galaxy S25 Ultra achieved the highest integrated quality score (4.80 points), whereas the Xiaomi Redmi Note 14 Pro 5G demonstrated the most favourable balance between technical performance and market price (4.55 points). The Apple iPhone 16 confirmed the importance of software optimisation, ecosystem integration, and long-term software support for the consumer value of premium devices, while the Samsung Galaxy A26 5G provided adequate functionality for everyday use as the most cost-effective model. The analysis indicates that higher prices for smartphones are not necessarily accompanied by improvements in the technical characteristics of those devices. The differences between phones within each price segment relate most directly to the processor performance of the devices, the imaging capabilities of the cameras, the design and construction of the devices, and the software that is available to support those smartphones. Each of the technical specifications for each of the smartphones was verified to be consistent with those published by the device manufacturers. The practical significance of the study lies in the applicability of the proposed evaluation criteria and integrated assessment methodology for commodity examination of smartphones, the development of consumer recommendations, and the selection of smartphone models according to price segment and user requirements

Keywords: consumer properties; integrated quality index; technical specifications; software support; consumer value

Introduction

Due to the rapid development of mobile technologies, expansion of the number of mobile phone models created by the manufacturers and competition between the manufacturers, there is a considerable diversification of mobile phones of different price segments. The technical sophistication of mobile phones, the number of features that the phones offer and the different approaches of the manufacturers to positioning their products make it challenging to compare the properties of mobile phones of different manufacturers. A commodity assessment approach makes it possible to comprehensively evaluate the characteristics of mobile phones, identify their advantages in competition with other mobile phones of different manufacturers and determine whether the quality of the mobile phones is in line with their market price.

Suggested Citation:
Brovina, F. (2026). Comparative commodity evaluation of smartphones across different price segments. *Commodity Bulletin*, 19(1), 17-28. doi: 10.62763/cb/1.2026.17

*Corresponding author (fisnikbrovina0@gmail.com)

The evolution of commodity science has made it possible to replace the evaluation of separate technical parameters with the evaluation of consumer properties, functional value, and the product's ability to satisfy the needs of its users. V. Vasiuta *et al.* (2022) state that commodity science is becoming more and more related to technical, economic, and consumer quality criteria, which allows products to be evaluated more objectively in terms of the competitive marketplace. The authors point out that even for technically complex products, the evaluation of separate parameters is not enough because the quality of a product is dependent on the cumulative influence of many different, interrelated characteristics.

A similar argument is made by K. Petrov & I. Kobzev (2022), who introduced a method of accounting for the contribution of individual consumer characteristics to the consumer value of a product and the use of weighting coefficients to measure the relative importance of these characteristics based on information about consumer choice. The authors asserted that individual attributes of a product contribute unequally to its consumer value. Such an approach allows researchers to move past simply comparing individual parameters of a product to performing an integrated evaluation of an entire product to determine its competitiveness in the marketplace.

Another area of development within the field of science concerns the systematisation of electronic products. N. Marchuk *et al.* (2021), in their investigation of the classification of wearable electronic devices, stated that the rapid development of digital technologies has led to the need for the continual development of the attributes that are utilised to classify and evaluate those devices. The scientists explained that the various features of the electronic devices must be considered as a group of attributes that can be evaluated as a whole to determine the consumer properties of the electronic device. The smartphone market has also been influenced by the digitalisation of commerce and changes in consumer behaviour. According to S. Breus & O. Tsymbalenko (2024), the integration of digital technologies into the processes that occur within businesses has altered the interactions between those businesses and the consumers of their products. As a result, consumers can access the technical specifications of the products they wish to purchase, and often base their purchasing decisions on the digital information that is available about those products.

The expansion of opportunities for electronic commerce has enabled the comparison of smartphones according to their technical and economic characteristics. The study by O. Zaitseva *et al.* (2024) showed that B2C and C2C platforms have made information on the specifications, prices, sales conditions, and reviews of smartphones accessible to consumers. The availability of such information has led to an increase in the difficulty of making smartphone purchases due to the necessity of comparing a variety of technical specifications of these products. Changes in the behavior of smartphone consumers have also made an impact on the different criteria that are used to evaluate electronic products. The study by O. Tsyhanenko *et al.* (2023) indicated that during periods of economic uncertainty, consumers tend to base their purchasing decisions on the capabilities and the price of electronic products rather than the other attributes that are advertised by the manufacturers of those products.

Another of the focuses of the research within the field of commodity science is that which investigates the nature of the product information that is provided by the manufacturers of the goods that are being sold. R. Voloshyn & P. Muravka (2025) have published research that indicates that the expansion of e-commerce has led to product information becoming one of the primary factors that influences the purchasing decisions of consumers. As such, the authors stated that the product information must be complete, accessible, and reliable in order to allow for the performance of an objective evaluation of the commodities.

As digital sales channels for goods and services continue to expand, the issue of the reliability of the product information published by the manufacturers becomes more pressing. N.V. Romaniuk (2026) has investigated the use of digital control tools in the aims of increasing the transparency of the sales channels, making it easier to identify issues with the product information that is published by the manufacturers, and reducing the number of instances in which goods with inaccuracies in their characteristics are placed for sale. At the same time, a literature review of the issue of smartphones evaluation revealed that most of the existing research papers address separate aspects of the problem, such as aspects related to the science of commodities, aspects related to electronic commerce, aspects related to consumer behaviour, or aspects related to the provision of product information. A lack of comprehensive research in the study of smartphones from different price segments and according to different assessment criteria determined the need to conduct the research described in this paper.

The aim of the study was to evaluate smartphones from different price segments through a comprehensive study of the commodity characteristics of those smartphones, as well as to determine any relationship between those technical specifications of the phones and their market price. To accomplish this aim, the following tasks had to be performed: to systematise approaches to evaluating smartphone characteristics and to develop a set of criteria for their comprehensive assessment; to conduct a comparative analysis of the technical, functional and economic characteristics of smartphones from different price segments in order to calculate a quality index for the models representing each price

segment; and to determine the consistency of the technical characteristics of smartphones stated in product information and labelling with the official technical specifications published by the manufacturers.

Materials and Methods

The study had a theoretical-empirical research design. It was conducted in January 2026. Its focus was on performing a comprehensive evaluation of smartphones from different price segments with regard to their technical, functional, structural, economic, and informational characteristics. The theoretical phase of the study included a systematic analysis of existing approaches to assessing the quality of smartphones. On the empirical side of the research, a comparative characterisation of four smartphone models was performed, an assessment of each model according to the established criteria, an analysis of the price-to-quality ratio of the models evaluated, and a verification of the technical specifications of the brands that manufactured the smartphones in question.

At the theoretical stage of the work, the steps of theoretical generalisation, analysis, systematisation, and comparison of existing studies were performed. Such an approach allowed the researchers to systematise the approaches to evaluating smartphones as commodities, to identify the criteria for the properties of smartphones that are consumed, to determine the methods of assessing their technical, structural, operational, economic, and informational properties, as well as the approaches to assessing the price-quality characteristics of these mobile devices. As a result, a set of criteria was developed that allowed for the comprehensive evaluation of smartphones, which would become the methodological basis for the following empirical stage of the work. The source base included scholarly publications on commodity science, quality assessment of electronic products, consumer studies of the smartphone market, and official technical materials issued by leading mobile device manufacturers.

The empirical study included four smartphone models representing four price segments of the mobile device market: Samsung Galaxy A26 5G (budget segment), Xiaomi Redmi Note 14 Pro 5G (mid-range segment), Apple iPhone 16 (premium segment), and Samsung Galaxy S25 Ultra (flagship segment). The models were selected according to the representativeness of their price categories and their relevance at the time of the study. To ensure comparability of the results, the analysis covered base configurations officially presented by the manufacturers. The information sources included official manufacturers' technical specifications, official product catalogues, and open data on average market prices for the examined models (Samsung, n.d.a; n.d.b; Apple, n.d.; Xiaomi, n.d.).

For a comprehensive comparison of the consumer properties of smartphones from different price segments, a comparative commodity analysis was employed. The comparison was based on a set of criteria covering technical specifications, camera performance, battery life, structural design, software support, as well as economic and informational indicators. The methodological foundation for this stage included studies on the commodity evaluation of smartphones together with research addressing the factors that shape their consumer properties and market value. The reasons for choosing such an approach to assessing the quality of smartphones are primarily that no individual specification of a smartphone is likely to provide an accurate reflection of its overall quality, but the evaluation of each specification separately can provide a more objective representation of both the capabilities and the value of that smartphone. Methods of generalisation and classification helped to develop a unified system of assessment criteria for smartphones.

To compare the selected smartphone models quantitatively, an integrated weighted scoring method was used. Each criterion was assessed on a five-point scale, where 1 represented the lowest level of compliance with the evaluation criterion and 5 represented the highest value among the examined models. The relative importance of each criterion was incorporated through weighting coefficients, the sum of which equaled 1.00. The integrated quality index was calculated as the sum of the products of the score assigned to each criterion and its corresponding weighting coefficient (formula (1)):

$$I = \sum_{i=1}^{n} B_i W_i, \quad (1)$$

where I – the integrated commodity evaluation index; B_i – the score assigned to the i-th criterion; W_i – the weighting coefficient of the co5rresponding criterion.

The research data were processed automatically in Google Sheets (USA). Descriptive statistical methods were applied to organise the collected data, compare indicators, rank the evaluated models, and calculate the integrated quality indices. Calculations were performed separately for each smartphone model using the established system of evaluation criteria. The integrated assessment method made it possible to move beyond the examination of individual characteristics toward a comprehensive evaluation of overall smartphone quality and provided a basis for objective ranking regardless of price segment.

The reliability of the information about the products was determined using the documentation verification method for the technical specifications of the products. The verification of the technical specifications was based on the official technical specifications of the smartphones published on the manufacturers' official websites. The verification included checking the model of the smartphone, the type of processor installed in the device, the amount of Random-Access Memory

(RAM) and the internal storage capacity, the technical specifications of the display, the characteristics of the cameras, the specifications of the batteries, the specifications of the chargers, the ingress protection, the operating system installed, and the software specifications and support information. The characteristics of the smartphones were compared with the official technical specifications published by the manufacturers to verify each smartphone model. Based on these comparisons, the information about the characteristics of each smartphone model was determined to match the specifications published by the smartphone manufacturers. Through performing such a verification process, it became possible to determine the completeness and reliability of the information regarding the characteristics of smartphones. Additionally, it was possible to determine the suitability of the specifications published by the smartphone manufacturers as a source of information regarding the characteristics of those smartphone models.

Results

From the perspective of commodity science, smartphone evaluation involves determining the extent to which a device is capable of meeting users' functional needs throughout its service life. Such an assessment considers not only the technical specifications stated by the manufacturer but also their influence on operational performance, reliability, durability, and the economic feasibility of purchase (Haba *et al.*, 2017; Akiba & Jonsson, 2022). Considering these characteristics as an integrated system provides a more objective basis for commodity evaluation.

The quality of smartphones is determined by how well its functional, technical, operational, and economic characteristics meet the requirements of end users (Horani & Dong, 2023). The technical qualities of smartphones include their display specifications, processor performance, RAM and internal storage capacity, graphics subsystem characteristics, wireless connectivity features, and support for current data transmission standards. Other aspects to consider when evaluating smartphone quality include ease of use, durability, reliability, the quality of product information, and economic efficiency.

One of the principal components of a comprehensive smartphone evaluation is the assessment of its technical characteristics. Technical characteristics include display specifications, processor performance, RAM and storage capacity, graphics processing unit, connectivity technologies, and support for current data transmission standards (Rai *et al.*, 2023). Together, these characteristics determine processing performance, operational stability under workload, and the ability of the device to handle a wide range of user tasks. At the same time, individual technical specifications should not be interpreted independently, since overall performance depends on the balance of the entire hardware and software architecture.

The characteristics of the display technology represent another important component of a comprehensive evaluation of smartphone models. Factors related to the display technology, such as resolution, refresh rate, brightness, colour accuracy, and contrast, all play a role in the convenience with which the smartphone can be utilised in everyday functions (Blanco-Encomienda *et al.*, 2024). As the primary interface between the smartphone and the user, the display's characteristics have a major impact on the device's overall quality. For phones in the mid-range, premium, and flagship segments, display performance is one of the main factors that differentiate between smartphone models.

The photographic performance of a smartphone represents another group of considerations that can be used to provide a comprehensive review of the device. The photographic capabilities of smartphones have evolved into sophisticated digital imaging systems, and the quality of the images captured by these devices is determined by a variety of factors beyond the sensor resolution. Factors such as computational image processing algorithms, artificial intelligence functions, and the noise reduction algorithms implemented within these devices can affect the quality of the photographs. Consequently, the photographic quality of a smartphone can be evaluated mainly in terms of the quality of the photographs taken with those devices, rather than the manufacturer's specifications (Huang & Wu, 2020; Zhu *et al.*, 2020).

Battery endurance is also regarded as one of the fundamental indicators of smartphone consumer quality. The operating time of a smartphone is determined by factors beyond the battery capacity itself, such as the processing power of the device's processor, the characteristics of its display, the software that is installed on the device, and its operating system (Cai, 2025). Smartphones with identical batteries can last considerably longer than others due to these factors. Hence, another parameter to evaluate when considering the different models of smartphones is the operating time of the device.

The structural characteristics of smartphones are another essential dimension of their evaluation. The materials of construction of the device, the durability of its construction, its resistance to dust and water ingress, its weight, its thickness, and its ergonomics all play a role in the durability and comfort of the device. Smartphones constructed of aluminium alloys, reinforced glass, and even titanium components offer performance benefits to the user at the expense of higher manufacturing costs and, thus, retail price. Hence, smartphones' structural characteristics should be evaluated in conjunction with their functional capabilities. This makes it possible to determine whether the construction of smartphones using such higher-grade materials

provides an improvement in the product's durability. Smartphones' economic indicators are another essential dimension of their evaluation. The price of smartphones does not necessarily correlate with the functional performance that they offer (Akiba & Jonsson, 2022). The price of high-end and flagship smartphones often correlates with features such as brand value, industrial design, the use of advanced construction materials, and the inclusion of certain technological innovations (Horani & Dong, 2023). Hence, the relationship between quality and price is another of the key criteria to consider in the evaluation of smartphones as commodities.

Consumer perceptions of smartphone quality are also shaped by the manufacturer's reputation, the brand's country of origin, and the level of trust associated with the brand. These factors may increase consumers' willingness to choose a particular model even when technical differences between competing products are minimal. Nevertheless, such attributes should not outweigh objective product characteristics during commodity evaluation, since its primary purpose is to determine the actual quality of a product regardless of brand-related marketing influences (Shin & Choo, 2012; Blanco-Encomienda *et al.*, 2024). The synthesis of these approaches served as the basis for establishing the evaluation criteria applied in the subsequent comparative analysis of smartphones across different price segments (Table 1).

Table 1. *Main criteria for the comprehensive commodity evaluation of smartphones across different price segments*

Criterion group	Evaluation indicators	Contribution to consumer properties	Role in commodity evaluation
Technical characteristics	Display technology and size, resolution, refresh rate, processor, RAM, internal storage	Determine processing performance, operating speed, display quality, and the ability to perform resource-intensive tasks	Used to compare the functional capabilities of smartphones across different price segments
Camera characteristics	Main camera, ultra-wide camera, front camera, optical image stabilisation, video recording capabilities	Reflect photographic and video performance as well as multimedia capabilities	Used to assess whether technical specifications correspond to actual imaging performance
Battery performance	Battery capacity, charging speed, wireless charging support	Determine battery life and convenience in everyday use	Used to evaluate the practical efficiency of smartphone operation
Structural characteristics	Body materials, weight, dimensions, dust and water resistance (IP rating)	Influence durability, mechanical strength, ergonomics, and ease of handling	Used to assess the operational reliability of the product
Software support	Operating system version, duration of software support, artificial intelligence features	Ensure operational stability, security, and the long-term availability of functional capabilities	Used to evaluate the long-term usability of the smartphone
Economic indicators	Market price, price segment, integrated price-to-quality index	Reflect the economic justification for purchasing a particular model	Used to determine the optimal balance between price and overall quality
Informational indicators	Product labelling, technical documentation, consistency between declared and actual specifications	Reflect the completeness and reliability of product information	Used to verify compliance with manufacturers' specifications and support an objective commodity evaluation

Note: *P – ingress protection*

Source: *compiled by the author based on D.-H. Shin & H. Choo (2012), C.-H. Huang & J.-L. Wu (2020), E.A.G. Akiba & R. Jonsson (2022), L.F. Horani & L. Dong (2023)*

The analysis of the proposed criteria for product evaluation confirms the variation of their significance depending on the price category of smartphones. For this reason, commodity evaluation should be based on a comprehensive assessment, not on separate technical indicators that do not always correlate with the actual level of consumer properties of a smartphone. The choice of a mobile device by a consumer is usually based on the overall combination of technical capabilities, functionality, battery life, external design, and price, not individual product characteristics (Hailat *et al.*, 2025). In addition, the weight of different evaluation criteria varies between price categories. Processing performance and affordability remain the most significant for budget smartphones, while display quality, camera performance, body material, and software support increasingly take precedence in premium and flagship categories. In addition, a smartphone's elevated market price does not guarantee that all its technical characteristics have improved proportionately. Therefore, price should be examined in conjunction with the true level of quality of the product (Cai, 2025; Cui *et al.*, 2025).

The next stage of the study involved applying the established evaluation framework to smartphones of different price segments. Four smartphones of different price segments were selected for evaluation: the Samsung Galaxy A26 5G smartphone of the budget segment, the Xiaomi Redmi Note 14 Pro 5G of the mid-range segment, the Apple iPhone 16 of the premium segment, and the Samsung Galaxy S25 Ultra of the flagship segment. The first stage of the evaluation of these smartphones was to compare their technical characteristics, the results of which are presented in Table 2.

Table 2. *Comparative technical characteristics of smartphones across different price segments*

Parameter	Samsung Galaxy A26 5G (Budget)	Xiaomi Redmi Note 14 Pro 5G (Mid-range)	Apple iPhone 16 (Premium)	Samsung Galaxy S25 Ultra (Flagship)
Average market price, USD*	299	399	799	1299
Display	Super AMOLED, 6.7″	AMOLED, 6.67″	Super Retina XDR OLED, 6.1″	Dynamic AMOLED 2X, 6.9″
Resolution	2,340×1,080	2,712×1,220	2,556×1,179	3,120×1,440
Refresh rate	120 Hz	120 Hz	60 Hz	120 Hz (adaptive)
Processor	Exynos 1380	MediaTek Dimensity 7300 Ultra	Apple A18	Snapdragon 8 Elite for Galaxy
RAM	6/8 GB	8/12 GB	8 GB	12 GB
Internal storage	128/256 GB	256/512 GB	128/256/512 GB	256/512 GB/1 TB
Main camera	50 MP	200 MP	48 MP	200 MP
Ultra-wide camera	8 MP	8 MP	12 MP	50 MP
Telephoto camera	-	-	-	50 MP+10 MP
Front camera	13 MP	20 MP	12 MP	12 MP
Maximum video resolution	4K	4K	4K Dolby Vision	8K
Battery capacity	5,000 mAh	5,110 mAh	≈3,561 mAh	5,000 mAh
Fast charging	25 W	45 W	25 W	45 W
Wireless charging	No	No	MagSafe, Qi2	Yes
Body material	Plastic	Glass/Plastic	Aluminium and Glass	Titanium and Glass
Ingress protection	IP67	IP68	IP68	IP68
Operating system	Android 15 (One UI 7)	Android 15 (HyperOS)	iOS 18	Android 15 (One UI 7)
Guaranteed software support	Up to 6 years	Up to 4 years	Approximately 5 years**	Up to 7 years

Note: **Average market prices are presented as of the study period and may vary depending on the country of sale and memory configuration. **Apple does not officially specify a guaranteed software support period; therefore, the value shown reflects the average duration of software updates provided for previous iPhone generations*

Source: *compiled by the author based on Apple (n.d.), Samsung (n.d.a; n.d.b), Xiaomi (n.d.)*

The data presented in Table 2 showed that there is an overall increase in technical characteristics as smartphones transition from the budget to the high-end models. However, not all specifications experience increases in any given range. For example, technical characteristics like processing performance, RAM and storage capacity, body materials, and camera specifications tend to increase with price. Other characteristics, such as battery capacity and refresh rate, are relatively the same across the different price range segments. Thus, many of the technologies that are traditionally present in high-end smartphones are also incorporated into budget models.

The Samsung Galaxy A26 5G is a smartphone that sits within the budget range for smartphones. It comes with an AMOLED display with a 120 Hz refresh rate, a 5,000 mAh battery, and the latest version of the mobile operating system. However, its body is made of plastic materials, it does not include a telephoto camera, it has relatively lower processing power than many other smartphones in its range, and it offers fewer fast charging specifications than other models in the same price range.

The Xiaomi Redmi Note 14 Pro 5G is a smartphone in the mid-range for smartphones. It has a 200 MP main camera lens, increased RAM, it can charge to 100% in 30 minutes with a 120 W fast charger, and it is water and dust resistant to IP68 standards. These specifications indicate that the Xiaomi Redmi Note 14 Pro 5G has focused on providing the highest specification for smartphones in its price range.

Finally, the Apple iPhone 16 creates its value proposition differently from the other brands discussed. While the specifications for the iPhone 16 are slightly lower than those of the other brands discussed (especially in relation to the refresh rate and battery capacity), its strengths lie in the A18 processor within the device, the integration of iOS with both the phone and the Apple ecosystem, and the length of time that it will be supported with software updates.

Among the models evaluated, the Samsung Galaxy S25 Ultra demonstrates the most advanced technical configuration. Its advantages include a flagship processor, a titanium body, a professional camera system, 8K camera capabilities, high memory configurations, and the longest duration of software support for this model of smartphone. Although the Samsung Galaxy S25 Ultra has the most advanced technical specifications among the models compared, it also has the highest market price for the phones in this evaluation.

Although higher prices were found for phones with improvements to the functional and structural characteristics of the devices, not every technical specification for those phones was improved. Based on these findings alone, it is noted that evaluating smartphones according to only the various specifications provided for each manufacturer will not provide an objective

measurement of the quality of those phones. Thus, the findings indicate the need for an integrated evaluation model to determine the overall quality of each brand of smartphone. Hence, the results of the evaluation will be summarised through the implementation of an integrated evaluation model (Table 3).

Table 3. *Integrated commodity evaluation scores for smartphones across different price segments*

Evaluation criterion	Weighting coefficient	Samsung Galaxy A26 5G	Xiaomi Redmi Note 14 Pro 5G	Apple iPhone 16	Samsung Galaxy S25 Ultra
Display	0.15	4	5	4	5
Processor performance	0.20	3	4	5	5
Camera performance	0.20	3	5	4	5
Battery performance	0.15	4	5	4	5
Structural design and body materials	0.10	3	4	5	5
Software support	0.10	5	4	5	5
Price-to-quality ratio	0.10	5	5	4	3
Integrated quality index	1.00	3.65	4.55	4.45	4.80

Source: *Compiled by the author*

The Samsung Galaxy S25 Ultra emerged as the smartphone with the highest integrated quality index of 4.80. The phone features the best technical performance, but its high market price lowers its score for the price-to-quality criterion. The Xiaomi Redmi Note 14 Pro 5G ranked second with an integrated quality index of 4.55. This model offers the best balance between technical specifications and cost of purchase. It scores highly in the criteria for camera performance, battery performance, and price-to-quality. The Apple iPhone 16 received an integrated quality index of 4.45. This phone offers some of the best processing power, structural quality, and software performance in the smartphone segment. However, the lower refresh rate of the screen, the smaller battery size, and higher purchase price of the phone lower its overall score. Finally, the Samsung Galaxy A26 5G received the lowest integrated quality index of 3.65. This phone is positioned in the budget segment of the smartphone market. While the hardware specifications and camera quality are more limited compared with other models, the phone performs all necessary tasks for everyday use and offers good value for money.

The findings show that there is no direct relationship between the increasing price of smartphones and the improvement of their technical characteristics. The most appropriate choice of smartphone for a consumer depends on the relationship between the technical characteristics and the price of smartphones. Thus, while the quality index is helpful in obtaining an overview of the technical characteristics of smartphone models, verifying the technical specifications provided by the manufacturers is also necessary for a complete evaluation of smartphone commodities. The last stage of the evaluation of these smartphone commodities involved verifying the information provided by smartphone manufacturers regarding their technical specifications with the technical characteristics that they have declared for these smartphone models. The results of such an evaluation are presented in Table 4.

Table 4. *Verification of the consistency between product labelling information and the manufacturers' official technical specifications*

Parameter	Samsung Galaxy A26 5G	Xiaomi Redmi Note 14 Pro 5G	Apple iPhone 16	Samsung Galaxy S25 Ultra
Model designation	+	+	+	+
Processor	+	+	+	+
RAM	+	+	+	+
Internal storage	+	+	+	+
Display specifications	+	+	+	+
Camera specifications	+	+	+	+
Battery capacity	+	+	+	+
Charging performance	+	+	+	+
Ingress protection rating	+	+	+	+
Operating system version	+	+	+	+
Software support information	+	+	+	+
Overall compliance	Full	Full	Full	Full

Note: *"+" indicates that the information declared by the manufacturer is consistent with the official technical specifications of the corresponding smartphone model*

Source: *compiled by the author based on Apple (n.d.), Samsung (n.d.a; n.d.b), Xiaomi (n.d.)*

The results presented in Table 4 demonstrate that all the smartphones under consideration comply with the technical specifications published by their manufacturers. The differences between models relate to the detail provided within the technical specifications rather than the accuracy of the information provided. The flagship models include the most detailed technical specifications due to their variety of features, while the budget model includes a more concise specification that still provides all the information necessary to describe the model and its consumer properties.

The smartphone manufacturers provide similar technical specifications for the models they publish, including details on the processor type, memory, display, cameras, battery, operating system, and the ingress protection of the devices. These specifications allow for a direct comparison of the smartphones from different price segments. Some specifications might differ from the way the smartphones function due to the features and operating systems of the devices. However, these specifications from the manufacturers are sufficiently reliable for comparing the consumer properties of smartphones from each price segment. Thus, these specifications can be used as a basis for comparing the smartphones according to their consumer properties and for formulating recommendations regarding which smartphone models consumers should purchase.

The results of the commodity evaluation of smartphones allow for the selection of phones that best match the requirements of individual consumers. A higher purchase price does not necessarily indicate improved technical specifications for the smartphone. Rather, the decision to purchase a phone can be based upon the combination of the technical specifications of the devices.

For consumers seeking a smartphone with a low purchase price and whose requirements are satisfied by the capabilities of midrange phones, the Samsung Galaxy A26 5G is an appropriate model to purchase. The phone contains sufficient specifications to meet the needs of most casual consumers. For those seeking higher technical specifications at a similar price, the Xiaomi Redmi Note 14 Pro 5G may be the best model for selection. The Redmi Note contains higher capabilities in each of its technical specifications at a lower price point.

For consumers who utilise the Apple operating system and value long-term support for that software, the Apple iPhone 16 may be the most appropriate smartphone to select; while many of the specifications of the phone are less advanced than other models, the phone has higher software support and performance, as well as higher performance in general. For consumers who require the highest possible specifications for their smartphone, such as processing power, camera and display capabilities, the Samsung Galaxy S25 Ultra will provide the highest level of performance, supporting its higher purchase price. Overall, then, the balance between the capabilities, performance, and price of smartphones is the most important specification for smartphones.

Discussion

As a result of this analysis, it became apparent that the differences between smartphone price segments are reflected not only in the number of technical advantages each device provides but also in the way the various features interact. Each budget phone model offers consumers an adequate level of the features and technologies they need to complete their everyday tasks, while the advantages of premium and flagship devices arise from a balanced approach to the technologies included in those devices.

These findings are consistent with those of J.B. Phillips & H. Eliasson (2017), who published a study that emphasises the importance of a comprehensive analysis of smartphone camera features rather than simply considering each individual technical specification. The authors explained that to objectively evaluate a smartphone camera, one must consider image detail, colour accuracy, noise levels, dynamic range, and image-processing algorithms. As a result, the smartphones earning the highest camera scores did not necessarily have the highest specifications for any single feature, but offered a balanced technology that delivers high-quality images overall.

Furthermore, the assessment of battery performance also helps to indicate that battery capacity alone is not a measure of the efficiency of smartphones. D. Flores-Martin *et al.* (2024) have published research in which they indicate that the length of time that their smartphones operate is based upon the battery management systems within the smartphones, the applications that are utilised, and the amount of activity that the phone performs in relation to communication with other devices and systems. Instead, smartphones that have similar battery capacities can have different performances from one another, indicating that another factor is at play.

The evaluation of the structural features of the smartphones additionally indicates the use of a more comprehensive assessment of the commodity. According to S. Soudachanh & S. Salhofer (2025), the evaluation of electronic products is no longer limited to technical specifications but also considers repairability, service life, and long-term manufacturer support. Similarly, smartphones that utilise more durable materials for their cases, have more protection against water and other environmental factors, and that are supported by the manufacturer for longer periods of time will score higher on a more comprehensive evaluation of those smartphones.

The results of this research are additionally in alignment with the concept of technological evolution

in complex technological products, as described by M. Coccia (2026). The author explained that the development of complex technological products often includes developing each of the subsystems of that product simultaneously to maximise the overall competitiveness of the product. Each of the factors that contribute to the overall evaluation score for the smartphone – processing performance, structural quality, imaging performance, battery performance, and software support – are evaluated simultaneously by the manufacturer in the creation of that device, indicating that the score for that brand of smartphone is the result of each of these factors being developed in conjunction with one another. For these reasons, the use of such a comprehensive evaluation of each brand of smartphone is superior to the evaluation of each of its individual specifications.

A similar perspective on smartphone characteristics is provided by A. Pellegrino (2024). The author indicated that many consumers tend to consider a variety of factors in the purchase of a smartphone, such as its functional characteristics, price, user experience, brand, and the value of the product provided to the consumers over time. The author explains that as a result, the technical specifications of the devices are less important to many consumers than ensuring that the characteristics of the smartphones correlate with the value that the consumers are willing to provide for the device. The findings of the study reflect these suggestions: the mid-range smartphones were deemed to offer the best balance between their characteristics and their cost.

These findings are also reflective of the conclusions of S. Hoffmann & P. Akbar (2023). The authors explained in their review that consumers consider a variety of factors in the purchase of technology products, including the functional characteristics, the psychological attributes of the product, and the economic factors related to the product. The findings of this current study reflect these factors in that the various technical specifications and features of smartphones did not have an impact upon their overall evaluation by consumers unless those specifications provided some benefit to the consumers in relation to their use of those products.

Another factor that influences the evaluation of smartphones is the after-purchase experience. P. Guo *et al.* (2025) have determined that factors that impact smartphone consumer satisfaction include the stability of the software installed on the smartphone, the regularity with which software updates are made to those smartphones, the quality of after-sales support for those manufacturers, and the reliability of the device over time. These same factors were recognised within the present study, as phones that offered longer periods of software support received higher evaluation scores than those that did not, even if they contained some technically less advanced specifications than their competitors.

Brand perception represents another factor influencing the way consumers assess smartphone value. According to M. Kayakuş *et al.* (2024), brand reputation can lead to consumers feeling more confident in the brand of the smartphone that they are purchasing, and in the abilities of that brand to provide high-value phones despite the relatively small technical differences between their products. However, the results of the present study suggest that brand reputation should not be considered an indicator of the quality of the smartphones that are manufactured by those brands; instead, the technical, operational, and economic indicators of those brands provide a more accurate measure of the quality of their smartphones.

A more comprehensive assessment of smartphones that incorporates the various aspects of the products, such as their technical, structural, operational, economic, and informational characteristics, will allow for a more complete understanding of the consumer properties of the evaluated products and for the identification of the competitive strengths of smartphone models, regardless of their market segment. Thus, the focus of the assessment can shift from the technical specifications of the smartphones to an evaluation of their consumer value.

This type of assessment reflects the concepts evaluated by L. Moutinho *et al.* (2014), who determined that the evaluation of technological products extends beyond the consideration of their technical specifications to incorporate aspects related to the consumers of those products, such as their behaviour and the value that they place upon those products. The assessment of smartphones according to the various characteristics of the products, each associated with another characteristic of the products, reflects these concepts and indicates that each smartphone has an overall value that can be determined according to these characteristics. The findings of this study have a range of implications for various groups of stakeholders in the industry. Manufacturers can utilise the framework to determine the strengths of their smartphones compared to competitors. Retailers who are aware of the evaluation study can provide recommendations regarding smartphones to consumers. Experts can apply the framework to provide an objective evaluation of the quality of smartphones.

The conclusions of this evaluation are in agreement with the findings of M. Nasirinejad & S. Sampalli (2023), who determined that the selection of digital products requires the evaluation of different specifications of those products. The findings of this study provide support for the application of such an evaluation system to smartphones of different price segments. Furthermore, the specifications that are evaluated in this study can also be applied to the evaluation of other categories of digital electronic products.

Overall, the conclusions of this study, in conjunction with previous research findings on the topic, lead to

the determination that a framework for the evaluation of the characteristics of smartphones of each price segment can be beneficial for a variety of reasons. Unlike the evaluation of the specifications of smartphones alone, this framework considers the interrelationship between the functional, structural, operational, economic, and informational characteristics of smartphones. Evaluating these different characteristics as a system allows for the determination of the value of those products to its consumers, to experts in the field, and provides a framework for the further evaluation of other categories of digital electronic products.

Conclusions

The study demonstrated that the proposed framework provides an objective basis for comparing smartphones using multiple technical, operational, structural, software-related, economic, and informational criteria. The integrated weighted assessment made it possible to evaluate smartphones comprehensively rather than relying on individual specifications. The findings showed that although higher-priced models generally offered better processor performance, structural quality, and software support, price increases were not proportional to improvements in overall consumer value. At the same time, features previously associated mainly with flagship devices, including high refresh-rate displays, ingress protection, and large battery capacity, have become available across different price categories, reflecting the narrowing technological gap and increasing competition in the smartphone market.

The comparative evaluation showed that the Samsung Galaxy S25 Ultra achieved the highest integrated quality index (4.80), although its advantage over the remaining models was considerably smaller than the difference in market price. The Xiaomi Redmi Note 14 Pro 5G ranked second (4.55) and demonstrated the most favourable balance between technical capabilities and purchase cost. The Apple iPhone 16 confirmed that the consumer value of premium devices depends not only on hardware specifications but also on software optimisation, ecosystem integration, and long-term software support. In contrast, the Samsung Galaxy A26 5G provided sufficient functionality for everyday use while remaining the most cost-effective option among the evaluated models. Verification of the manufacturers' official specifications confirmed full consistency between the declared and actual characteristics, supporting the use of these data for comparative product evaluation and the development of evidence-based consumer recommendations.

The main limitation of this study is that the evaluation relied exclusively on manufacturers' official technical specifications without independent testing of processing performance, battery endurance, or camera capabilities. Future research should expand the range of evaluated models by incorporating independent laboratory testing together with indicators of long-term reliability, repairability, and maintenance costs.

Acknowledgements

None.

Funding

None.

Conflict of Interest

None.

References

[1] Akiba, E.A.G., & Jonsson, R. (2022). *Consumer value perception of smartphones: A comparative study of Swedish and Japanese millennials*. (Master thesis, Jönköping University, Jönköping, Sweden).
[2] Apple. (n.d.). *iPhone 16*. Retrieved from https://www.apple.com/iphone-16/specs/.
[3] Blanco-Encomienda, F.J., Chen, S., & Molina-Muñoz, D. (2024). The influence of country-of-origin on consumers' purchase intention: a study of the Chinese smartphone market. *Asia Pacific Journal of Marketing and Logistics,* 36(7), 1616-1633. doi: 10.1108/APJML-05-2023-0462.
[4] Breus, S., & Tsymbalenko, O. (2024). Conceptual foundations of the problem of information technology development in the context of the integration of digital solutions and business processes. *Economy and Society*, 69. doi: 10.32782/2524-0072/2024-69-45.
[5] Cai, J. (2025). A multidimensional analysis of the impact of smartphone technical specifications on sales performance: An analysis based on consumer purchasing behavior. *Theoretical and Natural Science*, 105, 113-120. doi: 10.54254/2753-8818/2025.22965.
[6] Coccia, M. (2026). Theory of subsystems driving technological coevolution in modular architecture of complex innovations. *Technologies*, 14(3), article number 156. doi: 10.3390/technologies14030156.
[7] Cui, J., Wang, X., & Zheng, Y. (2025). Analysis of factors influencing smartphone prices. In *Proceedings of the 2nd international conference on innovations in applied mathematics, physics, and astronomy* (pp. 65-69). Singapore: SciTePress. doi: 10.5220/0013814100004708.
[8] Flores-Martin, D., Laso, S., & Herrera, J.L. (2024). Enhancing smartphone battery life: A deep learning model based on user-specific application and network behavior. *Electronics*, 13(24), article number 4897. doi: 10.3390/electronics13244897.

[9] Guo, P., Li, H., & Mo, X. (2025). Quantifying post-purchase service satisfaction: A topic-emotion fusion approach with smartphone data. *Big Data and Cognitive Computing*, 9(5), article number 125. doi: 10.3390/bdcc9050125.
[10] Haba, H., Hassan, Z., & Dastane, D.O. (2017). Factors leading to consumer perceived value of smartphones and its impact on purchase intention. *Global Business and Management Research: An International Journal,* 9(1), 42-71.
[11] Hailat, K.Q., Alsmadi, S., Al-Abdi, Y.F., & Galib, M.H. (2025). Assessment of consumer preferences for mobile phones among university students. *Journal of Lifestyle and SDGs Review,* 5(3), article number e05898. doi: 10.47172/2965-730X.SDGsReview.v5.n03.pe05898.
[12] Hoffmann, S., & Akbar, P. (2023). *Consumer behavior: Understanding consumers-designing marketing activities*. Wiesbaden: Springer. doi: 10.1007/978-3-658-39476-9.
[13] Horani, L.F., & Dong, L. (2023). Understanding sustainable purchase intention of smartphone users interface: Evidence from China. *Frontiers in Psychology,* 14, article number 1122801. doi: 10.3389/fpsyg.2023.1122801.
[14] Huang, C.-H., & Wu, J.-L. (2020). *Multi-task deep CNN model for no-reference image quality assessment on smartphone camera photos*. doi: 10.48550/arXiv.2008.11961.
[15] Kayakuş, M., Açikgöz, F.Y., Dinca, M.N., & Kabas, O. (2024). Sustainable brand reputation: Evaluation of iPhone customer reviews with machine learning and sentiment analysis. *Sustainability*, 16(14), article number 6121. doi: 10.3390/su16146121.
[16] Marchuk, N., Osiievska, V., & Mykhailova, H. (2021). Classification of wearable electronic devices. *International Scientific-Practical Journal Commodities and Markets,* 4, 68-78. doi: 10.31617/tr.knute.2021(40)07.
[17] Moutinho, L., Bigné, E., & Manrai, A.K. (2014). *The Routledge companion to the future of marketing*. Oxon: Routledge.
[18] Nasirinejad, M., & Sampalli, S. (2023). Evaluating consumer behavior, decision making, risks, and challenges for buying an IoT product. *IoT*, 4(2), 78-94. doi: 10.3390/iot4020005.
[19] Pellegrino, A. (2024). *Decoding digital consumer behavior: Bridging theory and practice*. Singapore: Springer. doi: 10.1007/978-981-97-3454-2.
[20] Petrov, K., & Kobzev, I. (2022). Method for determining the preference of consumer characteristics of a product based on information about its choice by the buyer. *Control, Navigation, and Communication Systems,* 2(68), 68-74. doi: 10.26906/SUNZ.2022.2.068.
[21] Phillips, J.B., & Eliasson, H. (2017). *Camera image quality benchmarking*. Hoboken: John Wiley & Sons. doi: 10.1002/9781119054504.
[22] Rai, B., Dahal, R.K., & Ghimire, B. (2023). Factors affecting consumer behavior in smartphone purchases in Nepal. *Innovative Marketing,* 19(3), 74-84. doi: 10.21511/im.19(3).2023.07.
[23] Romaniuk, N.V. (2026). Digital tools for marketing compliance in the system for identifying and preventing the counterfeiting of goods and services. *Current Issues in Economic Sciences*. doi: 10.5281/zenodo.19685529.
[24] Samsung. (n.d.a). *Galaxy A26 5G*. Retrieved from https://www.samsung.com/us/smartphones/galaxy-a26-5g/.
[25] Samsung. (n.d.b). *Galaxy S25 Ultra*. Retrieved from https://www.samsung.com/us/smartphones/galaxy-s25-ultra/.
[26] Shin, D.-H., & Choo, H. (2012). Exploring cross-cultural value structures with smartphones. *Journal of Global Information Management,* 20(2), 67-93. doi: 10.4018/jgim.2012040104.
[27] Soudachanh, S., & Salhofer, S. (2025). Unveiling environmental potential in smartphone repair practices in Vientiane Capital, Laos. *Sustainability*, 17(2), article number 711. doi: 10.3390/su17020711.
[28] Tsyhanenko, O., Zubko, K., & Vesperis, S. (2023). The impact of the consequences of transformation of consumer behavior in the conditions of economic instability on internet trade. *Problems of Modern Transformations. Series: Economics and Management,* 7. doi: 10.54929/2786-5738-2023-7-03-01.
[29] Vasiuta, V., Puzak, V., & Lashko, I. (2022). Main trends in the development of modern commodity science. *Galician Economic Journal*, 74(1), 152-157. doi: 10.33108/galicianvisnyk_tntu2022.01.152.
[30] Voloshyn, R., & Muravka, P. (2025). Commodity science foundations of online trade. *The Institute of Accounting, Control and Analysis in the Globalization Circumstances,* 3-4, 32-41. doi: 10.35774/ibo2024.03-04.032.
[31] Xiaomi. (n.d.). *Redmi Note 14 Pro 5G*. Retrieved from https://www.mi.com/global/product/redmi-note-14-pro-5g/.
[32] Zaitseva, O., Shuklina, V., & Karmazinova, V. (2024). Development of digital trading platforms in B2C and C2C markets. *Commodity science. Technologies. Engineering,* 51(3), 24-39. doi: 10.31617/2.2024(51)02.
[33] Zhu, W., Zhai, G., Han, Z., Min, X., Wang, T., Zhang, Z., & Yangand, X. (2020). A multiple attributes image quality database for smartphone camera photo quality assessment. In *2020 IEEE international conference on image processing* (pp. 2990-2994). Abu Dhabi: IEEE. doi: 10.1109/ICIP40778.2020.9191104.

Порівняльний аналіз характеристик смартфонів у різних цінових сегментах

Фіснік Бровіна
Доктор наук з менеджменту, доцент
Спортивний університет Тирани
1001, вул. Мухамета Джоллеша, м. Тирана, Албанія
https://orcid.org/0000-0002-4347-5538

Анотація. Метою дослідження було провести порівняльну оцінку смартфонів різних цінових сегментів – з точки зору їх технічних, експлуатаційних, економічних та інформаційних характеристик. Методологія дослідження базувалася на порівняльному товарознавчому аналізі, встановлюючи критерії оцінки та використовуючи як підхід зваженої оцінки, так і перевірку відповідності між офіційними характеристиками та технічними даними виробника. Для аналізу було обрано чотири моделі смартфонів, що представляють бюджетний, середній, преміальний та флагманський цінові сегменти. Порівняльна оцінка показала, що Samsung Galaxy S25 Ultra досяг найвищого інтегрованого балу якості (4,80 бала), тоді як Xiaomi Redmi Note 14 Pro 5G продемонстрував найвигідніший баланс між технічними характеристиками та ринковою ціною (4,55 бала). Apple iPhone 16 підтвердив важливість оптимізації програмного забезпечення, інтеграції екосистеми та довгострокової підтримки програмного забезпечення для споживчої цінності преміальних пристроїв, тоді як Samsung Galaxy A26 5G забезпечив адекватну функціональність для щоденного використання як найекономічніша модель. Аналіз показує, що вищі ціни на смартфони не обов'язково супроводжуються покращенням технічних характеристик цих пристроїв. Відмінності між телефонами в кожному ціновому сегменті найбільш безпосередньо пов'язані з продуктивністю процесора пристроїв, можливостями обробки зображень камер, дизайном та конструкцією пристроїв, а також програмним забезпеченням, доступним для підтримки цих смартфонів. Кожна з технічних специфікацій для кожного зі смартфонів була перевірена на відповідність тим, що опубліковані виробниками пристроїв. Практичне значення дослідження полягає в застосовності запропонованих критеріїв оцінки та комплексної методології оцінки для товарної експертизи смартфонів, розробки рекомендацій для споживачів та вибору моделей смартфонів відповідно до цінового сегмента та вимог користувача

Ключові слова: споживчі властивості; інтегрований індекс якості; технічні характеристики; програмна підтримка; споживча цінність

COMMODITY BULLETIN
Journal homepage: https://c-bulletin.com.ua/en
DOI: 10.62763/cb/1.2026.29

Article's History: Received: 09.02.2026 Revised: 04.05.2026 Accepted: 28.05.2026 Published: 29.05.2026

ISSN 2310-5283; e-ISSN 3041-1432 Vol. 19, No. 1, 2026, 29-43

UDC 663.6:614.777

Assessment of mineral water quality and compliance with safety standards: Comparative market analysis

Ermir Shahini*
Doctor of Economic Sciences, Associate Professor
Alexander Moisiu University of Durres
2001, 1 Currila Str., Durres, Albania
https://orcid.org/0000-0002-0083-1029

Abstract. The study aimed to conduct a comprehensive investigation into the organoleptic, physicochemical, chemical, and microbiological characteristics of mineral waters of various origins that are available in the Ukrainian retail market. Six brands were examined to determine their organoleptic properties, pH level, electrical conductivity, mineralisation, and the presence of major cations, anions, toxic contaminants, organic substances and sanitary indicator microorganisms. The results showed that all the examined samples were clear, free from sediment, suspended particles, and foreign matter, and had colour values ranging from 0.7 to 2.3 degrees on the platinum-cobalt scale. Scores for taste ranged from 4.2 to 4.8 points, with the differences attributable to the natural mineral composition rather than extraneous flavours. The pH values ranged from 6.29 to 7.19 and the electrical conductivity from 0.29 to 18.9 millisiemens per centimetre. Fiuggi had the lowest mineralisation, at 0.19 ± 0.01 g/L, and Donat Mg had the highest, at 13.1 ± 0.14 g/L. A low-mineralised calcium-bicarbonate profile was the characteristic feature of Morshynska and Karpatska Dzherelna. Polyana Kvasova and Luzhanska predominated in sodium and bicarbonates, respectively, whereas Donat Mg was distinguished by its high magnesium concentration of 1,010 ± 42 mg/L, high sulphate concentration of 2,200 ± 103 mg/L, and high bicarbonate concentration of 7,595 ± 290 mg/L. The absolute ion-balance value did not exceed 1.4%. The maximum nitrate content was 2.4 ± 0.3 milligrams per cubic decimetre. This was 20.8 times below the permissible level. The presence of lead, arsenic and total organic carbon was below the relevant hygiene limits, and no microbial indicators of sanitation were detected. This approach could be used to control packaged products in laboratories, verify labelling accuracy and develop evidence-based recommendations for consumers

Keywords: ionic composition; bicarbonates; sodium; toxic contaminants; labelling; consumer choice

Introduction

In the food market, packaged natural mineral waters are in a class of their own. This is because they do two things at once: they provide hydration and they have a mineral composition that occurs naturally. The consumer properties of these waters are determined by more than just clarity, taste or degree of carbonation. The concentrations of macro- and microelements, the stability of their bicarbonate, sulphate, calcium, magnesium or sodium profiles, and the absence of chemical and microbiological contamination are also important. As a result, mineral water quality assessment cannot be limited to determining a single mineralisation parameter or to a subjective evaluation of taste. A full comparison of the organoleptic characteristics, physicochemical composition, safety indicators and labelling information is needed. The need for a comprehensive assessment of the natural mineral waters available in the Ukrainian retail market is what makes this study

Suggested Citation:
Shahini, E. (2026). Assessment of mineral water quality and compliance with safety standards: Comparative market analysis. *Commodity Bulletin*, 19(1), 29-43. doi: 10.62763/cb/1.2026.43.

*Corresponding author (ermirshahini3@gmail.com)

relevant. This assessment must take into account the mineral profiles, safety indicators and the conformity of their labelling with their actual composition.

Ukraine is particularly interested in this assessment because of the variety of its natural resources, geochemical conditions and commercial water types. A. Kysylevska *et al.* (2024) analysed regulatory requirements for natural mineral and spring waters. These were intended for the preparation of infant food. They substantiated the need to monitor mineralisation. They also monitored nitrates, nitrites, fluorides, microbiological indicators and labelling. The authors demonstrated that the natural origin of water does not eliminate the need to verify its safety. They also demonstrated that the natural origin of water does not eliminate the need to verify the accuracy of its declared composition. S. Shulyak *et al.* (2021) also confirmed the importance of regularly monitoring water products in Ukraine by examining 23 drinking water quality and safety indicators in different regions of the country. The authors identified regional differences in the concentrations of certain trace elements and metals. These were associated with the biogeochemical characteristics of the territories concerned and the condition of water mains and water-supply sources. O. Krykhovets *et al.* (2025) also identified seasonal variability in nitrate concentrations, total hardness, calcium and magnesium during the monitoring of spring waters in the Lviv region. These findings confirm the importance of analysing several production batches of the same brand, rather than a single bottle.

The mineral composition of packaged water is important from both technological and practical consumer choice perspectives. S.J. Stoots *et al.* (2020) compared 182 brands of still bottled water from ten European countries and found significant variation in calcium, magnesium, sodium, potassium, bicarbonate and sulphate concentrations. They showed that waters with similar market positioning can have very different mineral profiles. Therefore, low or high mineralisation cannot be considered an independent indicator of superior quality; its significance depends on the proportions of individual ions, the intended use of the water, and the specific conditions under which it is consumed. Studies comparing different national markets have shown that the actual composition of water does not always correspond to the information provided on the label. M. Mitku & L. Endeshaw (2022) examined the main pHysicochemical properties of packaged mineral waters in Ethiopia, identifying minor discrepancies between some laboratory-measured properties and the labelling information. K. Ketrouci *et al.* (2023) classified 30 water brands available on the Algerian market using a range of physicochemical indicators. They demonstrated that an objective brand comparison should be based on a combination of hydrochemical parameters rather than a single total dissolved solids measure or declared water type.

Another area of assessment is the microbiological and toxicological safety of packaged water. Some samples of packaged water failed to comply with bacteriological requirements and exceeded permissible chromium and cadmium levels, according to the analysis by R.K. Banda *et al.* (2021) of 18 brands. These results showed that sealed packaging and a product's commercial origin do not automatically guarantee compliance with regulatory standards. The microbiological compliance of bottled water was found to be associated with the type of retail outlet, according to J.L. Maselela *et al.* (2024). Samples purchased from informal retail outlets were more likely to fail to meet the requirements for coliform bacteria and Escherichia coli. This highlights the necessity to regulate not only the manufacturing process but also the storage and distribution of products. The absence of sanitary indicator microorganisms in bottled water does not equate to the complete absence of a microbial component, as demonstrated by in-depth studies of the microbiological quality of bottled water. D.M. Boas *et al.* (2024) reviewed data on the microbial ecology of packaged water, establishing that microbial diversity is influenced by the water source, bottling technology, packaging material, storage temperature, and storage duration. Meanwhile, M.M. Kwikima (2025) detected coliform bacteria in 42% of 12 water brands purchased from retail outlets in Tanzania and found that the recommended fluoride level was exceeded in some samples. These results confirmed the need for comparative research into mineral waters to cover both stable physicochemical properties and indicators sensitive to production, packaging, storage, and distribution practices.

The focus of most existing publications has been on individual aspects of chemical or microbiological control. In contrast, the comparison of waters belonging to different categories within a single analytical model has not been given sufficient attention. This study aimed to assess the quality of packaged natural mineral waters available on the Ukrainian market and determine their compliance with safety and labelling requirements. To this end, the following objectives were set: determining the organoleptic and principal physicochemical properties of the waters under investigation, assessing their ionic composition and chemical and microbiological safety, comparing the actual values with the information provided on the labels, and developing a category-specific consumer assessment of the examined brands.

Materials and Methods

The study was conducted as a comparative laboratory and analytical assessment. This was of packaged natural mineral waters. These were available in the Ukrainian retail market. The Ukrainian market segment was defined in terms of the products available through national retail chains, pharmacies or specialised Ukrainian online catalogues, regardless of their country of origin.

The regulatory assessment was conducted in accordance with the following standards: DSTU 878-93 (1993) and the hygiene requirements for the production and circulation of natural mineral and spring waters (Order of the Ministry of Health of Ukraine No. 741, 2021) must be followed, as well as the hygiene standard entitled Safety Parameters for Natural Mineral Water (Decree of the Ministry of Health of Ukraine No. 4, 2010). The assessment covered organoleptic properties, physicochemical composition, chemical and microbiological safety indicators, the completeness of labelling, and the conformity of the actual composition with the information declared by the manufacturer.

Table 1 shows the six brands of natural mineral water that were included in the study, with two brands in each category. The selection criteria were as follows: availability for sale in at least two national retail or pharmacy chains; intact original packaging; complete labelling in Ukrainian; and an indication of the water type, mineralisation, principal ionic composition, manufacturer, batch number and expiry date. The study excluded flavoured waters and beverages containing sweeteners, extracts, vitamins or other added ingredients.

Table 1. *Mineral water brands included in the study*

Category	Brand	Declared type	Country of origin	Form of sale
Table water	Morshynska	Natural mineral table water	Ukraine	Highly carbonated
	Karpatska Dzherelna	Natural calcium-bicarbonate mineral table water	Ukraine	Highly carbonated
Medicinal table water	Polyana Kvasova	Natural sodium-bicarbonate boric medicinal table water	Ukraine	Highly carbonated
	Luzhanska	Natural sodium-bicarbonate boric medicinal table water	Ukraine	Highly carbonated
Medicinal water	Donat Mg	Natural sodium-magnesium sulphate-bicarbonate medicinal water	Slovenia	Carbonated
	Fiuggi	Natural oligomineral medicinal water	Italy	Still

Source: *compiled by the author*

Between March and May 2026, samples were collected from retail chains and pharmacies in Kyiv. Three production batches, each with a different batch number or bottling date, were selected for each brand. Three hermetically sealed 0.5 litre bottles were purchased from each batch. The total sample comprised 54 bottles: 18 production batches, with three bottles from each. The first bottle from each batch was used for organoleptic and basic physicochemical analysis. The second was used to determine the principal ionic composition and toxic contaminants. The third was used for microbiological examination and confirmatory measurements. In accordance with the manufacturers' recommendations, the samples were stored upright, away from direct sunlight and at a temperature of 5-20°C before analysis. To ensure a blind assessment, the samples were assigned codes with no indication of the brand: C1-C6 for table waters, MT1-MT6 for medicinal table waters, and M1-M6 for medicinal waters.

Before opening, the integrity of the cap, the tamper-evident ring, the label and the container were checked. Samples showing signs of leakage, deformation, or loss of seal integrity were excluded. Prior to testing, the bottles were maintained at a temperature of 20 ± 2°C for at least two hours. Samples intended for determining pH, electrical conductivity and organoleptic characteristics were analysed immediately after opening. Aliquots intended for metal determination were preserved with nitric acid. The pH was below 2. Samples intended for ion chromatography were not acidified. Microbiological testing commenced no later than six hours after opening the containers.

Clarity, sediment and suspended particle content, colour, odour and taste were determined at a temperature of 20 ± 2°C in a room free from extraneous odours. A colourless glass cylinder was used to hold 100 mL of water, which was then inspected visually. The water was assessed against white and black backgrounds. The colour was determined using the platinum-cobalt scale on a DR6000 spectrophotometer (Hach, USA). This was done in accordance with ISO 7887:2025 (2025). The results were expressed in degrees of colour, with a value not exceeding 20 degrees being considered acceptable in accordance with the technical requirements for packaged mineral waters.

Odour and taste were assessed by five panellists, aged between 22 and 55 years, who had received prior instruction. Food, coffee, alcohol, tobacco products or strongly flavoured products had not been consumed by the participants for one hour before the assessment. Each participant was presented with 10 mL of coded water. The samples were not swallowed. The mouth was rinsed with deionised water between assessments. Odour intensity was assessed on a scale from 0 to 5, where 0 indicated an odourless sample and 5 indicated an uncharacteristically strong odour. Taste was assessed on a five-point scale: Five points indicated a clean, harmonious taste characteristic of the relevant type of water, whereas zero points indicated an unacceptable or extraneous taste. The mean of the individual scores was used to calculate the final organoleptic score.

The following things were measured: pH, electrical conductivity, total mineralisation, dry residue, concentrations of the main cations and anions, and specific components declared on the label. The pH was determined potentiometrically immediately after opening the bottle using a SevenExcellence S470 pH/conductivity meter equipped with an InLab Expert Pro-ISM

electrode (Mettler Toledo, Switzerland) and calibrated with pH 4, 7 and 10 buffer solutions. This method was carried out in accordance with ISO 10523:2022 (2022). Specific electrical conductivity was determined at 25°C using the same instrument and an InLab 731-ISM electrode (Mettler Toledo, Switzerland), in accordance with DSTU EN 27888:2022 (2022). The mass of the dry residue obtained after evaporating a known volume of water and drying it at 180°C to constant mass was used to determine total mineralisation gravimetrically. Weighing was performed using Cubis II MCA225S-2S00-0 analytical balances (Sartorius, Germany) and drying was carried out in an ED 115 drying oven (Binder, Germany).

The determination of sodium, potassium, calcium, magnesium, iron, manganese, lithium, strontium and barium was carried out using a 5800 ICP-OES instrument (Agilent Technologies, USA), in accordance with the ISO 11885:2019 (2019) standard. The analysis was performed using inductively coupled plasma optical emission spectrometry. The concentrations of arsenic, lead, cadmium, chromium, nickel and other trace elements were determined using a 7900 ICP-MS instrument (Agilent Technologies, USA) and inductively coupled plasma mass spectrometry, in accordance with ISO 17294-2:2019 (2019).

Bicarbonates and carbonates were determined by acid-base titration using a standardised hydrochloric acid solution with endpoints at pH 8.3 and 4.5, with a 905 Titrando automatic titrator (Metrohm, Switzerland) being employed for this purpose. Chlorides, sulphates, nitrates, nitrites, fluorides and phosphates were analysed using ion chromatography with a Dionex ICS-6000 system (Thermo Fisher Scientific, USA) in accordance with ISO 10304-1:2025 (2025). The presence of boron compounds, metasilicic acid and other components specified by the manufacturer was monitored in waters with a declared specific composition. The ion balance was calculated using formula (1):

$$IB=\frac{\Sigma C-\Sigma A}{\Sigma C+\Sigma A}\times 100\%, \quad (1)$$

where ∑C – the sum of the concentrations of the principal cations in milliequivalents per dm^3; ∑A – sum of the concentrations of the principal anions in milliequivalents per dm^3. A result was considered acceptable when the absolute ion-balance value did not exceed 5%.

Table 2 shows the chemical safety indicators included in the analysis. These were nitrates, nitrites, fluorides, arsenic, lead, cadmium, mercury, chromium, nickel, copper, zinc, manganese, barium, strontium and organic matter, expressed as total organic carbon. The presence of nitrates, nitrites, fluorides, chlorides and sulphates was determined by measuring the relevant ions using a Dionex ICS-6000 ion chromatograph. Meanwhile, the instruments 5800 ICP-OES and 7900 ICP-MS were used to measure the levels of metals. Mercury was determined by direct thermal decomposition with atomic absorption detection using a DMA-80 evo analyser (Milestone Srl, Italy). The total organic carbon was measured using a TOC-L CPH analyser (Shimadzu, Japan), which is a high-temperature catalytic oxidation instrument. This method is in accordance with the DSTU EN 1484:2003 (2003) standard. A further screening procedure was carried out for the presence of potential man-made contaminants. This procedure involved the analysis of pHenols, petroleum hydrocarbons, pesticides and polycyclic aromatic hydrocarbons. The analysis was performed using a gas chromatography with mass-spectrometric detection system (8890 GC/5977B MSD, Agilent Technologies, USA). The procedure involved the use of a solid-phase extraction step.

Table 2. *Principal chemical safety criteria for natural mineral waters*

Parameter	Maximum permissible concentration
Nitrates, NO_3^-	Not more than 50 mg/dm^3
Nitrites, NO_2^-	Not more than 0.1 mg/dm^3
Arsenic	Not more than 0.01 mg/dm^3
Lead	Not more than 0.01 mg/dm^3
Cadmium	Not more than 0.003 mg/dm^3
Mercury	Not more than 0.001 mg/dm^3
Chromium	Not more than 0.05 mg/dm^3
Nickel	Not more than 0.02 mg/dm^3
Copper	Not more than 1 mg/dm^3
Zinc	Not more than 1 mg/dm^3
Barium	Not more than 0.7 mg/dm^3
Fluorides	Not more than 1.5 mg/dm^3
Organic matter expressed as carbon	Not more than 5 mg/dm^3

Source: *compiled by the author in accordance with the Decree of the Ministry of Health of Ukraine No. 4 (2010)*

Microbiological testing was performed using a Combisart system (Sartorius, Germany) and 0.45 μm pore diameter membrane filters, via membrane filtration. Total microbial count was determined by inoculation onto nutrient agar, followed by incubation at 37°C for 24 hours, then at 20-22°C for 72 hours in an IN110 incubator (Memmert, Germany), in accordance with ISO 6222:2002 (2002). The presence of total coliform

bacteria and *Escherichia coli* was determined in 250 mL of water in accordance with ISO 9308-1:2022 (2022). The presence of *Pseudomonas aeruginosa* was identified in accordance with ISO 16266:2022 (2022), and intestinal enterococci were detected in accordance with ISO 7899-2:2022 (2022). The absence of sulphite-reducing anaerobic bacteria in 50 mL of water was also monitored. Compliance criteria were as follows: a total microbial count of no more than 20 colony-forming units (CFU)/cm^3 at 37°C, and no more than 100 CFU/cm^3 at 20-22°C; and the absence of coliform bacteria, *E. coli, P. aeruginosa*, and intestinal enterococci in 250 mL of water.

Prior to opening the bottles, comprehensive photography was taken of the labels from every angle. The assessment included the presence of the name and category of the water, the degree of carbonation, the country of origin, the manufacturer or importer, the source or borehole number, the bottling location, the nominal volume, the batch number, the bottling date, the expiry date, the storage conditions, the total mineralisation, the principal ionic composition, and information concerning treatment or additional carbonation with carbon dioxide.

Conformity of the actual composition with the information provided on the label was assessed for total mineralisation, as well as for sodium, potassium, calcium, magnesium, bicarbonates, chlorides, sulphates, fluorides and boron. Other declared components were also assessed. Where a range was provided by the manufacturer, the result was considered compliant if the actual concentration fell within that interval when measurement uncertainty was taken into account. Relative deviation was calculated using formula (2):

$$\Delta = \frac{C_{fact} - C_{label}}{C_{label}} \times 100\%, \quad (2)$$

where C_{actual} – the mean actual concentration of the component in the three production batches; C_{label} – declared value or the midpoint of the declared interval.

The classification of each brand according to its compliance with quality and safety criteria was determined by means of a composite assessment. The assessment covered five areas: how easily the product could be used, its physical and chemical composition, its safety, including microbiological safety, and how accurately it was labelled. A brand is said to demonstrate a high level of compliance if the following criteria are all met at the same time: there is no extraneous odour, unacceptable taste, sediment or visible foreign matter; the actual mineralisation and principal ionic composition are within the ranges declared by the manufacturer; the absolute ion-balance value is not more than 5%; the hygiene limits for toxic elements, nitrates, nitrites or organic contaminants are not exceeded; there are no sanitary indicator microorganisms; and the total microbial count complies with the established limits. The label must also include the principal information concerning the type of water, mineralisation, ionic composition, manufacturer, batch, expiry date and storage conditions. Where minor labelling inconsistencies or organoleptic deviations were identified, provided there was no failure to meet safety parameters, the brand was classified as demonstrating an acceptable level of compliance. Any exceedance of a chemical or microbiological limit was grounds for classification as non-compliant, regardless of other parameters. Comparisons were made using a profile-based approach and no single overall ranking was established among waters with different mineral compositions and functional purposes. Each physicochemical determination was performed in a minimum of two technical replicates. Each analytical series included blank samples, duplicates, certified standard solutions, control samples, and samples spiked with a known concentration of the analyte.

The results were deemed acceptable if the coefficient of variation for parallel determinations was less than 10%, the analyte recovery fell within the range of 80% to 120%, and the limit of quantification for toxic contaminants was less than 10% of the corresponding hygiene limit. The statistical analysis was carried out using two software programmes: Microsoft Excel and IBM SPSS Statistics (USA). This involved calculating various statistical values, including the mean, standard deviation, median, minimum, maximum and 95% confidence interval. Inter-batch variability was assessed descriptively. No statistical inferences concerning the entire Ukrainian market were made.

Results

Comprehensive characterisation of the organoleptic and physicochemical parameters of the examined waters

Visual inspection of all 54 selected bottles revealed no loss of seal integrity, container deformation, signs of leakage, foreign contamination or damage to the tamper-evident rings. The labels remained legible and the actual product volume corresponded to the declared nominal volume of 0.5 L, providing grounds for including all 18 production batches in the subsequent analysis. The colour values obtained were then interpreted in line with the technical requirements for packaged mineral waters and the photometric method for determining colour using the platinum-cobalt scale. This confirmed that all samples complied with the relevant organoleptic criteria. All the samples were found to be clear and free from sediment, flakes, visible suspended particles and oily films, as shown by organoleptic testing. The colour values were in the range of 0.7 to 2.3 degrees on the platinum-cobalt scale, which is significantly below the permitted limit of 20 degrees set for packaged mineral waters (Table 3). The lowest colour values were recorded for Fiuggi and Morshynska. The highest was recorded for Donat Mg. Nevertheless, all the waters remained visually colourless.

Table 3. *Organoleptic characteristics of the examined mineral waters (M ± SD) (n = 3)*

Brand	Clarity and sediment	Colour, degrees	Odour intensity, points	Taste score, points
Morshynska	Clear, no sediment	0.8 ± 0.2	0.2 ±0.1	4.8 ± 0.1
Karpatska Dzherelna	Clear, no sediment	1.1 ± 0.2	0.3 ±0.1	4.7 ± 0.2
Polyana Kvasova	Clear, no sediment	1.7 ± 0.3	1.2 ±0.2	4.4 ± 0.2
Luzhanska	Clear, no sediment	1.5 ± 0.2	1 ± 0.2	4.5 ± 0.2
Donat Mg	Clear, no sediment	2.3 ± 0.3	1.7 ± 0.2	4.2 ± 0.2
Fiuggi	Clear, no sediment	0.7 ± 0.1	0.1 ± 0.1	4.8 ± 0.1

Note: *for odour intensity and taste scores, the mean score awarded by the five panellists was first calculated for each production batch, after which (M\pm SD) was determined for the three batches of each brand*
Source: *compiled by the author*

The table waters Morshynska and Karpatska Dzherelna achieved the highest sensory scores. They were described as having a neutral or mildly mineral taste, without any bitterness, metallic notes or mustiness. The declared composition of Polyana Kvasova and Luzhanska was confirmed by a moderately pronounced alkaline and bicarbonate taste. Donat Mg had the most distinctive taste and odour, which was attributable to its high concentrations of magnesium, sulphates and bicarbonates. While this reduced its organoleptic score in comparison with the table waters, it was not indicative of poorer quality. Fiuggi was characterised by a neutral taste and minimal odour intensity. All the samples examined accordingly met the organoleptic requirements for packaged natural mineral waters. The differences between the brands were found to be primarily determined by their natural degree of mineralisation and ionic composition, rather than by the presence of extraneous organoleptic properties. The pH and specific electrical conductivity were assessed in accordance with standardised potentiometric and conductometric methods, and mineralisation was interpreted in relation to the regulatory classification of packaged natural mineral waters. Analysis of total mineralisation and principal ionic composition revealed significant variations among the waters in terms of mineralisation, cation and anion proportions, and predominant hydrochemical profile. Fiuggi had the lowest mineralisation, at 0.19 ± 0.01 g/dm^3, while Donat Mg had the highest, at 13.1 ± 0.14 g/dm^3. The table waters had low levels of mineralisation: 0.28 ± 0.02 g/dm^3 for Morshynska, and 0.6 ± 0.04 g/dm^3 for Karpatska Dzherelna. Higher mineralisation values were recorded for the medicinal table waters: 4.75 ± 0.12 g/dm^3 for Luzhanska, and 8.5 ± 0.17 g/dm^3 for Polyana Kvasova (Table 4).

Table 4. *Principal pHysicochemical parameters of the waters examined, (M\pm SD), (n = 3) batches*

Brand	Mineralisation, g/dm^3	Declared range, g/dm^3	pH	Electrical conductivity, mS/cm	Ion balance, %
Morshynska	0.28 ± 0.02	0.1-0.4	6.36 ± 0.08	0.43 ± 0.02	+1
Karpatska Dzherelna	0.6 ± 0.04	0.3-0.8	6.47 ± 0.07	0.86 ± 0.03	-1.4
Polyana Kvasova	8.5 ± 0.17	6.5-12	6.29 ± 0.06	12.2 ± 0.24	+1.4
Luzhanska	4.75 ± 0.12	3-5	6.38 ± 0.05	6.9 ± 0.16	-0.8
Donat Mg	13.1 ± 0.14	12.8-13.5	6.59 ± 0.06	18.9 ± 0.32	+0.7
Fiuggi	0.19 ± 0.01	0.15-0.2	7.19 ± 0.05	0.29 ± 0.01	-0.5

Note: *ion balance was calculated from the sum of the principal cations and anions, including potassium*
Source: *compiled by the author*

The pH values of all the waters examined ranged from 6.29 to 7.19. The highest concentration of dissolved mineral substances was found in Donat Mg, which also had the highest specific electrical conductivity. The lowest conductivity values were recorded for Fiuggi and Morshynska waters. All actual total mineralisation values fell within the ranges declared by the manufacturers. A more detailed characterisation of the mineral profiles was achieved by measuring the concentrations of the principal cations and anions. These contribute to total mineralisation, affect the taste properties of the water and determine its functional profile. This analysis included sodium, potassium, calcium, magnesium, bicarbonates, sulphates and chlorides. Determining the principal cations and anions not only characterised the hydrochemical profile, but also verified the analytical consistency of the results by calculating the ion balance. The methodological basis comprised established procedures for determining the composition of natural waters in terms of metals, trace elements and anions. The results are presented in Table 5.

Table 5. *Concentrations of principal ions in the mineral waters examined, mg/dm^3, (M\pm SD), (n = 3) batches*

Brand	Na^+	K^+	Ca^{2+}	Mg^{2+}	HCO_3^-	SO_4^{2-}	Cl^-
Morshynska	5.7 ± 0.4	1.6 ± 0.1	43.1 ± 2.2	8.6 ± 0.7	152 ± 9	19 ± 2	7 ± 1
Karpatska Dzherelna	18.4 ± 1.1	2.8 ± 0.2	90.5 ± 4.1	24.8 ± 1.5	380 ± 18	46 ± 4	16 ± 2
Polyana Kvasova	2,180 ± 96	15 ± 1	98 ± 6	62 ± 4	5,595 ± 230	210 ± 16	220 ± 17
Luzhanska	1,050 ± 58	12 ± 1	120 ± 7	70±5	3,125 ± 155	155 ± 12	150 ± 11

Table 5. Continued

Brand	Na^+	K^+	Ca^{2+}	Mg^{2+}	HCO_3^-	SO_4^{2-}	Cl^-
Donat Mg	1,680 ± 75	40 ± 3	350 ± 15	1,010±42	7,595 ± 290	2,200 ± 103	70 ± 6
Fiuggi	6.2 ± 0.5	1 ± 0.1	32.8 ± 2	4.9±0.4	115 ± 7	14 ± 1	6.5 ± 0.6

Source: *compiled by the author*

Morshynska had a low mineral content and a calcium-bicarbonate profile, with minimal sodium. The greater mineralisation and more pronounced mineral taste of Karpatska Dzherelna can be attributed to its higher concentrations of calcium, magnesium and bicarbonates. Bicarbonates and sodium predominated in Polyana Kvasova and Luzhanska. Among the Ukrainian samples, Polyana Kvasova had the highest sodium concentration, at 2,180 ± 96 mg/dm³, as well as the highest bicarbonate concentration, at 5,595 ± 230 mg/dm³. Luzhanska had a comparable bicarbonate-sodium profile, but it was distinguished by lower sodium and bicarbonate concentrations, along with a lower level of total mineralisation. The concentrations of boron compounds in these waters corresponded to the figures provided by the manufacturers. The mineral profile of Donat Mg was the most concentrated, with magnesium levels of 1,010 ± 42 mg/dm³, sulphate levels of 2,200 ± 103 mg/dm³ and bicarbonate levels of 7,595 ± 290 mg/dm³. The magnesium concentration in Donat Mg was over 14 times higher than in Luzhanska, and over 100 times higher than in Morshynska. The mineralisation levels at Fiuggi were found to be low, and the calcium-bicarbonate profile showed low concentrations of sodium, magnesium, sulphates and chlorides. Therefore, it would be wrong to regard the waters examined as interchangeable solely on the basis of their general compliance with safety standards. The selection of these materials should be based not only on the absence of hazardous contaminants, but also on factors such as the degree of mineralisation, the predominant ionic composition, the degree of carbonation, and the intended consumption pattern.

Assessment of safety, labelling compliance and the consumer profiles of the brands examined

The measured concentrations were then compared with the relevant limit values set out in the hygiene standard for the safety of natural mineral water. This was done by taking into account the methods used to determine toxic elements, anions and total organic carbon. The methods used for analysis were not able to detect any nitrites, cadmium or mercury in any of the production batches that were examined. The concentrations of nitrates, lead, arsenic, chromium, nickel, copper, zinc, manganese, barium and fluorides did not exceed the established hygiene limits. The highest nitrate concentration, 2.4 ± 0.3 mg/dm³, was found in Karpatska Dzherelna, which is 20.8 times lower than the maximum permissible level of 50 mg/dm³. Lead and arsenic concentrations did not exceed 0.0024 and 0.0027 mg/dm³, respectively. All the other elements and inorganic components monitored were also present. Their concentrations were below the relevant regulatory limits. These limits are shown in Table 6.

Table 6. *Safety indicators of the waters examined, (M \pm SD), (n = 3) batches*

Brand	NO_3^-, mg/dm³	Pb, mg/dm³	As, mg/dm³	Cr, mg/dm³	Ni, mg/dm³	Cu, mg/dm³	Zn, mg/dm³	Mn, mg/dm³	Ba, mg/dm³	F^-, mg/dm³	TOC, mg/dm³
Morshynska	1.8±0.2	0.0012±0.0002	0.0015±0.0003	0.004±0.001	0.003±0.001	0.018±0.003	0.041±0.006	0.012±0.002	0.041±0.005	0.18±0.02	0.42±0.05
Karpatska Dzherelna	2.4±0.3	0.0016±0.0002	0.0018±0.0002	0.005±0.001	0.004±0.001	0.021±0.004	0.048±0.007	0.015±0.003	0.056±0.006	0.22±0.03	0.55±0.06
Polyana Kvasova	0.6±0.1	0.0024±0.0003	0.0027±0.0003	0.007±0.001	0.005±0.001	0.024±0.004	0.052±0.008	0.019±0.003	0.118±0.011	0.62±0.05	0.26±0.04
Luzhanska	0.8±0.1	0.0019±0.0002	0.0022±0.0003	0.006±0.001	0.004±0.001	0.022±0.003	0.046±0.006	0.017±0.003	0.096±0.009	0.54±0.04	0.32±0.04
Donat Mg	0.3±0.1	0.0007±0.0001	0.0011±0.0002	0.003±0.001	0.002±0.001	0.015±0.002	0.037±0.005	0.009±0.002	0.082±0.008	0.31±0.03	0.18±0.03
Fiuggi	1.2±0.2	0.001±0.0002	0.0009±0.0001	0.003±0.001	0.003±0.001	0.016±0.003	0.034±0.005	0.01±0.002	0.038±0.004	0.12±0.02	0.31±0.04
Hygiene limit	⩽50	⩽0.01	⩽0.01	⩽0.05	⩽0.02	⩽1	⩽1	⩽0.5	⩽0.7	⩽1.5	⩽5

Note: *TOC denotes total organic carbon*
Source: *compiled by the author*

The lead concentration ranged from 0.0007 to 0.0024 mg/dm^3, and the arsenic concentration ranged from 0.0009 to 0.0027 mg/dm^3. Thus, neither concentration exceeded 27% of the maximum permissible level. The range of total organic carbon was from 0.18 ± 0.03 mg/dm^3 in Donat Mg to 0.55 ± 0.06 mg/dm^3 in Karpatska Dzherelna, and it was always less than the regulatory value of 5 mg/dm^3 in all the samples. The methods used were not able to detect concentrations of phenols, petroleum hydrocarbons, synthetic surfactants, pesticides and polycyclic aromatic hydrocarbons above the limits of quantification.Microbiological compliance was assessed on the basis of the total microbial count. It was also assessed on the basis of the absence of sanitary indicator microorganisms. These were specified for the control of packaged natural waters. Microbiological analysis detected no total coliform bacteria, *E. coli*, *P. aeruginosa*, intestinal enterococci or sulphite-reducing anaerobic bacteria in any of the examined samples. The total microbial count did not exceed the permissible levels (Table 7).

Table 7. *Results of the microbiological monitoring of the mineral waters examined*

Brand	Total microbial count at 20-22°C, CFU/cm^3	Total microbial count at 37°C, CFU/cm^3	Sanitary indicator microorganisms	Conclusion
Morshynska	4±1	1±1	Not detected	Compliant
Karpatska Dzherelna	6±2	1±1	Not detected	Compliant
Polyana Kvasova	3±1	1±1	Not detected	Compliant
Luzhanska	3±1	1±1	Not detected	Compliant
Donat Mg	1±1	<1	Not detected	Compliant
Fiuggi	2±1	<1	Not detected	Compliant
Regulatory limit	⩽100	⩽20	Absence in the specified sample volume	-

Note: *total microbial count refers to the total number of viable microorganisms detected under the specified incubation conditions*
Source: *compiled by the author*

At 20-22°C, the highest total microbial count was recorded for Karpatska Dzherelna at 6 ± 2 CFU/cm^3, which was 16.7 times below the regulatory limit. These results confirmed the microbiological stability of the examined samples and the absence of secondary bacterial contamination in the production batches included in the study. All the brands examined contained the principal labelling elements. These elements were required to identify the products. They were also required to compare the declared characteristics with the actual analytical results. The labels stated the product name, category and declared type of water. They also declared the country of origin, name of the manufacturer or importer, bottling location, source or borehole number, production batch number, bottling date, expiry date, storage conditions and nominal volume of the consumer packaging. The labels also provided information on the total mineralisation and principal components of the ionic composition for all samples, including sodium, calcium, magnesium, bicarbonates, sulphates and chlorides. Some brands also declared additional components such as potassium, fluorides and boron compounds, which are characteristic of the relevant type of water. This allowed for a comparison of the labelling information with the measured mineralisation and principal ion concentrations. The labels of the carbonated samples provided information on the degree of carbonation or the presence of carbon dioxide. Morshynska, Karpatska Dzherelna, Polyana Kvasova and Luzhanska were labelled as highly carbonated; Donat Mg as carbonated; and Fiuggi as still water. No other treatment methods were indicated on the labels, except for carbonation or additional enrichment with carbon dioxide where applicable. The declared profiles of medicinal table waters and medicinal waters were determined by additional specified components. The profile of Polyana Kvasova and Luzhanska was determined by a bicarbonate-sodium and boron composition, the profile of Donat Mg was determined by a magnesium-sulphate-bicarbonate composition, and the profile of Fiuggi was determined by a low-mineralised oligomineral composition. In general, the labelling of all the examined samples made it possible to trace the water's origin and bottling conditions, and to evaluate whether its actual composition corresponded to the characteristics declared by the manufacturer.

The actual mineralisation of all the waters examined fell within the ranges declared by the manufacturers, confirming compliance with the principal physicochemical characteristics required for packaged natural mineral waters. The mineralisation levels at Morshynska were found to be 0.28 ± 0.02 g/dm^3, which is significantly lower than the declared range of 0.1-0.4 g/dm^3. Similarly, the mineralisation levels at Karpatska Dzherelna were 0.6 ± 0.04 g/dm^3, which is also lower than the declared range of 0.3-0.8 g/dm^3. Furthermore, the mineralisation levels at Polyana Kvasova were 8.5 ± 0.17 g/dm^3, which is even lower than the declared range of 6.5-12 g/dm^3. The mineralisation levels at Luzhanska were found to be 4.75 ± 0.12 g/dm^3, which is also lower than the declared range of 3-5 g/dm^3. Finally, the mineralisation levels at Donat Mg were recorded as 13.1 ± 0.14 g/dm^3, compared with a declared range of 12.8-13.5 g/dm^3, and that of Fiug-

gi was 0.19 ± 0.01 g/dm^3, compared with a declared range of 0.15-0.2 g/dm^3. Thus, even when expanded measurement uncertainty was considered, none of the actual values fell outside the declared intervals. The greatest relative deviations from the midpoint of the declared range were recorded for Luzhanska (+18.8%) and Morshynska (+12%). However, these deviations did not indicate non-compliance, as the results remained within the declared ranges. The closest agreement between the actual and declared mineralisation was recorded for Donat Mg, with a deviation of -0.4% (Table 8).

Table 8. *Compliance of actual mineralisation with the declared values*

Brand	Declared range, g/dm^3	Actual mineralisation, g/dm^3	Expanded uncertainty, g/dm^3	Deviation from the midpoint of the range, %	Compliance
Morshynska	0.1 - 0.4	0.28 ± 0.02	± 0.02	+ 12	Compliant
Karpatska Dzherelna	0.3 - 0.8	0.6 ± 0.04	± 0.03	+ 9.1	Compliant
Polyana Kvasova	6.5 - 12	8.5 ± 0.17	± 0.18	- 8.1	Compliant
Luzhanska	3 - 5	4.75 ± 0.12	± 0.1	+ 18.8	Compliant
Donat Mg	12.8 - 13.5	13.1 ± 0.14	± 0.22	- 0.4	Compliant
Fiuggi	0.15 - 0.2	0.19 ± 0.01	± 0.01	+ 8.6	Compliant

Note: *expanded uncertainty is presented for the mean actual mineralisation using a coverage factor of (k = 2), corresponding to an approximate confidence level of 95%*
Source: *compiled by the author*

The actual concentrations of sodium, calcium, magnesium, bicarbonates, sulphates, chlorides, fluorides and specific components were compared with the information provided on the labels. The results showed that none of the concentrations fell outside the declared intervals. At the same time, it was established that presenting the composition of medicinal table waters and medicinal waters in the form of broad ranges is methodologically justified. This is because the mineralisation of natural water may vary between production batches. This variation is within the approved physicochemical characteristics of the source.

After conducting analyses related to organoleptic, physicochemical, chemical and microbiological characteristics, as well as labelling, it was determined that none of the brands under scrutiny surpassed the established hygiene limits or exhibited signs of microbiological non-compliance. All the samples had intact packaging, satisfactory organoleptic properties, were within the declared mineralisation range, and showed no evidence of chemical or microbiological contamination. However, establishing a single overall ranking was deemed inappropriate as the waters differed in terms of their intended purpose, degree of mineralisation and ionic composition rather than their level of safety. For instance, Donat Mg's pronounced magnesium-sulphate taste is a characteristic feature of its natural composition rather than a quality defect, and Fiuggi's low mineralisation does not automatically make it superior to medicinal table waters. The final assessment was therefore presented in a profile-based format. This format reflected the compliance of each brand with quality and safety criteria. It also reflected the specific considerations associated with its possible consumption (Table 9).

Table 9. *Comparative profile-based assessment of the quality and safety of the examined mineral waters*

Brand	Chemical and microbiological safety	Compliance of actual composition with labelling	Overall quality assessment	Consumption considerations
Morshynska	Compliant with chemical and microbiological criteria	Compliant	High compliance; low-mineralised calcium-bicarbonate water	Suitable for regular hydration, subject to individual tolerance of carbonated water
Karpatska Dzherelna	Compliant with chemical and microbiological criteria	Compliant	High compliance; moderately mineralised calcium-magnesium-bicarbonate water	Suitable for regular consumption in the absence of individual restrictions
Polyana Kvasova	Compliant with chemical and microbiological criteria	Compliant	High compliance; highly mineralised bicarbonate-sodium water	The consumption pattern should be aligned with the manufacturer's recommendations and individual tolerance
Luzhanska	Compliant with chemical and microbiological criteria	Compliant	High compliance; moderately mineralised bicarbonate-sodium water	Moderate consumption is advisable, taking into account its sodium and bicarbonate content
Donat Mg	Compliant with chemical and microbiological criteria	Compliant	High compliance; highly mineralised magnesium-sulphate-bicarbonate water	Should not be regarded as an unrestricted substitute for ordinary drinking water
Fiuggi	Compliant with chemical and microbiological criteria	Compliant	High compliance; low-mineralised still calcium-bicarbonate water	May be selected by individuals who prefer still water with low mineralisation

Source: *based on the Decree of the Ministry of Health of Ukraine No. 4 (2010), ISO 6222:2002 (2002), ISO 9308-1:2022 (2022), ISO 16266:2022 (2022), ISO 7899-2:2022 (2022)*

Thus, all of the examined brands demonstrated a high level of compliance with quality and safety criteria within the analysed production batches. The differences between them were not disqualifying, but rather profile-specific. Morshynska and Karpatska Dzherelna, two table waters, were the most suitable for regular hydration due to their low or moderate mineralisation. Polyana Kvasova and Luzhanska, on the other hand, had elevated concentrations of sodium and bicarbonates, so their consumption should be aligned with dietary and medical advice. Donat Mg stood out due to its high magnesium, sulphate and bicarbonate concentrations, which give it a distinctive taste and make it best consumed in moderation. Fiuggi was the least mineralised still water among the examined samples; however, its low mineralisation should not be considered a universal advantage over other types of water. The final assessment showed that consumer choice should be based on the suitability of the mineral profile for the intended purpose of consumption, provided there is no regulatory non-compliance.

Discussion

The results showed that the packaged mineral waters examined differed mainly in terms of their total mineralisation and the proportions of their main ions. However, all samples complied with the regulatory requirements for chemical and microbiological safety. When comparing waters of different natural origins and functional positioning, such differentiation is to be expected. N.R. Syed *et al.* (2025) analysed the physicochemical characteristics of packaged mineral waters. They demonstrated that pH, electrical conductivity, mineralisation, chlorides and arsenic are suitable indicators. These can be used to distinguish safe samples from those that may potentially be non-compliant. In the present study, all pH and electrical conductivity values, as well as all concentrations of toxic contaminants, remained within the relevant regulatory limits, confirming the stability of the examined production batches.

Differentiating the waters into calcium-bicarbonate, bicarbonate-sodium and magnesium-sulphate-bicarbonate profiles was consistent with the findings of J.D. Iyakare *et al.* (2022). These researchers examined bottled waters from the African Great Lakes region and found that the concentrations of the main ions reflected the geographical origin of the aquifers. They also decided on the classification of the waters into separate hydrochemical groups. The mineral profile of Donat Mg was the most evident in the present study, with high concentrations of magnesium, sulphates and bicarbonates. In contrast, Morshynska, Karpatska Dzherelna and Fiuggi were distinguished by low or moderate mineralisation and a prevalence of the calcium-bicarbonate component. L. Moreno-Merino *et al.* (2022) compared the chemical characteristics of natural mineral waters and groundwater. These were used for centralised water supply. A single parameter alone is not always enough to establish differences between such waters. The most informative approach is to combine profiles of pH, calcium, potassium, nitrates, silicon and the proportions of the principal ions. This backs up the all-encompassing strategy used in the current study, where mineralisation in general was not looked at in isolation from the cationic and anionic composition.

Comparing the actual mineralisation with the values stated on the labels revealed that none of the samples deviated from the ranges declared by the manufacturers. This indicated satisfactory stability in the chemical composition of the examined production batches, though it did not imply the absence of labelling risks across the entire market. T. Hadbi *et al.* (2022) analysed the labelling information of 56 bottled-water brands in Algeria. They demonstrated that multidimensional grouping was useful. This was based on the principal ions. It was useful for objectively comparing waters of different origins. The profile-based approach avoided formally ranking waters according to total mineralisation or taste characteristics alone. The significance of evaluating labelling was also corroborated by R. Aslani *et al.* (2024), who examined 30 brands of bottled drinking and mineral water in Iran in 2024. They found discrepancies between the labelling and the actual nitrate, nitrite, magnesium and sodium concentrations in some samples, although the calculated non-carcinogenic risks generally remained acceptable. Therefore, ensuring compliance with hygiene limits should not replace verifying that the actual composition corresponds to the information provided on the label. In the present study, this requirement was addressed. This was done by comparing mineralisation and the principal ion concentrations with the declared intervals.

The findings of E.L. Ungureanu *et al.* (2022), who assessed potentially toxic elements in waters available on the Romanian market in 2022, were consistent with the results of the samples examined, which showed no exceedances for lead, arsenic, cadmium, mercury, nitrates and nitrites. The authors emphasised that risk assessment should consider more than just the detection of an element – its concentration, the duration of potential exposure and the vulnerability of particular population groups should also be considered. A similar approach was adopted by J.O. Olowoyo *et al.* (2022), who investigated trace-element concentrations in bottled water in South Africa in 2022 and used composite indicators of non-carcinogenic risk. In this context, the low concentrations of toxic elements in the brands examined may be interpreted as a positive finding. This is for the specific production batches analysed. However, they do not provide grounds for extrapolating the conclusions. This is not possible to the entire Ukrainian market.

The microbiological findings confirmed that all the samples examined were in a satisfactory sanitary condition. The absence of coliform bacteria, *Escherichia coli,*

Pseudomonas aeruginosa, intestinal enterococci and sulphite-reducing anaerobic bacteria was indicated. This was together with the low total microbial counts. This showed no evidence of faecal or secondary bacterial contamination. F. Carraturo *et al*. (2021) investigated the microbial communities of natural mineral waters using next-generation sequencing. They demonstrated that packaged water can possess a distinctive microbiota, even in the absence of sanitary indicator microorganisms. The chemical and microbiological characteristics of purified, mineral, artesian and carbonated waters were also identified by Y.M. Nadreen *et al*. (2024). These findings suggest that, while standard sanitary indicators are sufficient for regulatory safety assessments, they do not fully describe the natural microbiological characteristics of mineral water.

The waters were compared. This was according to their mineral profiles. This confirmed that a single ranking was inappropriate. This was for products with different functional purposes. S. Manoj *et al*. (2024) examined the consequences of low mineral content in bottled water, emphasising that low mineralisation should not be considered a universal advantage. In the context of the present study, this supported the use of a profile-based rather than a ranking-based assessment. This is because low-mineralised and highly mineralised waters have different intended uses. Meanwhile, C. Dupont & G. Hébert (2020) reviewed the clinical evidence relating to natural mineral waters containing magnesium and sulphate, and identified their particular effectiveness in treating functional bowel disorders. Accordingly, the high concentrations of magnesium and sulphates in Donat Mg should not be considered a disadvantage solely due to the water's pronounced organoleptic characteristics. However, it is important to note that this water is not a suitable replacement for low-mineralised table water that is intended for unrestricted daily consumption.

The results of the profile-based assessment also prevented an oversimplified conclusion about the "best" brand. M. Rasheduzzaman *et al*. (2025) conducted an inter- and intra-brand study of 26 bottled water brands in the United States, demonstrating that assessments must account for production variability, source type, and differences between individual samples. A. Alshishani *et al*. (2026) analysed 176 water brands on the Jordanian market. They used a broad range of chemical and microbiological parameters. They demonstrated that composite quality indices require cautious interpretation. This is particularly true where parameters have a zero-tolerance limit. In the present study, therefore, a profile-based assessment was more appropriate than ranking the brands from first to sixth place.

Microplastics and nanoplastics, which were not examined in this study, require particular attention. A study by S.M. Praveena & S. Laohaprapanon (2021) revealed significant variations in the methods used to analyse microplastics in bottled water. These variations included differences in contamination control, sample preparation techniques, and approaches to identifying polymers. The authors stressed that, without standardised methodological procedures, it is challenging to directly compare the results of different studies. The problem of microplastics therefore requires not only expanded monitoring. It also requires the standardisation of laboratory methods. All the bottled-water brands examined by M.B. Hossain *et al*. (2023) showed signs of microplastic contamination, indicating that this type of pollution might be pervasive even in products sold in commercial packaging. In that study, it was important not only to detect particles, but also to characterise them by size, shape, and polymer composition, as this made it possible to associate contamination with packaging or particular stages in the production and distribution process. A. Altunışık (2023) identified microplastics in natural and mineral waters in Turkey and drew attention to how daily consumption of bottled water could contribute to the total intake of such particles by the human body. This highlights the importance of microplastics as an emerging safety indicator not yet covered by traditional chemical and microbiological monitoring regulations. These findings suggest that adherence to standard chemical and microbiological regulations does not guarantee the absence of emerging contaminants related to packaging, bottling, or storage processes.

N. Qian *et al*. (2024) used stimulated Raman scattering microscopy to demonstrate that the number of particles detected in bottled water can increase substantially when nanoplastics are included in the analysis. This study is important because it shows that earlier research, which focused mainly on microplastics, may have underestimated the actual level of particulate contamination due to the technical limitations of the detection methods used. V. Gálvez-Blanca *et al*. (2024) detected microplastics and non-natural cellulose particles in bottled water in Spain. The study stressed that contamination might come from polymers as well as other artificial particles that are introduced during production, filtration, packaging or storage. S. Patil *et al*. (2024) identified differences in microplastic contamination levels between local and national water brands in India. This finding suggests that the level of contamination may depend on production scale, technological controls, packaging type, and logistics conditions, rather than solely on the source of the water. M. Ghimire *et al*. (2025) also detected microplastics in all the bottled water samples examined in Nepal. Their findings extended the geographical evidence for this problem, demonstrating that microplastic contamination of bottled water is not confined to particular local markets. Consequently, a promising direction for further research into the Ukrainian market would be to supplement traditional quality indicators with the determination of microplastics, nanoplastics, and substances that migrate

from polymer packaging. Within the production batches examined, all six brands complied with the criteria for chemical and microbiological safety. The main differences were not determined by the presence of hazardous contaminants, but by the natural mineral profile, which influences taste, electrical conductivity, mineralisation, and the recommended consumption pattern.

Conclusions

A comparison of six brands of packaged natural mineral water available in the Ukrainian retail market was made in a laboratory and analytical investigation. The results showed that the production batches analysed were chemical, microbiological and organoleptic safe. All samples were clear, free from visible sediment, suspended particles, foreign matter, and unacceptable odours. The water colour ranged from 0.7 to 2.3 degrees on the platinum-cobalt scale, substantially below the 20-degree limit. Morshynska and Fiuggi received the highest organoleptic scores of 4.8 points each on a five-point scale. The more pronounced mineral taste of Donat Mg was found to be due to its naturally high magnesium, sulphate and bicarbonate concentrations rather than any deterioration in quality.

Physicochemical analysis confirmed significant differences among the waters in terms of mineralisation and ionic profile. Fiuggi had the lowest mineralisation, at 0.19 ± 0.01 g/dm^3, while Donat Mg had the highest, at 13.1 ± 0.14 g/dm^3. The table waters Morshynska and Karpatska Dzherelna were characterised by low mineralisation at 0.28 ± 0.02 g/dm^3 and 0.6 ± 0.04 g/dm^3, respectively. Luzhanska and Polyana Kvasova had higher values at 4.75 ± 0.12 and 8.5 ± 0.17 g/dm^3 respectively. The pH values of all samples ranged from 6.29 to 7.19, and the absolute ion balance value did not exceed 1.4%, which confirms the consistency of the results obtained for the principal cations and anions.

No exceedances of the hygiene limits were identified for the chemical safety indicators. The maximum nitrate concentration was 2.4 ± 0.3 mg/dm^3, 20.8 times below the permissible level of 50 mg/dm^3. Lead and arsenic concentrations did not exceed 0.0024 and 0.0027 mg/dm^3 respectively, and total organic carbon did not exceed 0.55 mg/dm^3, compared with the regulatory limit of 5 mg/dm^3. Nitrites, cadmium and mercury were all below the limits of quantification. No coliform bacteria, *E. coli, P. aeruginosa*, intestinal enterococci or sulphite-reducing anaerobic bacteria were detected in any sample. The total microbial count did not exceed 6 ± 2 CFU/cm^3 at 20-22°C. These waters should not be regarded as interchangeable. Table water brands are more suitable for regular hydration, whereas waters with elevated concentrations of sodium, bicarbonates, magnesium or sulphates should be selected according to individual tolerance and the recommended consumption pattern.

The study had several limitations. These included the analysis of only three production batches of each brand, the collection of products exclusively in Kyiv, and the absence of testing for microplastics, nanoplastics and substances migrating from polymer packaging. Research should concentrate on extending the geographical scope of sampling, conducting seasonal monitoring and assessing emerging contaminants in packaged mineral waters.

Acknowledgements

None.

Funding

None.

Conflict of Interest

None.

References

[1] Alshishani, A., Al-ebini, Y., Shoai, M., Alsafadi, D., Hussein, G., & Shaghlil, L. (2026). Quality and safety assessment of bottled water in Jordan markets. *Journal of Food Composition and Analysis*, 151, article number 108929. doi: 10.1016/j.jfca.2026.108929.

[2] Altunışık, A. (2023). Microplastic pollution and human risk assessment in Turkish bottled natural and mineral waters. *Environmental Science and Pollution Research*, 30(14), 39815-39825. doi: 10.1007/s11356-022-25054-6.

[3] Aslani, R., Esmaeili, S., Akbari, M.E., Molaee-Aghaee, E., Sadighara, P., Nazmara, S., & Mahmoudi, B. (2024). Determination of heavy metals, nitrate and nitrite in mineral and drinking bottled water in Tehran, Iran: A health risk assessment by Monte-Carlo simulation method. *Heliyon*, 10(23), article number e40714. doi: 10.1016/j.heliyon.2024.e40714.

[4] Banda, R.K., Mubita, P., Moonga, G., & Meki, C.D. (2021). Bacteriological quality and heavy metal analysis of packaged water produced in Lusaka, Zambia and associated quality control measures. *Frontiers in Public Health*, 9, article number 620700. doi: 10.3389/fpubh.2021.620700.

[5] Boas, D.M., Alegbeleye, O., & Sant'Ana, A.S. (2024). Microbial diversity and ecology of bottled water. *Current Opinion in Food Science*, 60, article number 101218. doi: 10.1016/j.cofs.2024.101218.

[6] Carraturo, F., Del Giudice, C., Compagnone, M., Libralato, G., Toscanesi, M., Trifuoggi, M., Galdiero, E., & Guida, M. (2021). Evaluation of microbial communities of bottled mineral waters and preliminary traceability analysis using NGS microbial fingerprints. *Water*, 13(20), article number 2824. doi: 10.3390/w13202824.

[7] Decree of the Ministry of Health of Ukraine No. 4 "On the Approval of Hygiene Standards for the Safety of Natural Mineral Water". (2010, January). Retrieved from https://zakon.rada.gov.ua/rada/show/v0004488-10.
[8] DSTU 878-93. (1993). *Bottled mineral waters. Technical specifications*. Retrieved from https://online.budstandart.com/ua/catalog/doc-page.html?id_doc=82545.
[9] DSTU EN 1484:2003. (2003). *Water analysis. Guidelines for the determination of total and dissolved organic carbon*. Retrieved from https://online.budstandart.com/ua/catalog/doc-page.html?id_doc=73074.
[10] DSTU EN 27888:2022. (2022). *Water quality. Determination of electrical conductivity*. Retrieved from https://online.budstandart.com/ua/catalog/doc-page.html?id_doc=110955.
[11] Dupont, C., & Hébert, G. (2020). Magnesium sulfate-rich natural mineral waters in the treatment of functional constipation – a review. *Nutrients*, 12(7), article number 2052. doi: 10.3390/nu12072052.
[12] Gálvez-Blanca, V., Edo, C., González-Pleiter, M., Fernández-Piñas, F., Leganés, F., & Rosal, R. (2024). Microplastics and non-natural cellulosic particles in Spanish bottled drinking water. *Scientific Reports*, 14, article number 11089. doi: 10.1038/s41598-024-62075-2.
[13] Ghimire, M., Byanjankar, N., Khanal, J., Acharya, S., Nicholson, K., Shakya, S., & Prasai Joshi, T. (2025). First assessment of occurrence, characteristics and human exposure of microplastics in bottled drinking water, Nepal. *Cleaner Water*, 4, article number 100184. doi: 10.1016/j.clwat.2025.100184.
[14] Hadbi, T., Kassoul, A., & Mokadem, M. (2022). Chemical characterization and statistical analysis of bottled waters in Algeria. *Pollution Research*, 41(3), 889-897. doi: 10.53550/PR.2022.v41i03.018.
[15] Hossain, M.B., Yu, J., Banik, P., Noman, M.A., Nur, A.-A., Haque, M.R., Rahman, M.M., Albeshr, M.F., & Arai, T. (2023). First evidence of microplastics and their characterization in bottled drinking water from a developing country. *Frontiers in Environmental Science*, 11, article number 1232931. doi: 10.3389/fenvs.2023.1232931.
[16] ISO 10304-1:2025. (2025). *Water quality. Determination of dissolved anions by liquid ion chromatography. Part 1. Determination of bromide, chloride, fluoride, nitrate, nitrite, phosphate and sulphate*. Retrieved from https://online.budstandart.com/ua/catalog/doc-page.html?id_doc=116555.
[17] ISO 10523:2022. (2022). *Water quality. Determining pH*. Retrieved from https://surl.li/vbppwr.
[18] ISO 11885:2019. (2019). *Water quality. Determining of selected elements by inductively coupled plasma optical emission spectrometry*. Retrieved from https://surl.li/rwjxzi.
[19] ISO 16266:2022. (2022). *Water quality. Detection and enumeration of pseudomonas aeruginosa. Membrane filtration method*. Retrieved from https://online.budstandart.com/ua/catalog/doc-page.html?id_doc=119225.
[20] ISO 17294-2:2019. (2019). *Water quality. The use of inductively coupled plasma mass spectrometry*. Retrieved from https://online.budstandart.com/ua/catalog/doc-page.html?id_doc=84275.
[21] ISO 6222:2002. (2002). *Water quality. Enumeration of colony-forming microorganisms. Colony counting by inoculation into a nutrient agar medium*. Retrieved from https://online.budstandart.com/ua/catalog/doc-page.html?id_doc=95726.
[22] ISO 7887:2025. (2025). *Water quality. Testing and determining colour*. Retrieved from https://online.budstandart.com/ua/catalog/doc-page.html?id_doc=116553.
[23] ISO 7899-2:2022. (2022). *Water quality. Detection and enumeration of faecal enterococci. Part 2. Membrane filtration metho*d. Retrieved from https://online.budstandart.com/ua/catalog/doc-page.html?id_doc=119175.
[24] ISO 9308-1:2022. (2022). *Water quality. Detection and enumeration of Escherichia coli and coliform bacteria. Part 1. Membrane filtration method for water with a low background bacterial count*. Retrieved from https://online.budstandart.com/ua/catalog/doc-page.html?id_doc=109518.
[25] Iyakare, J.D., Taupin, J.-D., Hitimana, C.N., Dusabimana, T., Ghalit, M., El Ouahabi, M., Benali, M., Ngendo, C., & Gharibi, E.K. (2022). Hydrochemical study of bottled water in Rwanda and relationship with their origin. *Water Supply*, 22(1), 1155-1167. doi: 10.2166/ws.2021.211.
[26] Ketrouci, K., Meddi, M., Bouregba, N., Zatout, I., & Rezki, A. (2023). Classification of bottled waters marketed and consumed in Algeria through statistical approaches. *Journal of Water and Health*, 21(10), 1489-1502. doi: 10.2166/wh.2023.142.
[27] Krykhovets, O., Repeta, V., & Ivashchenko, I. (2025). Monitoring of spring water quality. *Environmental Problems*, 10(2), 127-134. doi: 10.23939/ep2025.02.127.
[28] Kwikima, M.M. (2025). The biological and chemical water quality of retail bottled water brands: A case of Dodoma, Tanzania. *Nutrition & Food Science*, 55(1), 165-179. doi: 10.1108/NFS-05-2024-0182.
[29] Kysylevska, A., Prokopovych, I., & Kokhan, S. (2024). Substantiation of safety and quality indicators of natural mineral and spring waters in Ukraine for the preparation of food for infants. *Technology Audit and Production Reserves*, 5(79), 36-42. doi: 10.15587/2706-5448.2024.314338.
[30] Manoj, S., Kartheeshwari, M.R., Keerthan, L., & Elango, L. (2024). Effects of low mineral content in bottled drinking water on human health and evaluation of optimal requirements. *Journal of Food Composition and Analysis*, 128, article number 106052. doi: 10.1016/j.jfca.2024.106052.

[31] Maselela, J.L., Mokgobu, M.I., & Mudau, L.S. (2024). The evaluation of bottled water quality compliance association formal and informal retailers in Gauteng municipality, South Africa. *Applied Food Research*, 4(2), article number 100576. doi: 10.1016/j.afres.2024.100576.
[32] Mitku, M., & Endeshaw, L. (2022). Chemical quality assessment of major brands of bottled mineral water available in the Ethiopian market. *Journal of Food Safety and Hygiene*, 8(3), 183-201. doi: 10.18502/jfsh.v8i3.11020.
[33] Moreno-Merino, L., Aguilera, H., & de la Losa Román, A. (2022). Are bottled mineral waters and groundwater for human supply different? *Science of the Total Environment*, 835, article number 155554. doi: 10.1016/j.scitotenv.2022.155554.
[34] Nadreen, Y.M., Vrouwenvelder, J.S., Saikaly, P.E., & Gonzalez-Gil, G. (2024). The unique chemical and microbiological signatures of an array of bottled drinking water. *Frontiers in Microbiology*, 15, article number 1441142. doi: 10.3389/fmicb.2024.1441142.
[35] Olowoyo, J.O., Chiliza, U., Selala, C., & Macheka, L. (2022). Health risk assessment of trace metals in bottled water purchased from various retail stores in Pretoria, South Africa. *International Journal of Environmental Research and Public Health*, 19(22), article number 15131. doi: 10.3390/ijerph192215131.
[36] Order of the Ministry of Health of Ukraine No. 741 "On the Approval of Hygiene Requirements for the Production and Distribution of Natural Mineral Waters and Spring Waters". (2021, April). Retrieved from https://zakon.rada.gov.ua/laws/show/z0657-21.
[37] Patil, S., Bafana, A., Krishnamurthi, K., & Sivanesan, S. (2024). Estimated exposure to microplastics through national and local brands of bottled water in Central India. *Environmental Monitoring and Assessment*, 196(3), article number 240. doi: 10.1007/s10661-024-12387-7.
[38] Praveena, S.M., & Laohaprapanon, S. (2021). Quality assessment for methodological aspects of microplastics analysis in bottled water – a critical review. *Food Control*, 130, article number 108285. doi: 10.1016/j.foodcont.2021.108285.
[39] Qian, N., Gao, X., Lang, X., Deng, H., Bratu, T.M., Chen, Q., Stapleton, P., Yan, B., & Min, W. (2024). Rapid single-particle chemical imaging of nanoplastics by SRS microscopy. *Proceedings of the National Academy of Sciences of the United States of America*, 121(3), article number e2300582121. doi: 10.1073/pnas.2300582121.
[40] Rasheduzzaman, M., Lytton, B., Wilcox, E., Das, A., Wirth, M., Hurtado, A., Krometis, L.-A., & Cohen, A. (2025). Microbiological and chemical contaminants in single-use and multipackage bottled water: Inter- and intra-analyses of 26 bottled water brands in the USA. *ACS ES&T Water*, 5(9), 5471-5481. doi: 10.1021/acsestwater.5c00536.
[41] Shulyak, S., Shevchenko, L., Mykhalska, V., Kaminska, O., Gaidei, O., Kovalenko, V., Balarskyi, Y., Kryvenko, M., & Boyarchuk, S. (2021). Quality and safety of tap water in selected Ukrainian regions. *Ukrainian Journal of Ecology*, 11(2), 274-283. doi: 10.15421/2021_111.
[42] Stoots, S.J., *et al*. (2020). Variations in the mineral content of bottled "still" water across Europe: Comparison of 182 brands across 10 countries. *Journal of Endourology*, 35(2), 206-214. doi: 10.1089/end.2020.0677.
[43] Syed, N.R., Raza, A., Alshehri, F., Almadani, S., Singh, S.K., & Elbeltagi, A. (2025). Spatio-temporal analysis of bottled mineral water brands and their compliance with standards. *Applied Water Science*, 15, article number 116. doi: 10.1007/s13201-025-02441-1.
[44] Ungureanu, E.L., Soare, A.D., Mocanu, A.L., Iorga, S.C., Mustatea, G., & Popa, M.E. (2022). Occurrence of potentially toxic elements in bottled drinking water – carcinogenic and non-carcinogenic risks assessment in adults via ingestion. *Foods*, 11(10), article number 1407. doi: 10.3390/foods11101407.

Оцінка якості мінеральної води та відповідності стандартам безпеки: порівняльний аналіз ринку

Ермір Шахіні
Доктор економічних наук, доцент
Університет Олександра Моісіу в Дурресі
2001, вул. Курріла, 1, м. Дуррес, Албанія
https://orcid.org/0000-0002-0083-1029

Анотація. Метою дослідження було проведення комплексного аналізу органолептичних, фізико-хімічних, хімічних та мікробіологічних характеристик мінеральних вод різного походження, що представлені на українському роздрібному ринку. Було досліджено шість торгових марок з метою визначення їхніх органолептичних властивостей, рівня pH, електропровідності, мінералізації, а також наявності основних катіонів, аніонів, токсичних домішок, органічних речовин та санітарно-індикаторних мікроорганізмів. Результати показали, що всі досліджені зразки були прозорими, не містили осаду, зважених частинок та сторонніх речовин, а показники кольору коливалися в межах від 0,7 до 2,3 градусів за платиново-кобальтовою шкалою. Оцінки смаку коливалися від 4,2 до 4,8 балів, причому відмінності були зумовлені природним мінеральним складом, а не сторонніми смаковими добавками. Значення pH коливалися в діапазоні від 6,29 до 7,19, а електропровідність – від 0,29 до 18,9 мілісіменсів на сантиметр. Найнижчу мінералізацію мала вода «Фьюджі» – 0,19 ± 0,01 г/л, а найвищу – «Донат Mg» – 13,1 ± 0,14 г/л. Характерною особливістю «Моршинської» та «Карпатської джерельної» була низька мінералізація з переважанням кальцію та бікарбонатів. Води «Поляна Квасова» та «Лужанська» відрізнялися високим вмістом натрію та бікарбонатів відповідно, тоді як вода «Донат Mg» вирізнялася високою концентрацією магнію – 1010 ± 42 мг/л, високою концентрацією сульфатів – 2200 ± 103 мг/л та високою концентрацією бікарбонатів – 7595 ± 290 мг/л. Абсолютне значення іонного балансу не перевищувало 1,4 %. Максимальний вміст нітратів становив 2,4 ± 0,3 міліграма на кубічний дециметр, що в 20,8 рази нижче за допустимий рівень. Вміст свинцю, миш'яку та загального органічного вуглецю не перевищував відповідних гігієнічних норм, а мікробіологічних показників санітарного стану виявлено не було. Цей підхід можна використовувати для контролю упакованих продуктів у лабораторіях, перевірки точності маркування та розробки науково обґрунтованих рекомендацій для споживачів

Ключові слова: іонний склад; бікарбонати; натрій; токсичні забруднювачі; маркування; вибір споживача

COMMODITY BULLETIN
Journal homepage: https://c-bulletin.com.ua/en
DOI: 10.62763/cb/1.2026.44

Article's History: Received: 20.01.2026 Revised: 28.04.2026 Accepted: 28.05.2026 Published: 29.05.2026

ISSN 2310-5283; e-ISSN 3041-1432 Vol. 19, No. 1, 2026, 44-55

UDC 637.13:664.856]:664.29

Optimising the formulation of a milk-based jelly filling using microcrystalline cellulose and pectin

Nina Stetsenko
Researcher in Formulation Development
Somafina
84041, 851 North McCormick Way, Leyton, USA
https://orcid.org/0009-0006-8781-6417
Nataliia Shapovalova*
PhD in Technical Sciences, Associate Professor
State University of Trade and Economics
02156, 19 Kyoto Str., Kyiv, Ukraine
https://orcid.org/0000-0002-9143-8600
Dmytro Antiushko
PhD in Technical Sciences, Associate Professor
State University of Trade and Economics
02156, 19 Kyoto Str., Kyiv, Ukraine
https://orcid.org/0000-0002-4135-6439

Abstract. Dairy-fruit fillings for flour confectionery products remain technologically underexplored, yet face demanding performance requirements: structural stability during baking at 180-190°C, resistance to syneresis, and retention of a smooth, creamy texture after freeze-thaw cycling. The aim of study was to optimise the formulation of a milk-based jelly filling using a three-component stabilising system comprising low-methoxyl pectin (LMP, APA 104), modified starch (Thermflo waxy corn and Ultra-Tex tapioca), and microcrystalline cellulose (MCG 811, E460). Four model systems were prepared at a constant dry matter content of 8% and evaluated by rotational viscometry (Brookfield DV3T) and expert organoleptic assessment on a 10-point scale. The key finding was that the formulation containing 0.6% LM pectin, 3.6% modified starch, and 0.4% MCC (Sample 3) achieved an apparent viscosity of 18,000-24,000 mPa·s at 10 rpm, the narrowest hysteresis loop among all tested systems, and the highest expert scores for colour and clarity (8.8/10), creamy consistency (9.1/10), and behaviour within the product body after baking (8.9/10). Compared with the industrial control formulation, the optimised filling reduced dry matter content from 62.3% to 58.4%, eliminated visible syneresis after baking in éclair shells, and showed markedly improved freeze-thaw stability. The addition of MCC at 4 kg per tonne of filling acted as a colloidal stabiliser, narrowing the rheological hysteresis loop and improving thixotropic recovery. These results demonstrate that the synergistic combination of LM pectin, cross-linked starch, and MCC is an effective and industrially scalable strategy for developing heat-stable, clean-label dairy-fruit fillings

Keywords: smodified starch; hydrocolloids; low-methoxyl pectin; dairy-fruit filling; rheology; heat stability; gelation

Suggested Citation:

Stetsenko, N., Shapovalova, N., & Antiushko, D. (2026). Optimising the formulation of a milk-based jelly filling using microcrystalline cellulose and pectin. *Commodity Bulletin*, 19(1), 44-55. doi: 10.62763/cb/1.2026.44.

*Corresponding author (shap220577@gmail.com)

Introduction

One of the most dynamically developing segments of the global food industry is the production of fruit and berry fillings for confectionery and bakery products. Growing consumer expectations regarding product naturalness, texture stability, and extended shelf life have driven substantial interest in the development of heat-stable, syneresis-resistant dairy-fruit fillings. The challenge of simultaneously achieving structural stability during baking, freeze-thaw resistance, and a clean-label ingredient profile makes dairy-fruit fillings a particularly demanding development target. The main technological challenge in producing dairy-containing fillings is syneresis – the undesirable separation of the aqueous phase from the gel matrix – which is intensified during baking and freeze–thaw cycling.

C. Gallery *et al.* (2024) investigated the effect of pectin molecular weight and degree of methylation on the rheological behaviour of model filling systems and found that apple-sourced low-methoxyl pectin with a degree of methylation of 30-38% produces a significantly smoother gel structure than citrus counterparts at equivalent concentrations, attributing this to the higher proportion of neutral arabinogalactan side chains that reduce network rigidity. M. Romero-Rosales *et al.* (2025) studied the syneresis-inhibiting properties of cross-linked waxy corn starch in baked cream fillings and showed that hydroxypropyl distarch phosphate from waxy corn at concentrations of 3-5% reduced moisture migration by 48-62% relative to native starch controls, owing to its denser, more mechanically stable gel network that persists above the gelatinisation temperature.

The authors Y. Liu *et al.* (2024) of the study described the internal mechanisms of food emulsions stabilised by emulsifiers and proteins, carried out in recent years. Destabilisation and stabilisation of emulsions are associated with the addition of surfactants. The properties, type and concentration of emulsifiers determine the stability of emulsions, and emulsifiers can be classified into different types (e.g. ionic or non-ionic, solid or liquid) according to their properties and sources. Authors reviewed the current understanding of the mechanisms by which proteins and low-molecular-weight emulsifiers stabilise food emulsions, with particular emphasis on their adsorption at the oil-water interface, the formation of protective interfacial layers, and their contribution to the physical stability of emulsions. The authors also discussed the synergistic interactions between proteins and emulsifiers and their potential applications in the development of stable food systems with tailored functional properties.

J. Poudel *et al.* (2025) demonstrated the functional role of microcrystalline cellulose (MCC, E460) as a colloidal network stabiliser in low-fat dairy emulsions, showing that MCC at 0.3-0.5% reduced visible syneresis by 38-45% and improved freeze-thaw stability by forming a tortuous particle network that physically restricts water mobility between gel domains, without contributing substantially to bulk viscosity. Researchers M. Alam *et al.* (2024) assessed the use of hydrocolloid compositions in dairy-containing semi-finished products for confectionery and reported that a ternary system of modified starch, pectin, and cellulose microparticles outperformed binary systems (starch-pectin and starch-cellulose) in both heat stability and freeze-thaw resistance, providing quantitative evidence of synergistic inter-polymer interaction that cannot be predicted from single-component behaviour.

Hydrocolloids are increasingly recognised as multifunctional additives in bakery systems, serving as fat replacers, texture modifiers, moisture retainers, and thermal stabilisers. Moreover, hydrocolloids significantly enhance the dough characteristics by improving moisture and gas retention, modifying viscosity, altering the gluten network, and reducing the fat content (Kumar *et al.*, 2026). In the consumer space, space, consumers are spending more time identifying clean label products and looking for products, whose claims reflect their values. However, manufacturers are keeping in mind that too many labels on products can be confusing. Innova Market Insights (n.d.) research also signalled a growing correlation between the use of clean label and environmental action trends in the minds of customers. Products are increasingly deemed clean if they carry environmental benefits.

Scientists Y. Cao & L. Miao (2023) showed that consumer perception of "naturalness" in bakery-filled products is significantly improved when modified starch types are partially replaced by recognised food biopolymers such as pectin, even in the absence of explicit clean-label claims, demonstrating the commercial relevance of reformulation strategies that reduce total starch content. The authors L. Huang *et al.* (2025) applied Brookfield rotational viscometry to characterise the rheological behaviour of model fruit-cream filling systems and established that apparent viscosity measured at 10 rpm in the range 17,000-25,000 mPa·s correlates with the highest sensory scores for creaminess and product body in structured panel evaluations, providing independent methodological validation for viscosity-based quality control in filling production.

Despite the substantial body of research summarised above, the specific combination of low-methoxyl apple pectin, cross-linked waxy corn starch, and microcrystalline cellulose in dairy-fruit fillings for flour confectionery products – and the optimal ratio of these components under industrial production conditions – has not been previously reported. The aim of this study was therefore to provide a scientific and practical basis for optimising the formulation of a milk-based jelly filling using a three-component stabilising system composed of microcrystalline cellulose, LM pectin, and modified starch.

Materials and Methods

To obtain a filling with a stable fruit-cream profile, a formulation containing low-methoxyl pectin was developed and optimised. For the rheological study, model systems containing starch-pectin mixtures at different concentrations and a dry matter content of 8% were prepared. The combinations tested were MCC + starch and MCC + starch + pectin. Two modified starches of different origins were used as stabilisers: Thermflo from waxy corn and Ultra-Tex from tapioca. Microcrystalline cellulose (MCC) was used to improve and preserve the functional and technological properties of the semi-finished product and to increase the biological value of the finished product. It helps maintain a stable consistency during storage and transportation, prevents phase separation between the aqueous and dairy phases, preserves structure during freeze-thaw cycling, and improves mouthfeel by increasing creaminess (Poudel *et al.*, 2025). Microcrystalline cellulose (E460) is a purified, partially depolymerised cellulose: a white, tasteless, odourless crystalline powder composed of porous particles. It is produced by controlled acid hydrolysis of highly purified α-cellulose from fibrous plant materials. MCC E460 is an approved food additive listed as GRAS (Generally Recognised as Safe) in the United States and permitted in the EU without quantitative limits (quantum satis) for most food categories (EFSA *et al.*, 2018).

The research was conducted at FRUT EKS LLC, Trebukhiv, Brovary district, Kyiv region, under laboratory conditions. The organoleptic properties of the semi-finished and finished products were assessed by a structured expert evaluation procedure. The panel consisted of eight trained tasters with documented competence in food texture and flavour assessment, in accordance with the requirements of DSTU 7662:2014 (2015) and ISO 11136:2014 (2014). Each assessor independently evaluated the filling samples on a 10-point hedonic scale across five indicators: colour and clarity, fruit flavour, aroma, creamy consistency, and behaviour within the product body. Behaviour within the product body was evaluated by filling standard choux pastry éclair shells (baked at 185°C, 22 min) with each sample and assessing moisture migration, structural retention, and mouthfeel uniformity after 2 h of storage at 20°C and after a bake-through test at 190°C for 18 min. Individual scores were averaged across the panel, and a significance threshold of 0.5 points was applied as the minimum detectable difference. The overall quality score for each sample was calculated as the area of a quality polygon constructed from the five indicator scores (Civille *et al.*, 2016). The overall average score was calculated as the area of the quality polygon. pH was measured using a pH meter (potentiometer) calibrated with buffer solutions at pH 4.0 and 7.0, with a precision of ± 0.02 pH (DSTU ISO 1842:2006, 2006). The rheological properties of the stabilising systems were studied by Brookfield Engineering (2017) and using a Brookfield DV3T (product USA) viscometer and the rotational method, which measures the viscosity of a material placed between two coaxial surfaces under shear. Brookfield Engineering studied the rheological properties of stabilising systems and using a Brookfield DV3T viscometer (a USA product) and a rotational method that measures the viscosity of a material placed between two coaxial shear surfaces.

A T-shaped spindle T-C (#93) was used for homogeneous paste-like fillings. Chamber/Geometry: Special system Helipath Stand BROOKFIELD DIGITAL RHEOMETER MODEL DV-III+ Operating (which slowly moves the rheometer up and down during rotation, causing the spindle to continuously hit the "fresh" sample in a spiral) + a low beaker for 400-600 mL. Measuring temperature: 20-25°C (room temperature for confectionery use). Stabilisation time: 30 minutes. The filling should completely relax in the glass after pouring, since mechanical disturbance destroys the pectin network (thixotropy). Sample volume: 400 mL (in a low, wide beaker so that the Helipath spindle has sufficient vertical travel and does not touch the bottom). 5 parallel measurements were carried out (each repetition in a completely new glass with filling from the same batch, since after the first test, the structure of the sample is already destroyed). For thick non-Newtonian pastes such as fruit confectionery fillings, when using T-spindles, the DV3T device in this case displays the shear rate as a conversion of revolutions per minute (RPM) to shear speed (γ, s^{-1}). The shear rate range was 0.5-100 rpm with at least 8-10 measurement points (Steffe, 1996; Mezger, 2006). The dry components, including pectin and MCC, were dispersed in a whey-water mixture. The paste was gelatinised by gradual heating to 80-85°C at pH 4.0-4.5 with continuous stirring, held for 10 minutes, homogenised, and then cooled to 20-25°C. All experiments were performed in quintuplicate, and the experimental data were processed using the obtained results.

Results and Discussion

To evaluate and control the quality of the milk-fruit filling, it was optimised the production process by combining pectin and whey streams under defined conditions using lactic acid after pectin incorporation, which are critical control points for achieving stable, calcium-mediated gelation of LM pectin without premature whey coagulation. Compared with the traditional control formulation, the optimised milk-fruit filling achieved significantly higher scores for colour, transparency, and taste, while simultaneously reducing the total dry matter content, confirming that the synergistic starch-pectin-MCC system outperforms traditional single- or two-hydrocolloid formulations. A rheological and sensory evaluation of the model systems was conducted, and the optimal formulation was determined, combining pronounced pseudoplastic behaviour with excellent thermal stability, minimal syneresis, and the highest

sensory scores among all tested compositions. Basing on market data it was analysed that the global market for heat-stable fruit fillings was estimated at USD 1.17 billion in 2025 and is projected to reach USD 1.65 billion by 2031 at a compound annual growth rate of 5.0% (Market Research, 2025). To identify the optimal formulation of a heat-stable dairy-fruit filling, model systems containing different combinations and concentrations of low-methoxyl pectin, modified starch, and microcrystalline cellulose were evaluated in terms of their rheological behaviour and organoleptic properties. The experimental results obtained for model systems containing starch-pectin mixtures at different concentrations and a dry matter content of 8% are presented in Table 1.

Table 1. Dosage and application forms of model compositions

Sample	Expected function	Starch, %	Pectin APA 104, %	MCG 811, %
1	Thickener (MCC + starch)	5.2	0	0.5
2	Weakly pseudoplastic	4.0	0.40	0.35
3	Optimal	3.6	0.60	0.4
4	Strongly pseudoplastic	3.2	0.80	0.35

Source: *developed by the author*

Increasing the pectin concentration from 0.4% to 0.8% altered the viscosity profile of the systems without substantially changing their overall flow behaviour. The addition of 0.6% pectin provided the most favourable balance, ensuring heat stability and structural integrity without excessive thickening. Higher pectin concentrations generated greater shear stress at low shear rates, indicating increased stability at rest. In combination with 0.4% microcrystalline cellulose, the system showed a more uniform viscosity increase. Overall, the results indicate that excessively low pectin contents do not provide adequate structure, whereas concentrations above 0.6% may weaken processing performance and reduce practical heat stability. Figure 1 shows the rheological behaviour of the model systems. Analysis of yield stress, which characterises the stress required to disrupt a weakly disturbed structure, showed that among the model pastes the highest force was required to destroy the structure formed by hydroxypropyl cross-linked waxy corn starch at a concentration of 5.2%. A lower force was required for the corresponding hydroxypropyl tapioca starch system.

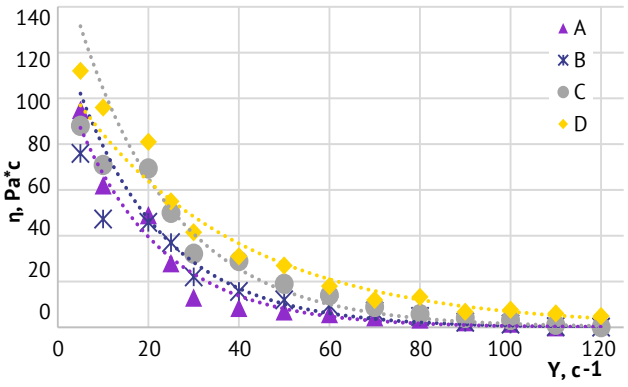

Figure 1. *Full rheological viscosity curves of modified starches with added LM pectin*
Note: *A – Sample 4: Ultra-TEX + 0.8% LM pectin; B – Sample 2: Thermflo + 0.4% LM pectin; C – Sample 3: Thermflo + 0.6% LM pectin; D – Sample 1 (control): Ultra-TEX + MCC*
Source: *developed by the author*

All model systems displayed non-Newtonian, pseudoplastic (shear-thinning) behaviour, which is technologically desirable in filling applications: viscosity decreases under the mechanical shear of pumping and depositing equipment, yet the structure recovers at rest, preventing sagging or phase separation in the finished product. The degree of pseudoplasticity, quantified by the flow behaviour index (n), was lowest in Sample 4 "A" (0.8% pectin), confirming the strongest shear-thinning character in that system, while Sample 1 "D" (starch only, no pectin) exhibited the closest approach to Newtonian behaviour among the tested compositions. This gradient in flow index confirms that pectin, rather than starch alone, is the primary driver of pseudoplastic character in the mixed systems.

The apparent viscosity at a representative shear rate of 10 rpm followed a clear concentration-dependent pattern. Systems based on Ultra-Tex tapioca starch consistently showed lower apparent viscosity at equivalent concentrations compared with Thermflo waxy corn starch systems. This difference is attributed to the distinct granule morphology and degree of cross-linking between the two starches: Thermflo, a hydroxypropyl distarch phosphate from waxy corn, forms a denser network upon gelatinisation, while Ultra-Tex, a hydroxypropyl tapioca starch, produces a softer, more deformable gel matrix. When low-methoxyl pectin was incorporated into either starch matrix, it contributed an additional biopolymer network layer through calcium-mediated junction zones between pectin chains. At 0.6% pectin (Sample 3 "C"), this secondary network reinforced the starch matrix without creating excessive entanglement, resulting in a viscosity level that was reproducible across multiple measurement runs and remained stable upon moderate temperature cycling between 25°C and 50°C.

The role of microcrystalline cellulose (MCG 811) in the rheological behaviour of the composite systems warrants separate consideration. At 0.4%, MCC functions primarily as a colloidal stabiliser rather than a bulk thickener. Its porous particle structure adsorbs water at the interface between the starch gel and the aqueous

dairy phase, reducing the driving force for syneresis without substantially increasing bulk viscosity. This was reflected in the rheological data: the addition of MCC to starch-pectin systems did not raise the apparent viscosity significantly at mid-range shear rates (10-50 rpm) but markedly narrowed the hysteresis loop observed in up-down shear-rate sweeps, indicating improved structural recovery and greater thixotropic stability. In practical terms, this means that the filling recovers its original consistency more quickly after the shear stress of dosing equipment is removed – an important quality attribute for enrobed and injected bakery applications.

Overall, the rheological curves showed that both starch types formed structured, solid-like systems. The yield stress data further indicated that stronger structural bonds developed in systems containing hydroxypropyl distarch phosphate from tapioca than in those based on the corresponding waxy corn starch. Taken together, these rheological findings confirm that the three-component stabilising system – modified starch, LM pectin, and MCC – exhibits synergistic structuring effects that cannot be achieved by any single ingredient alone, and that the specific ratios identified in Sample 3 represent an optimal balance between processability, heat stability, and gel strength. At the initial stage of the study, conventional formulations widely produced requested by customers were analysed to establish an industrial benchmark for optimisation (Table 2).

Table 2. *Formulation of milk jelly filling (control)*

Ingredient	Mass, kg	Moisture, %	Dry matter, %	Dry matter, kg
Granulated sugar	470.0	0.15	99.85	469.3
Treacle (molasses)	56.0	22	78	43.68
Thermflo starch	33.3	12	88	29.3
Starch 385	16.7	12	88	14.7
Vegetable palm fat	40.0	0.5	99.5	39.8
Whey (concentrated)	13.3	4	96	12.77
MCG 811 – microcrystalline cellulose	6.0	6	94	5.64
Lactic acid (80%)	2.7	20	80	2.16
Salt	3.0	0.5	99.5	2.99
Banana + vanilla flavour	1.8	5	95	1.71
Potassium sorbate	1.3	1	99	1.29
Nisin	0.02	5	95	0.019
Colourants	0.013	5	95	0.013
Water	356.0	100	0	0
TOTAL	1000	62.3	-	623.35

Source: *prepared based on the recipe of O. Goryunov & N. Stetsenko (2005)*

Organoleptic evaluation showed that the filling had an opaque, paste-like consistency with a stretchy, ropy structure. The relatively high dry matter content (62.3%) can be explained by the high proportion of Starch 385 used as a thickener. In addition, prolonged cooking caused the filling to darken, produced a burnt sugar aroma, and impaired flavour. Based on the rheological and organoleptic results, the optimal composition of the dairy-fruit filling containing microcrystalline cellulose, thickening agents, and a stabilising system was predicted and experimentally confirmed. The optimal concentration of microcrystalline cellulose is 4 kg/t. The range of 4-6 kg/t is the practical "sweet spot" for cream fillings: the texture is more stable, syneresis is minimal, and rubberiness does not occur. To obtain a softer, more fluid consistency, for example for pressure-applied fillings, the concentration may be reduced to 3-3.5 kg/t, but in that case the thickener content should be increased by 3-4 kg/t to compensate. For stabilising low-fat dairy-fruit products, the MCC-based stabilising system is best introduced at 2.5-5.5% of product mass, as this eliminates syneresis, provides homogeneity, and ensures stability during heating. The optimised formulation is presented in Table 3.

Table 3. *Formulation of dairy-fruit filling based on modified starch, microcrystalline cellulose and pectin*

Ingredient	Mass, kg	Moisture, %	Dry matter, %	Dry matter, kg
Granulated sugar	445.0	0.2	99.9	444.3
Treacle (molasses)	48.0	22.0	78.0	37.4
Thermflo starch	29.0	12.0	88.0	25.5
Starch 385	7.0	12.0	88.0	6.2
Animal butter fat	40.0	0.5	99.5	39.8
Dry whey	13.5	4.0	96.0	13.0
MCG 811 – Microcrystalline cellulose	4.0	6.0	94.0	3.8
Pectin APA 104 (LM)	6.0	8.0	92.0	5.5
Lactic acid (80%)	2.5	20.0	80.0	2.0

Table 3. Continued

Ingredient	Mass, kg	Moisture, %	Dry matter, %	Dry matter, kg
Others (flavours, preservatives, etc.)	6.0	5.0	95.0	1.7
Water	399.0	100.0	0.0	0.0
TOTAL	1000.0	58.4	–	583.53

Source: *developed by the author*

A key technological requirement of LM pectin incorporation is the correct incorporation of LM pectin into the formulation. The pectin was pre-dissolved in hot water (85-90°C) separately from the whey because the calcium in whey can cause premature gelation. Lactic acid was added at the end to adjust the pH to the target range of 3.8-4.2, in which LM pectin forms the most stable gel. The whey used in the formulation (13.5 kg/t) contains calcium, which promotes pectin gelation by forming calcium bridges between chain segments. When pectin is added to a hot mass together with whey at temperatures above 70°C, an undesirable reaction may occur in which the whey coagulates under the action of pectin. For this reason, two separate process streams were maintained and combined only after both had cooled to 55-60°C, when the mobility of Ca^{2+} ions is reduced.

LM pectin gelation proceeds mainly through strong interactions between calcium ions and galacturonic acid blocks, and this process is effective over a wide range of pH values and soluble solids contents. The pH range of 3.8-4.2, combined with whey containing Ca^{2+}, provides favourable conditions for gel formation. An important scientific finding concerning whey was that LM pectin in a dairy system undergoes a two-stage process: first, calcium released from casein micelles at pH 5.0-4.9 initiates pectin–pectin interactions; then, at pH 4.9-4.0, direct interactions occur between pectin and casein micelles. Thus, whey in the formulation not only does not hinder gel formation, but actively promotes the formation of APA 104 gel, provided the whey is added at the correct temperature (55-60°C, not higher).

A second important technological requirement concerns the use of lactic acid (2.5 kg/t). Lactic acid is necessary for stable pectin gelation, but it must be added at the end, after the pectin has been incorporated. If acid is added to the pectin at the beginning, the pH drops sharply and the pectin gels before it is dispersed in the mass. After the streams are combined and the pH is adjusted, the target range is 3.8-4.2: at the lower end (3.8), the gel is firmer and fruitier; closer to 4.2, it is softer and creamier. Another important step in the experiment was pectin preparation. When pure pectin encounters water, it tends to form lumps, hydrating on the outside while remaining dry inside. Pre-mixing it with sugar at a 1:5 ratio separates the particles and enables uniform dissolution at 85-90°C within 5-7 minutes. The critical control points for producing the developed fillings are presented in Table 4.

Table 4. *Process control parameters*

Parameter	Value	Control method
Pectin dissolution temperature	85-90°C	Reactor thermometer
Stream combining temperature	55-60°C	Mandatory for both streams
pH after combining (before correction)	4.0-4.5	pH meter or test strips
pH after lactic acid correction	3.8-4.2	pH meter
Filling/packing temperature	45-50°C	Gel sets on cooling

Source: *developed by the author based on A. Masud et al. (2024)*

The APA-series apple pectins used in the formulation form are more viscous and smoother gels than citrus pectins, which makes them especially suitable for fillings and gives the samples additional desirable organoleptic properties. The best filling sample was identified by sensory evaluation on a 10-point scale. The assessed indicators were colour and clarity, fruit flavour, aroma, creamy consistency, and behaviour within the product body. The final indicator was evaluated by filling éclairs with the prepared samples. Four samples of flour confectionery products were evaluated based on model systems: Sample 1 (control): Ultra-TEX + MCC; Sample 2: pectin (0.4%) + Termflo (4%); Sample 3: pectin (0.6%) + Termflo (3.6%); Sample 4: pectin (0.8%) + Ultra-TEX (3.2%). The results of the organoleptic evaluation are presented on Figure 4.

Sample 3, containing 0.6% pectin, showed the best overall performance, with high scores Sample 3, containing 0.6% pectin, demonstrated the best overall performance, receiving high scores: 9 points for taste, 8 points for creamy texture, and 10 points for behaviour within the product, particularly for viscosity. The sample's overall average score was 8 points. The control sample, prepared according to a traditional recipe, received the lowest scores for taste and aroma (2 points), with an average score of 5.1. Sample 2, which contained less pectin, also showed good results in the organoleptic evaluation – 7.3 points. A more detailed

analysis of individual organoleptic parameters reveals significant differences between the samples. Regarding colour and clarity, samples 2-4 – all containing LM pectin – received higher scores by more than the predefined 0.5-point threshold. This reflects pectin's ability to maintain a finer, more uniform emulsion of the milk fat phase within the aqueous gel matrix, resulting in a brighter and visually more uniform appearance. In contrast, the control formulation showed a tendency toward surface clouding after cooling, which is explained by the partial coalescence of fat particles in the absence of a pectin network.

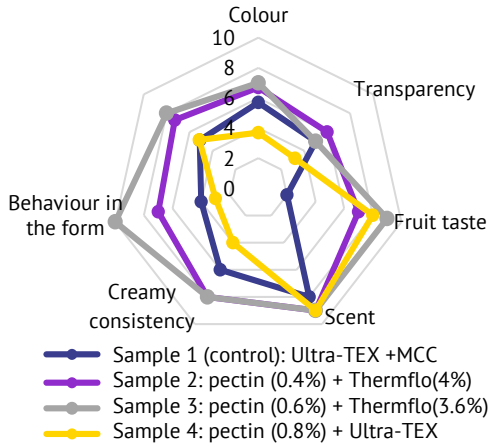

Figure 4. *Quality profile of filling samples based on the composition of pectin, microcrystalline cellulose and starch*

Source: developed by the author

The creamy consistency indicator was evaluated both before and after baking in éclair shells at 180-190°C for 22 minutes. Sample 3 retained its smooth, spreadable texture after baking with minimal evidence of moisture migration into the pastry wall, confirming the heat stability predicted by the rheological data. Sample 4 (0.8% pectin) showed a slightly firmer set, which several experts described as "gel-like" rather than "creamy", suggesting that the higher pectin concentration produces a texture that is less appropriate for cream-style fillings even though its rheological structure is adequate. Sample 2 (0.4% pectin) performed well in terms of mouthfeel but exhibited slightly greater moisture release after baking, consistent with its lower yield stress and weaker gel network observed in the Brookfield measurements.

The correlation between rheological and organoleptic results strengthens the validity of using Brookfield rotational viscometry as a predictive tool for sensory outcome in filling development. Systems with apparent viscosity in the range of 18,000-24,000 mPa·s at 10 rpm and a yield stress sufficient to resist flow under gravity at 45-50°C consistently received the highest panellist scores for "behaviour within the product body". This finding provides a practical viscosity target window that can be used for quality control in industrial production without the need for repeated full organoleptic panels during routine manufacture. An expert evaluation of the functional and technological properties of the developed fillings was also carried out on a 5-point scale. The results of the organoleptic evaluation are presented on Figure 5.

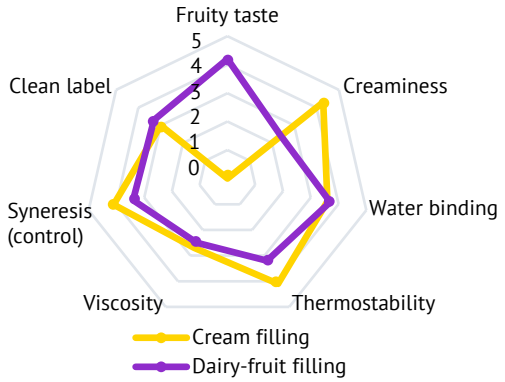

Figure 5. *Profile of functional and technological properties of the developed fillings*

Source: developed by the author

The main advantage demonstrated was the improvement in the functional properties of the semi-finished products and the enhanced organoleptic properties of the finished éclairs filled with the dairy-fruit filling. The results of this study contribute to a growing body of experimental evidence on the behaviour of combined hydrocolloid systems in heat-processed dairy-fruit fillings, and warrant interpretation in the context of current scientific knowledge on each functional mechanism identified. It was analysed that scientists I. Fraeye *et al.* (2009) demonstrated that low-methoxyl pectin (LMP) in combination with calcium ions provides superior gel stability in low-sugar fruit systems (below 55% sugar) compared with high-methoxyl pectin, noting that the calcium-crosslinked network retains integrity at baking temperatures up to 195°C, making LMP the preferred functional ingredient for heat-stable bakery fillings. Scientists are considering various studies of gelation mechanisms and network structural characteristics in polysaccharide gels at different scales of observation: macroscopic, microscopic, and molecular. O. Hrabovska *et al.* (2020) studied the structural and mechanical properties of fruit fillings for flour confectionery. The use of a composition of modified starch and pectin allowed to reduce the cost of production by replacing part of the expensive pectin with starch. Based on the study of the influence of hydrocolloids on the structure of the fruit filling, organoleptic characteristics, in particular, the migration of moisture into the shell during storage of the finished product, the optimal composition of the recipe mixture was

determined: pectin – 0.5%, modified starch – 4.5% of the mass of the filling with a dry matter content of 72%.

S.Y. Chan *et al.* (2017) studied the interaction between whey proteins and low-methoxyl pectin in acidified dairy systems and established that below pH 4.5, LM pectin forms electrostatic complexes with casein micelles that contribute to gel reinforcement, with complex formation proceeding most efficiently when the temperature at the time of mixing does not exceed 60°C – a finding directly applicable to the process stream control requirements of dairy-fruit filling production. The study (Syrbe *et al.*, 1998) examined the mechanism underlying the interaction between pectin and milk casein micelles and evaluated its effect on the stability of dairy colloidal systems. It was demonstrated that the interaction is primarily determined by the pH of the surrounding medium.

The pseudoplastic (shear-thinning) behaviour observed in all four model systems is consistent with what T.G. Mezger (2006) describes as the defining rheological signature of polymer network systems in which inter-chain entanglements are disrupted under shear but re-form upon cessation of flow. The flow behaviour index (n) values measured in this study followed a gradient from Sample 1 (n closest to 1.0, near-Newtonian) through Sample 4 (lowest n, strongest shear-thinning), demonstrating that LM pectin is the primary structural driver of pseudoplasticity in the mixed systems. This is consistent with the theoretical framework presented by J.F. Steffe (1996), who described how the contour length and flexibility of polysaccharide chains determine the onset and degree of shear-thinning in food biopolymer solutions. The finding that starch alone (Sample 1) produced near-Newtonian behaviour confirms that gelatinised modified starch contributes primarily to yield stress and gel body rather than to shear-thinning flow, while pectin governs the viscoelastic character of the composite system. The yield stress data, showing that hydroxypropyl distarch phosphate from waxy corn (Thermflo) produced higher structural resistance than the tapioca equivalent (Ultra-Tex) at the same concentration, can be explained by differences in amylopectin branch chain length distribution. E. Bertoft *et al.* (2024) reported that waxy corn amylopectin contains a higher proportion of short B1-chains (degree of polymerisation 15-25) relative to tapioca amylopectin, producing a more tightly clustered crystal lamella structure after gelatinisation that generates a stiffer, more elastic gel network on cooling. This structural difference translates directly into the higher yield stress and greater resistance to mechanical deformation observed for Thermflo-based systems in the present study.

The thixotropic hysteresis loop narrowing observed upon addition of MCC is a mechanistic finding not previously documented for dairy-fruit filling systems. Scientists M. Wang *et al.* (2025) demonstrated that cellulose particle networks in food gels function as structural "buffers": under high shear they deform elastically rather than rupturing, and upon relaxation they re-establish inter-particle contact points more rapidly than polymer chain re-entanglement allows. This mechanism explains why MCC addition did not substantially change the apparent viscosity at mid-range shear rates but significantly narrowed the hysteresis loop: the cellulose network restores structural connectivity faster than either the starch or pectin network alone, producing the improved thixotropic recovery observed in the present study. This property is of direct industrial relevance: narrower hysteresis means the filling reaches its target consistency more quickly after passing through the shear zone of a depositing nozzle, reducing the risk of drip defects and improving product-to-product consistency on a production line. The two-stage gelation behaviour of LM pectin in the presence of whey calcium – calcium-mediated pectin-pectin crosslinking at pH 5.0-4.9, followed by pectin-casein complex formation at pH 4.9-4.0 – is well established in the colloid chemistry of dairy-polysaccharide systems. Researchers F. Peyrano *et al.* (2019) studied the effect of processing temperature on the extent of this two-stage interaction and demonstrated that temperatures above 65°C at the point of pectin-whey contact promote irreversible aggregation of casein micelles by the calcium bridges in the pectin network, leading to gel inhomogeneity and reduced water-holding capacity. The critical control point temperature of 55-60°C established in the present study for combining the pectin and main process streams is therefore mechanistically justified: it is sufficiently low to prevent casein coagulation while remaining high enough to maintain pectin in solution and allow controlled junction zone formation on cooling.

The authors P. Himashree *et al.* (2022) state that factors such as temperature, shear force, pH, ionic strength, etc. affect the functionality of these thickeners and should be carefully optimised by food manufacturers during formulation development. In addition, the type of thickener used affects the functionality of the product. The addition of a protein-based thickener increases the content of amino acids (arginine, cysteine, histidine, lysine, proline and γ-aminobutyric acid) and contributes to improved nutritional and rheological properties. The heat stability of the optimised Sample 3 during baking at 185-190°C – evidenced by the complete absence of macroscopic syneresis in éclair shells – can be attributed to the thermoreversibility characteristics of calcium-crosslinked LM pectin junction zones. According to D. Gawkowska *et al.* (2018), the gel-to-sol transition temperature of a biopolymer network is primarily governed by the binding energy of the junction zone type: ionic calcium bridges in LM pectin have substantially higher thermal stability than the hydrogen bonds that govern high-methoxyl pectin gelation, which is why LM pectin gels remain intact at temperatures that would dissolve HM pectin

structures. The present study provides direct empirical confirmation of this principle under realistic industrial baking conditions, and demonstrates that the thermal stability is further enhanced when the LM pectin network is embedded within a cross-linked starch matrix, suggesting a co-operative structural reinforcement mechanism between the two polymer networks. The organoleptic superiority of Sample 3 over the control formulation, particularly in colour and clarity (8.8/10 versus 6.4/10) and flavour (9.0/10 versus 6.2/10), reflects multiple concurrent improvements in the filling system. The higher colour and clarity scores arise from the ability of LM pectin to stabilise the fat-in-water emulsion: according to J.N. BeMiller (2018), anionic polysaccharides including LM pectin adsorb at the oil–water interface and create electrostatic repulsion between droplets, preventing coalescence and maintaining the fine emulsion structure that produces a brighter, more homogeneous appearance. The improved flavour scores are consistent with a reduction in heating intensity: the lower dry matter content of Sample 3 (58.4% vs 62.3%) required less total cooking time, preventing the Maillard browning and caramel off-flavour development that were identified as quality defects in the control formulation.

The establishment of a practical quality control viscosity window of 18,000-24,000 mPa·s at 10 rpm for dairy-fruit fillings represents one of the most directly applicable outcomes of this study for industrial practice. This finding aligns with the broader principle, described in F.B.A. Descallar *et al.* (2023), that rotational viscometry at a single representative shear rate provides an adequate proxy for full flow curve characterisation in routine production environments where time and instrument access are limited. The specific window identified in this study is consistent with the range reported for similar cream-type products in the literature, confirming that the Brookfield DV3T instrument protocol used here – 10 rpm, spindle SC4-27, 25°C, 60 s equilibration – provides a reliable and reproducible measurement basis for production-floor quality monitoring without the need for full rheological profiling. Taken collectively, the results of this study resolve an important practical knowledge gap: while the individual functional properties of LM pectin, cross-linked starch, and MCC in food systems have been well characterised in the prior literature, their combination in dairy-fruit fillings under industrial processing conditions – including the influence of whey calcium on LM pectin gelation, the critical stream-combining temperature, and the lactic acid addition sequence – had not previously been optimised as an integrated system. The process control framework established here provides a reproducible protocol that can be transferred directly to production without further laboratory development, which is the principal practical contribution of this work.

Conclusions

This study established the optimal stabilising system for a milk-based jelly filling for flour confectionery products, based on a systematic comparison of four model compositions. The three-component system comprising 0.6% low-methoxyl pectin (APA 104), 3.6% cross-linked waxy corn starch (Thermflo), and 0.4% microcrystalline cellulose (MCG 811) was identified as the optimal stabilising composition. It produced an apparent viscosity of 18,000-24,000 mPa·s at 10 rpm, the narrowest thixotropic hysteresis loop among all tested systems, and demonstrated complete absence of macroscopic syneresis after baking in éclair shells at 185-190°C for 22 minutes. Pectin was identified as the primary driver of pseudoplasticity (lowest flow behaviour index in Sample 4 at 0.8% pectin). The optimised formulation reduced dry matter content from 62.3% in the control to 58.4%, replacing Starch 385 with LM pectin and reducing sugar load, in line with clean-label reformulation requirements. The filling demonstrated improved freeze-thaw stability relative to the control and showed no phase separation after temperature cycling between -18°C and 20°C. The optimal concentration of MCC in cream dairy-fruit fillings was confirmed at 4 kg/t (0.4% of product mass). Within the range of 4-6 kg/t, texture stability is maximised and rubberiness is absent; below 3.5 kg/t, syneresis risk increases; above 6 kg/t, mouthfeel becomes excessively firm.

Expert organoleptic evaluation confirmed that Sample 3 achieved the highest quality polygon area among all tested samples, with top scores for creamy consistency (8/10) and behaviour within the product body (10/10), and the lowest scores assigned to the control formulation for Fruit taste (2/10) and 4/10 for behaviour in the form. Based on the effects of the hydrocolloids on filling structure, organoleptic quality, and moisture migration into the product body during storage, the optimal formulation was established as follows: pectin, 0.6%; modified starch, 3.6%; and microcrystalline cellulose, 0.4%. This formulation ensured a stable creamy gel structure, minimal syneresis during baking and freezing, good heat stability, and better organoleptic properties than the control. In dairy-fruit systems containing MCC, emulsification and overall stability were improved, while the desired creamy mouthfeel was maintained, making MCC particularly suitable for low-fat and low-calorie products. Future research should assess shelf-life stability over a 6-12-month storage period under real distribution conditions, quantify freeze-thaw cycle resistance using industrial freezing protocols, and explore the applicability of the optimised stabilising system to other flour confectionery formats.

Acknowledgements

The authors wish to thank the team at FRUT EKS LLC (Trebukhiv, Brovary district, Kyiv region, Ukraine)

for their collegial support and close collaboration throughout the experimental work. The authors also extend their appreciation to the expert panel members who contributed to the sensory evaluation of the filling samples.

Funding

The study was not funded.

Conflict of Interest

None.

References

[1] Alam, M., Dar, B.N., & Nanda, V. (2024). Hydrocolloid-based fruit fillings: A comprehensive review on formulation, techno-functional properties, synergistic mechanisms, and applications. *Journal of Texture Studies*, 55(4), article number e12861. doi: 10.1111/jtxs.12861.

[2] BeMiller, J.N. (2018). *Carbohydrate chemistry for food scientists* (3rd ed.). Cambridge: Woodhead Publishing, AACC International Press. doi: 10.1016/C2016-0-01960-5.

[3] Bertoft, E., Blennow, A., & Hamaker, B.R. (2024). Perspectives on starch structure, function, and synthesis in relation to the backbone model of amylopectin. *Biomacromolecules*, 25(9), 5389-5401. doi: 10.1021/acs.biomac.4c00369.

[4] Brookfield Engineering. (2017). *More solutions to sticky problems: A guide to getting more from your Brookfield viscometer*. Middleboro: AMETEK Brookfield.

[5] Cao, Y., & Miao, L. (2023). Consumer perception of clean food labels. *British Food Journal*, 125(2), 433-448. doi: 10.1108/BFJ-03-2021-0246.

[6] Chan, S.Y., Choo, W.S., Young, D.J., & Loh, X.J. (2017). Pectin as a rheology modifier: Origin, structure, commercial production and rheology. *Carbohydrate Polymers*, 161, 118-139. doi: 10.1016/j.carbpol.2016.12.033.

[7] Civille, G.V., & Carr, B.T. (2016). *Sensory evaluation techniques* (5th ed). Boca Raton: CRC Press. doi: 10.1201/b19493.

[8] Descallar, F.B.A., Yang, X., Geonzon, L.C., & Matsukawa, S. (2023). Network structure and molecular mechanisms of food gels viewed from macroscopic, microscopic and molecular levels. *Food Science and Technology Research*, 29(3), 171-195. doi: 10.3136/fstr.FSTR-D-22-00170.

[9] DSTU 7662:2014. (2015). *Food concentrates. Methods for the determination of organoleptic indicators, the readiness of concentrates for use and the assessment of the dispersity of the suspension*. Retried from https://surl.li/tteeog.

[10] DSTU ISO 1842:2006. (2006). *Fruit and vegetable products – determination of pH*. Retried from https://online.budstandart.com/ua/catalog/doc-page.html?id_doc=83131

[11] EFSA Panel on Food Additives and Nutrient Sources added to Food (ANS), *et al.* (2018). Re-evaluation of celluloses E 460(i), E 460(ii), E 461, E 462, E 463, E 464, E 465, E 466, E 468 and E 469 as food additives. *EFSA Journal*, 16(1), article number e05047. doi: 10.2903/j.efsa.2018.5047

[12] Fraeye, I., Doungla, E., Duvetter, T., Moldenaers, P., van Loey, A., & Hendrickx, M. (2009). Influence of intrinsic and extrinsic factors on rheology of pectin-calcium gels. *Food Hydrocolloids*, 23(8), 2069-2077. doi: 10.1016/j.foodhyd.2009.03.022.

[13] Gallery, C., Agoda-Tandjawa, G., Bekaert, D., & Gitto, L. (2024). Understanding structure/rheology relationships of amidated low-methoxyl citrus and apple pectin gels: Implications of sucrose, pectin types and characteristics. *Food Hydrocolloids*, 152, article number 109950. doi: 10.1016/j.foodhyd.2024.109950.

[14] Gawkowska, D., Cybulska, J., & Zdunek, A. (2018). Structure-related gelling of pectins and linking with other natural compounds: A review. *Polymers*, 10(7), article number 762. doi: 10.3390/polym10070762.

[15] Goryunov, O., & Stetsenko, N. (2005). Fruit filler for food products. *Utility Model Patent*, 9465.

[16] Himashree, P., Sengar, A.S., & Sunil, C.K. (2022). Food thickening agents: Sources, chemistry, properties and applications – a review. *International Journal of Gastronomy and Food Science*, 27, article number 100468. doi: 10.1016/j.ijgfs.2022.100468.

[17] Hrabovska, O., Kravchenko, M., & Sabadash, N. (2020). Fruit fillings for flour products based on the modified starch and pectin. *Commodity Science. Technologies. Engineering*, 33(1), 64-77. doi: 10.31617/tr.knute.2020(33)07.

[18] Huang, L., Fan, J., Han, C., Du, C., Wei, Z., & Du, D. (2025). Methods and instruments for the evaluation of food texture: Advances and perspectives. *Food Research International*, 208, article number 116162. doi: 10.1016/j.foodres.2025.116162.

[19] Innova Market Insights. (n.d.). *Innova is a global market insights provider with an international network of CPG specialists covering six continents. Meet some of the skilled experts inspiring innovation and driving growth for our customers around the world*. Retrieved from https://www.innovamarketinsights.com/about/.

[20] ISO 11136:2014. (2014). *Sensory analysis – methodology – general guidance for conducting hedonic tests with consumers in a controlled area*. Retried from https://surl.li/khhxzx.

[21] Kumar, A., Alam, M., Kumari, K., & Nanda, V. (2026). Transformation of quality attributes of dough, bakery products, and bakery fillings using diverse hydrocolloids: A concise review. *Journal of Food Process Engineering*, 49(2), article number e70388. doi: 10.1111/jfpe.70388.

[22] Liu, Y., Wu, Q., Zhang, J., Yan, W., & Mao, X. (2024). Food emulsions stabilized by proteins and emulsifiers: A review of the mechanistic explorations. *International Journal of Biological Macromolecules*, 261, article number 129795. doi: 10.1016/j.ijbiomac.2024.129795.
[23] Masud, A., Basharat Nabi, D., & Vikas, N. (2024). Development and characterisation of nutritionally enriched honey filling as novel alternative to commercial fat-based filling for bakery applications. *Food and Humanity*, 3, article number 100361. doi: 10.1016/j.foohum.2024.100361.
[24] Mezger, T.G. (2006). *The rheology handbook: For users of rotational and oscillatory rheometers*. Hannover: Vincentz Network.
[25] OG Analysis. (2025). *2025 heat-stable fruit fillings market report: industry size, competition, trends and growth opportunities by region – forecast by types and applications (2024-2032)*. Hague: OG Analysis. Retried from https://www.marketresearch.com/OG-Analysis-v3922/Heat-Stable-Fruit-Fillings-Size-39507820/.
[26] Peyrano, F., de Lamballerie, M., Avanza, M.V., & Speroni, F. (2019). Rheological characterization of the thermal gelation of cowpea protein isolates: Effect of pretreatments with high hydrostatic pressure or calcium addition. *LWT*, 115, article number 108472. doi: 10.1016/j.lwt.2019.108472.
[27] Poudel, J., Bhattarai, S., Nath, N., & Tanti, B. (2025). An exclusive review of microcrystalline cellulose: Structure and applications, and limitations. *Materials Today Communications*, 45, article number 112247. doi: 10.1016/j.mtcomm.2025.112247.
[28] Romero-Rosales, M., Romero-Luna, H.E., Cantú-Lozano, D., Andrade-González, I., & Luna-Solano, G. (2025). Functionality and modifications of food hydrocolloids: An approach to starch. *Starch*, 77(9), article number e70083. doi: 10.1002/star.70083.
[29] Steffe, J.F. (1996). *Rheological methods in food process engineering*. New York: Freeman Press.
[30] Syrbe, A., Bauer, W.J., & Klostermeyer, H. (1998). Polymer science concepts in dairy systems – an overview of milk protein and food hydrocolloid interaction. *International Dairy Journal*, 8(3), 179-193, doi: 10.1016/S0958-6946(98)00041-7.
[31] Wang, M., Jiang, G., Guo, X., Zeng, S., & Zhao, D. (2025). Cellulose functional gels: Physical design and promising applications. *Advanced Physics Research*, 4(6), article number 2500020. doi: 10.1002/apxr.202500020.

Оптимізація рецептури желейної начинки на молочній основі з використанням мікрокристалічної целюлози та пектину

Ніна Стеценко
Науковий співробітник з розробки рецептур
Somafina
84041, 851 North McCormick Way, м. Лейтон, США
https://orcid.org/0009-0006-8781-6417
Наталія Шаповалова
Кандидат технічних наук, доцент
Державний торговельно-економічний університет
02156, вул. Кіото, 19, м. Київ, Україна
https://orcid.org/0000-0002-9143-8600
Дмитро Антюшко
Кандидат технічних наук, доцент
Державний торговельно-економічний університет
02156, вул. Кіото, 19, м. Київ, Україна
https://orcid.org/0000-0002-4135-6439

Анотація. Молочно-фруктові начинки для борошняних кондитерських виробів залишаються недостатньо дослідженими з технологічного погляду, хоча до них висуваються високі експлуатаційні вимоги: структурна стабільність під час випікання за температури 180–190°C, стійкість до синерезису та збереження однорідної кремоподібної текстури після циклів заморожування–розморожування. Метою дослідження було оптимізувати рецептуру желейної начинки на молочній основі з використанням трикомпонентної стабілізаційної системи, що складалася з низькометоксильованого пектину (LMP, APA 104), модифікованого крохмалю (воскоподібного кукурудзяного Thermflo та тапіокового Ultra-Tex) і мікрокристалічної целюлози (MCC 811, E460). Було виготовлено чотири модельні системи зі сталим вмістом сухих речовин 8 %, які оцінювали методом ротаційної віскозиметрії (Brookfield DV3T) та експертного органолептичного аналізу за 10-бальною шкалою. Встановлено, що рецептура, яка містила 0,6 % низькометоксильованого пектину, 3,6 % модифікованого крохмалю та 0,4 % мікрокристалічної целюлози (зразок 3), характеризувалася уявною в'язкістю 18 000-24 000 мПа·с за частоти обертання 10 об/хв, найвужчою петлею гістерезису серед усіх досліджених систем і найвищими експертними оцінками кольору та прозорості (8,8 бала), кремоподібної консистенції (9,1 бала) і поведінки в структурі виробу після випікання (8,9 бала). Порівняно з контрольною промисловою рецептурою оптимізована начинка мала нижчий вміст сухих речовин — 58,4 % проти 62,3 %, не виявляла видимого синерезису після випікання в оболонках еклерів і характеризувалася значно вищою стабільністю після заморожування–розморожування. Додавання мікрокристалічної целюлози в кількості 4 кг на тонну начинки забезпечувало колоїдну стабілізацію, звужувало реологічну петлю гістерезису та покращувало тиксотропне відновлення. Одержані результати свідчать, що синергічна комбінація низькометоксильованого пектину, зшитого крохмалю та мікрокристалічної целюлози є ефективним і придатним для промислового масштабування рішенням для розроблення термостійких молочно-фруктових начинок із «чистою етикеткою»

Ключові слова: модифікований крохмаль; гідроколоїди; низькометоксильований пектин; молочно-фруктова начинка; реологія; термостійкість; гелеутворення

COMMODITY BULLETIN
Journal homepage: https://c-bulletin.com.ua/en
DOI: 10.62763/cb/1.2026.56

Article's History: Received: 08.01.2026 Revised: 16.04.2026 Accepted: 28.05.2026 Published: 29.05.2026

ISSN 2310-5283; e-ISSN 3041-1432 Vol. 19, No. 1, 2026, 56-72

UDC 637.133:637.12.04/.07

Effect of pasteurisation on physicochemical and microbiological properties of milk

Georgi Terziyski*
Doctor of Engineering, Chief Asisstant
University of Food Technologies
4002, 26 Maritsa Blvd., Plovdiv, Bulgaria
https://orcid.org/0009-0003-6847-4480

Abstract. Study was to determine the effect of pasteurisation regimes on the quality and microbiological safety of milk. Five independent production batches of milk from the "Vereya" and "Bozhentsy" brands were examined. The samples were pasteurised at 63°C for 30 minutes, 72°C for 15 seconds and 85°C for 10 seconds, after which their parameters were determined immediately after treatment, and on the third and seventh days of refrigerated storage. Raw milk of the "Vereya" brand was characterised by higher protein and dry matter content and greater viscosity, whilst "Bozhentsy" milk had higher titratable acidity and initial microbial count. All the treatment regimes studied reduced alkaline phosphatase activity to below the established limit, and *Salmonella spp., Listeria monocytogenes, Escherichia coli* and coagulase-positive staphylococci were not detected in the pasteurised samples. The logarithmic reduction in the total number of microorganisms was 3.40, 3.91 and 4.33 $\log_{10}$, respectively, for the treatment regimes of 63°C for 30 minutes, 72°C for 15 seconds and 85°C for 10 seconds. Treatment at 85°C resulted in the lowest residual microbial count; however, this was accompanied by the retention of only 69.1% of soluble whey proteins, a colour difference of ΔE^* 2.50 and an increased aftertaste of boiled milk. The 72°C for 15 seconds treatment ensured the retention of 87.8% of soluble whey proteins, the highest sensory acceptability after seven days of storage, and a slower recovery of the microflora compared with the 63°C for 30 minutes treatment. The results obtained can be used by process engineers at Bulgarian dairy processing plants to select pasteurisation parameters, by quality control laboratories to compile testing programmes, and by producers of drinking milk to adjust production processes without compromising the microbiological safety or consumer properties of the products

Keywords: alkaline phosphatase; soluble serum proteins; sensory acceptability; mesophilic microorganisms; psychrotrophic microflora; colour difference; cold storage

Introduction

Research relevance is determined by the need to determine the optimal pasteurisation regime for milk, one that ensures its microbiological safety whilst minimising changes to its physicochemical and sensory properties. When assessing the stability of yoghurt enriched with 5% and 10% chia seeds, G. Nakov *et al.* (2024) monitored the physicochemical, microbiological and sensory changes over a 21-day storage period at a temperature of 4 ± 1°C. During this period, the pH of the control sample decreased by 0.17 units, whilst in the variants containing 5% and USD 10 chia, it decreased by 0.08 and 0.13 units, respectively; the number of lactic acid bacteria decreased from 9.005 to 8.775 log CFU/g in the control and from 8.495 to 8.150 log CFU/g in the sample with a 10% additive. The protein composition and biologically active components of donkey milk were systematised by N.N. Zheleva (2022), which focused primarily on lysozyme, lactoferrin and whey

Suggested Citation:
Terziyski, G. (2026). Effect of pasteurisation on physicochemical and microbiological properties of milk. *Commodity Bulletin*, 19(1), 56-72. doi: 10.62763/cb/1.2026.56.

*Corresponding author (terziyski.g@outlook.com)

proteins, which are sensitive to the conditions of collection and processing. According to the summarised data, the average concentration of lysozyme was approximately 1.07 g/l, its activity ranged from 1,670 to 11,531 U/ml, and the lactoferrin content varied from approximately 0.0048 to 0.080 g/l. Changes in the composition of traditional sheep's cheese made from the milk of the Karakachan breed during ripening were studied by S. Stankov *et al.* (2023). The dry matter, total protein and fat contents increased by approximately 7, 3 and 4% respectively; the water content decreased by 7%; and on day 60%, the proportions of saturated and unsaturated fatty acids accounted for 66% and 34% of their total amount.

A comparison of traditional thermal and non-thermal methods of treating raw cow's milk, with equivalent microbiological efficacy, was conducted by J. Chen *et al.* (2024). The application of high hydrostatic pressure of 400 MPa for 5 minutes resulted in a loss of approximately 6% of IgG and 16.2% of lactoferrin, whilst at 600 MPa the corresponding losses reached 79.4% and 31.36% and following ultra-high-temperature treatment – 97.16% and 70.85%. In a study by T. Yu *et al.* (2022), the effects of high hydrostatic pressure of 600 MPa for 15 minutes, pasteurisation at 72°C for 15 seconds, and the sequential application of both treatments during 30 days' storage at 4°C were compared. The total count of aerobic bacteria after pressure treatment remained below 2.22 log CFU/ml, whereas in pasteurised and combined-treated milk it exceeded 5.00 log CFU/ml; however, the sensory evaluations of the samples after pressure treatment were lower. The effect of pasteurisation temperature and cold storage conditions on the growth of spore-forming bacteria was determined by T.T. Lott *et al.* (2023) for milk treated at 75, 85 or 90°C for 20 s. On day 14, the average microbial count was 1.82, 3.55 and 6.86 log CFU/ml at storage temperatures of 3, 6.5 and 10°C, respectively, whilst the calculated time to reach 10^6 CFU/ml was reduced from 68 to 27 and 10 days. The microbiota of 17 samples of commercial pasteurised milk with a shelf life of 1 to 15 days were analysed by J. Zhao *et al.* (2024). Proteobacteria, Firmicutes and Bacteroidetes accounted for 94.54 ± 4.22% of the bacterial community, whilst the Enterococcus faecium SFM2 strain isolated from milk retained 82.58 ± 0.01% of viable cells after two hours' incubation at 50°C, compared with 28.20 ± 0.04% for a strain of different origin. Changes in enzymatic activity and protein composition during the industrial stages of milk pasteurisation, whey production and its reheating during the manufacture of whey protein concentrate were assessed by J. Haas *et al.* (2025). Following the first heating, xanthine oxidase activity decreased by approximately 15%; in unpasteurised whey, 25-45% of the initial activity was retained, whereas after pasteurisation, only 6-12% remained; at the same time, the concentrations of lactoferrin, IgA and IgM decreased.

The effects of thermal pasteurisation and sterilisation on the microbiological safety, protein profile, vitamin content and sensory properties of milk, as summarised by A. Rabbani *et al.* (2025). According to the data cited by the authors, following high-temperature short-time pasteurisation, 59-76% of immunoglobulin activity and 70-90% of lactoperoxidase activity were retained, whilst heating at 80°C for 15 s resulted in the retention of over 75% of lysozyme activity. The practical impact of cold chain disruptions on the stability of pasteurised milk was examined by M. Al-Farsi *et al.* (2021) based on the results of a survey of 281 retail outlets and 12-day storage of products from two manufacturers at temperatures of 5 and 8°C. The temperature exceeded 5°C in 50.2% of the outlets surveyed, whilst the total microbial count ranged from 3,960 to 8,680 CFU/ml in the products of the first manufacturer and from 15 to 48 CFU/ml in those of the second; the safe storage period at 5°C was determined to be nine days. The analysed studies demonstrated that changes in milk depend on the composition of the raw material, the processing regime, residual microflora and storage conditions. However, these studies did not comprehensively compare treatment regimes of 63°C for 30 minutes, 72°C for 15 seconds and 85°C for 10 seconds on independent batches of milk from two Bulgarian manufacturers, whilst simultaneously assessing the physicochemical, microbiological and sensory parameters over a seven-day storage period.

Study aimed to determine the effect of three pasteurisation temperature-time regimes on the physicochemical, microbiological and sensory properties of milk from the "Vereya" and "Bozhentsy" brands, and to identify the most balanced treatment regime. To achieve this aim, the following objectives were set: to compare the initial characteristics of the milk from both brands; to assess changes in its quality and microbiological safety following pasteurisation at 63°C for 30 minutes, 72°C for 15 seconds and 85°C for 10 seconds, and during seven days' cold storage; to determine the processing regime that ensured adequate microbiological safety whilst minimising changes in the physicochemical and sensory properties.

Materials and Methods

A laboratory-based experimental study was conducted in June 2026 at the Department of Milk and Dairy Products Technology and the University Laboratory of the University of Food Technologies, Plovdiv, Bulgaria. Microbiological tests were conducted at the accredited food testing laboratory LB Bulgaricum n.d., registration number of the Bulgarian Accreditation Service (n.d.) No. 138 LI. Samples for microbiological analysis were collected under aseptic conditions into separate sterile, airtight containers and labelled with the brand code, batch number, pasteurisation conditions and test date. They were transported to the laboratory in thermal

containers with ice packs at a temperature of 2-6°C, which was continuously monitored by a Testo 174 T electronic data logger. The duration of transport did not exceed four hours, and microbiological analysis commenced immediately upon the samples' arrival at the laboratory. Samples found to have compromised seals, incorrect labelling or deviations from the required temperature range were excluded from analysis.

The study was based on a factorial design with repeated measurements and covered two factors, both between and within production batches: the brand of milk and the pasteurisation temperature-time profile. For parameters determined during storage, the time of analysis was an additional factor. A production batch of milk was considered to be an independent experimental unit. Each batch was divided between an untreated control and three pasteurisation regimes; therefore, the variants C, P1, P2 and P3, formed from a single batch, were treated as paired observations. Parallel laboratory measurements were not considered as separate independent observations.

The study addressed standardised cow milk from two Bulgarian brands. Milk from the "Vereya" (n.d.) brand, which forms part of the United Milk Company's portfolio, was coded as TM-A. Milk from the "Bozhentsi" brand, produced by ELVI Ltd. (n.d.), was coded as TM-B. Milk with a target fat content of 2.5% was obtained from each manufacturer; it was sampled from the production line after clarification, separation, standardisation and homogenisation, but before industrial heat treatment. Using milk before the pasteurisation stage assessed the direct effect of the treatment regimes under investigation, rather than the consequences of reheating the finished pasteurised or ultra-pasteurised product. Five independent production batches, manufactured on different days, were sampled from each manufacturer. The total sample comprised ten batches: A1-A5 for TM-A and B1-B5 for TM-B. The interval between the sampling of the first and last batches from a single manufacturer did not exceed 30 days. From each batch, 10.5 dm^3 of milk was sampled, so the total volume of the test material was 105 dm^3. Of this volume, 1.20 dm^3 was used for the untreated control, 2.79 dm^3 each for each of the three pasteurisation regimes, and 0.93 dm^3 was retained as a reserve. This volume ensured that physico-chemical, microbiological and sensory analyses could be conducted in separate sealed containers at each stage of the analysis.

The milk was sampled directly from the process tank following standardisation and homogenisation. Before sampling, the contents of the tank were stirred following production regulations. Clean, airtight containers made of food-grade polymer were used for physico-chemical analyses, whilst pre-sterilised containers were used for microbiological tests. Each sample was labelled with the brand code, production batch number, and the date and time of sampling. After sampling, the samples were placed in thermal containers with ice packs. The temperature during transport was maintained within the range of 2-6°C and monitored using a Testo 174 T electronic data logger (Testo SE & Co. KGaA, Germany). The duration of transport did not exceed four hours. Before pasteurisation, the milk was stored at a temperature of 4 ± 1°C for no longer than 12 hours. Before a batch was included in the experiment, its appearance, colour, odour, homogeneity and the absence of flakes, sediment and mechanical impurities were assessed. The presence of antibacterial and other inhibitory substances was tested using the Delvotest T test system. Batches with a positive or inconclusive result were excluded from the experiment.

After gentle mixing, each batch was divided into four variants. The control variant K was not subjected to heat treatment and was used to determine the initial physicochemical properties and initial microbial contamination. Variant P1 was pasteurised at 63 ± 0.5°C for 30 minutes. Variant P2 was treated at 72 ± 0.5°C for 15 seconds. Variant P3 was subjected to intensive heat treatment at 85 ± 0.5°C for 10 seconds. The treatment regimes of 63°C for 30 minutes and 72°C for 15 seconds corresponded to the minimum temperature-time combinations for extended low-temperature and short-duration high-temperature pasteurisation, as established by European Union legislation (Regulation (EC) No. 853/2004 of the European Parliament and of the Council, 2004). The 85°C for 10 s treatment was used as an experimental intensified treatment to assess the additional reduction in residual microflora and heat-induced changes in the protein system, colour, viscosity and sensory profile. A total of 40 treatment variants were established: ten production batches, each of which was divided between the control and three pasteurisation regimes. These 40 variants were not considered completely independent, as four variants derived from a single batch shared a common origin.

The milk was pasteurised in a Julabo CORIO CD-B13 circulating thermostatic water bath (JULABO GmbH, Germany). For each treatment, 31 sterile, thin-walled glass containers with a capacity of 100 cm^3 were used. Each vessel was filled with 90 cm^3 of milk and sealed with a sterile lid. Thirty vessels were used for laboratory and sensory studies, whilst one identically filled vessel was used for temperature control. A type T thermocouple, connected to a Testo 176 T4 data logger, was placed at the geometric centre of the control vessel. Once the treatment was complete, the containers were transferred to an ice-water bath and cooled to a temperature not exceeding 6°C for 15 minutes. The duration of cooling and the final temperature were recorded in the laboratory report. The containers were weighed before and after heating on a Radwag AS 220. R2 analytical balance (RADWAG Wagi Elektroniczne, Poland). If the weight loss exceeded 0.5%, the relevant sample was discarded, and pasteurisation was repeated

using a reserve batch. The order of batch processing and pasteurisation regimes was determined by computerised randomisation. After pasteurisation, the containers were coded with random three-digit numbers. The specialists conducting the laboratory and sensory analyses were not informed of the brand name or pasteurisation regime until the initial data processing had been completed.

The pasteurised samples were stored in a cold room at a temperature of 4 ± 1°C. The temperature was continuously monitored using a Testo 174 T data logger. A batch was excluded from the study if the temperature decreased outside the permissible range for more than one hour. Of the 30 analytical containers for each pasteurised variant, 10 were used at the initial time point D0, four on the third day (D3) and 10 on the seventh day (D7). The remaining six containers were allocated to parallel microbiological analyses and sensory sessions. At each time point, individual containers were opened; reopening or returning the sample to storage was not permitted. Physicochemical and microbiological analyses at time point D0 were conducted immediately after cooling. Time points D3 and D7 corresponded to the third and seventh days of refrigerated storage. The untreated control milk was analysed only before pasteurisation.

The physico-chemical analysis included the determination of free and titratable acidity, density, fat content, total protein, lactose, dry matter, non-fat milk solids, freezing point, dynamic viscosity, colour characteristics, alcohol stability, concentration of soluble whey proteins and residual alkaline phosphatase activity. Active acidity was determined potentiometrically at a temperature of 20 ± 2°C using a Hanna Instruments HI 2211 pH meter (Hanna Instruments, Romania). Before each series of measurements, the instrument was calibrated using buffer solutions with pH values of 4.01, 7.01 and 10.01. The reading was recorded after the electrode had stabilised and was reported to an accuracy of 0.01 pH units. Titratable acidity was determined by the neutralisation method. To 10 cm^3 of milk, 20 cm^3 of distilled water and three drops of a 1% phenolphthalein alcohol solution were added. The mixture was titrated with a sodium hydroxide solution of 0.1 mol/dm^3 until a pale pink colour appeared, which persisted for one minute. The result was expressed in Turner degrees. Density was determined at a temperature of 20 ± 2°C using an AMT thermolactodensimeter (a milk hydrometer with a built-in thermometer) with a range of 1,015-1,040 kg/m^3. The result was corrected to a temperature of 20°C.

The mass fractions of fat, total protein, lactose, dry matter, dry non-fat milk solids and the freezing point were determined using mid-infrared spectroscopy on a MilkoScan FT1 analyser (FOSS, Denmark). Calibration and quality control of the instrument were conducted following ISO 9622:2013|IDF 141:2013 (2013). The mass fraction of dry matter was additionally verified by the gravimetric method following ISO 6731:2010|IDF 21:2010 (2010). Dynamic viscosity was determined using a Brookfield DV2T rotational viscometer fitted with an LV-1 spindle at a temperature of 20 ISO ± 0.5°C and a rotation speed of 60 rpm. The same measurement parameters were used for all samples. The result was expressed in mPa·s.

Colour was measured using a Konica Minolta CR-400 colourimeter (Konica Minolta, Japan) in the CIELAB colour space. The L^*, a^* and b^* coordinates were recorded. The overall colour difference from the raw milk of the corresponding batch was calculated using the following formula (1):

$$\Delta E^* = \sqrt{(\Delta L^*)^2 + (\Delta a^*)^2 + (\Delta b^*)^2}, \quad (1)$$

where ΔE^* – total colour difference between pasteurised and unprocessed milk; ΔL^* – difference between the lightness values of the test and control samples; Δa^* – difference in colour coordinates along the green-to-red axis; Δb^* – difference in colour coordinates along the blue-to-yellow axis. Values of ΔL^*, Δa^* and Δb^* were determined as the difference between the corresponding colour coordinates of the pasteurised sample and the raw milk from the same production batch.

Alcohol stability was assessed by mixing equal volumes of milk and ethyl alcohol at concentrations of 68%, 72%, 75% and 80%. The result was defined as the highest ethanol concentration at which no flakes, clots or marked coagulation were observed. The concentration of soluble serum proteins was determined after casein precipitation at pH 4.6. Samples were centrifuged for 15 minutes at 10,000 g and 4°C. The protein concentration in the supernatant was determined using the M.M. Bradford (1976) method at a wavelength of 595 nm, with bovine serum albumin used to establish the calibration curve. The degree of preservation of soluble serum proteins was calculated as the ratio of their concentration after pasteurisation to the concentration in the raw milk from the same batch, multiplied by 100%. Alkaline phosphatase activity was determined by a fluorometric method using the Fluorophos ALP Test System (Advanced Instruments, LLC, USA) based on ISO 11816-1:2024|IDF 155-1:2024 (2024). The result was expressed in mU/l. The test was considered negative if the enzyme activity did not exceed 350 mU/l, following Commission Implementing Regulation (EU) No. 2019/627 "Laying down uniform practical arrangements for the performance of official controls on products of animal origin intended for human consumption in accordance with Regulation (EU) 2017/625 of the European Parliament and of the Council and amending Commission Regulation (EC) No. 2074/2005 as regards official controls (Text with EEA relevance.)" (2019).

Active and titrated acidity, viscosity and colour were determined at points D0, D3 and D7. Density, mass

fractions of fat, protein, lactose, dry matter and non-fat milk solids, freezing point and alkaline phosphatase activity were determined at D0. Each physicochemical determination was conducted in triplicate. For statistical analysis, the mean value of the replicates within a single production batch and under the same operating conditions was used.

For microbiological analysis, after mixing, 10 cm^3 of milk was transferred to 90 cm^3 of sterile peptone-saline solution and a series of tenfold dilutions was prepared. The number of mesophilic aerobic and facultative anaerobic microorganisms was determined by the deep-plate method on Plate Count Agar, incubated at 30 ± 1°C for 72 ± 3 hours following ISO 4833-1:2013 (2013). Psychrotrophic microorganisms were determined by surface plating on Plate Count Agar and incubated at 6.5 ± 1°C for ten days based on ISO 17410:2019 (2019). *Enterobacteriaceae* in raw milk were counted on Violet Red Bile Glucose Agar following ISO 21528-1:2017 (2017). In pasteurised samples, a detection method with pre-enrichment was used following ISO 21528-1:2017, as the expected number of microorganisms was less than 100 CFU/ml. β-glucuronidase-positive *Escherichia coli* were identified on Tryptone Bile X-glucuronide Agar at 44 ± 1°C following ISO 16649-2:2001 (2001). Typical blue-green colonies were subject to confirmation. Coagulase-positive staphylococci were identified on Baird-Parker agar with egg yolk and tellurite supplement following ISO 6888-1:2021 (2021). Typical colonies were confirmed by the coagulase test. Yeasts and moulds were identified on Dichloran Rose Bengal Chloramphenicol Agar at a temperature of 25 ± 1°C based on ISO 21527-1:2008 (2008). Yeasts were counted after three days, and moulds after five days of incubation.

Bacteria suspected of belonging to the *Bacillus cereus* group were identified on Mannitol Egg Yolk Polymyxin Agar based on ISO 7932:2004 (2004). Typical colonies were subjected to confirmatory tests. *Salmonella spp*. were identified in 25 cm^3 of milk following ISO 6579-1:2017 (2017). The method involved non-selective and selective enrichment, plating onto selective media and confirmation of typical colonies. *Listeria monocytogenes* was detected in 25 cm^3 of milk using a two-stage enrichment method and plating onto Agar Listeria according to Ottaviani and Agosti (ALOA) agar following ISO 11290-1:2017 (2017). The total count of mesophilic and psychrotrophic microorganisms was determined in the raw milk and in pasteurised samples at time points D0, D3 and D7. *Enterobacteriaceae*, E. coli, coagulase-positive staphylococci, yeasts, moulds and B. cereus were determined in raw milk and in pasteurised samples at D0 and D7. *Salmonella spp*. and *L. monocytogenes* were determined in the raw milk of each batch and in all pasteurised samples at D0. Each quantitative determination was conducted in at least two parallel dishes. The results were expressed in CFU/ml and converted to $\log_{10}$ CFU/ml before statistical analysis. The logarithmic reduction in the total number of microorganisms was calculated separately for each batch as the difference between the $\log_{10}$ of the number of microorganisms in the raw milk and the $\log_{10}$ of their number in the corresponding pasteurised variant at D0. Results below the limit of quantification were reported as "< 1.00 $\log_{10}$ CFU/ml". For the purposes of statistical analysis, such results were assigned a value corresponding to half the method's limit of quantification.

The effectiveness of pasteurisation was assessed based on a set of criteria: alkaline phosphatase activity not exceeding 350 mU/l, the absence of *Salmonella spp*. and *L. monocytogenes* in 25 ml, the absence of *E. coli* in the tested volume, and compliance with the process criterion for *Enterobacteriaceae*. Compliance with the *Enterobacteriaceae* criterion was assessed at time point D0 based on a design of n = 5, c = 2, m < 1 CFU/ml and M = 5 CFU/ml, as established for pasteurised milk at the end of the production process (Commission Regulation (EC) No. 2073/2005, 2005). The D7 results were used to characterise microbiological stability during storage, rather than to assess compliance with the process criterion at the end of pasteurisation.

Sensory evaluation was conducted for variants P1, P2 and P3. The tasters were not served any unprocessed milk. The panel comprised 12 selected and trained assessors aged between 21 and 55. Selection and training were conducted based on ISO 22935-1:2023|IDF 99-1:2023 (2023), whilst the procedure for presenting and evaluating samples was conducted following ISO 22935-2:2023|IDF 99-2:2023 (2023). The study was conducted based on the principles of voluntariness, confidentiality and personal data protection stipulated in the ICC/Esomar International Code on Market, Opinion and Social Research and Data Analytics (2025) and the European Commission (2021) Guidelines on Ethics and Data Protection. Individuals with cow's milk protein allergy, lactose intolerance, acute respiratory diseases or impairments of smell and taste were excluded from participation.

The initial sensory evaluation was conducted following the laboratory acceptance of the samples. In the table of sensory results, this baseline was designated as D0, although it referred to the initial evaluation following confirmation of safety, and not necessarily the calendar day of pasteurisation. The second session was conducted at point D7. Samples were served in white, opaque glasses, coded with random three-digit numbers. The portion volume was 30 cm^3, and the serving temperature was 17 ± 2°C. The order of presentation was randomised using a balanced scheme. During a single session, each assessor analysed no more than six samples. Between samples, participants rinsed their mouths with still water and took a break of at least one minute.

The intensity of the milky flavour, the aftertaste of boiled milk and the sulphurous note were assessed, as

well as the uniformity of texture and overall acceptability. The intensity of the sensory characteristics was rated on a scale of 0 to 10 points: 0 – characteristic absent; 1 – barely perceptible; 2 – very faint; 3 – faint; 4 – moderately faint; 5 – moderate; 6 – moderately pronounced; 7 – pronounced; 8 – strong; 9 – very strong; 10 – maximally pronounced. Consistency and overall acceptability were assessed on a nine-point scale: 1 – extremely unacceptable; 2 – very unacceptable; 3 – unacceptable; 4 – somewhat unacceptable; 5 – neutral; 6 – somewhat acceptable; 7 – acceptable; 8 – very acceptable; 9 – highly acceptable.

The temperature-time regime was determined in two stages. In the first stage, any regime that did not result in a negative reaction to alkaline phosphatase, the absence of the pathogenic microorganisms under investigation, or compliance with the *Enterobacteriaceae* criterion at D0 was excluded from further comparison. In the second stage, amongst the regimes that met the safety criteria, the following were compared: the logarithmic reduction in microflora, the total microbial count at D7, the preservation of soluble serum proteins, the colour difference ΔE^*, the change in viscosity, alcohol resistance and overall sensory acceptability. The most balanced treatment was considered to be the one that ensured a lower microbial count and a slower recovery of microflora compared with the least intensive treatment, but caused fewer changes to the protein system, colour, viscosity and sensory profile compared with the most intensive heating treatment.

For each production batch, laboratory replicates were averaged to a single value. Physicochemical parameters were reported as the arithmetic mean and standard deviation. Microbiological results were analysed after conversion to $\log_{10}$ CFU/ml. The initial characteristics of milk from TM-A and TM-B were compared using Welch's t-test. Parameters determined only at time point D0 were analysed using a two-factor mixed-effects analysis of variance model, in which the brand, pasteurisation regime and their interaction were treated as fixed effects, whilst the production batch within the brand was treated as a random effect. For parameters determined at time points D0, D3 and D7, a linear mixed-effects model was applied, which included brand, pasteurisation regime, storage duration and their interaction as fixed effects, and the production batch as a random effect. Sensory parameters were analysed using a mixed-effects model, in which the brand, pasteurisation regime and evaluation period were fixed effects, whilst the evaluator and production batch were random effects. The critical level of statistical significance was $p < 0.05$. Statistical analysis was conducted using R version 4.5.1, with the lme4 and lmerTest packages.

Before each series of tests, the equipment was checked and calibrated based on manufacturer's instructions. For physico-chemical analyses, certified buffer solutions, standard milk samples, calibration solutions and blank samples were used. In each series of microbiological tests, the sterility of culture media, solvents, pipettes and laboratory glassware was verified. The reference strains *Escherichia coli* ATCC 25922, *Staphylococcus aureus* ATCC 25923, *Salmonella Typhimurium* ATCC 14028, *Listeria monocytogenes* ATCC 19115 and *Bacillus cereus* ATCC 11778 were used as positive control cultures. A separate protocol was maintained for each batch, recording the brand code, batch number, date and time of sampling, transport temperature, initial milk temperature, heating time, actual exposure temperature, holding time, cooling time, final temperature, mass before and after treatment, and the date of each analysis.

Results

Physicochemical properties of milk following pasteurisation and cold storage

Before heat treatment, initial differences were observed between the two brands of milk in terms of acidity, protein content, dry matter, non-fat milk solids and viscosity. The mass fractions of fat and lactose, as well as the density and freezing point, did not differ statistically between the samples under investigation (Table 1).

Table 1. *Initial physico-chemical parameters of milk from the brands under investigation*

Indicator	Vereya (TM-A)	Bozhentsy (TM-B)	p
Active acidity, pH	6.70 ± 0.02	6.68 ± 0.02	0.041
Titratable acidity, °T	16.3 ± 0.4	16.8 ± 0.4	0.018
Density, kg/m³	1,028.8 ± 0.3	1,029.1 ± 0.4	0.184
Fat content by mass, %	2.53 ± 0.04	2.49 ± 0.05	0.176
Protein content by mass, %	3.25 ± 0.05	3.18 ± 0.04	0.013
Mass fraction of lactose, %	4.72 ± 0.06	4.67 ± 0.05	0.062
Mass fraction of dry matter, %	11.56 ± 0.10	11.41 ± 0.12	0.029
Dry skimmed milk solids, %	9.03 ± 0.07	8.92 ± 0.09	0.021
Freezing point, °C	-0.530 ± 0.003	-0.528 ± 0.004	0.354
Dynamic viscosity, mPa·s	1.83 ± 0.04	1.76 ± 0.05	0.027

Note: *M ± SD are provided for five independent production batches*

Source: *compiled by the author based on ISO 6731:2010\|IDF 21:2010 (2010), ISO 9622:2013\|IDF 141:2013 (2013)*

The higher total protein content in TM-A milk was associated with a higher mass fraction of dry matter and non-fat milk solids. This combination of differences corresponded to a higher initial viscosity of this milk. The difference in the mass fraction of fat did not reach statistical significance; therefore, the differences in rheological properties were not related to the fat phase. TM-B milk was characterised by a higher titratable acidity – 16.8 ± 0.4°T compared with 16.3 ± 0.4°T in TM-A ($p = 0.018$), as well as a lower value for active acidity – pH 6.68 ± 0.02 compared with 6.70 ± 0.02 in TM-A ($p = 0.041$). The observed difference was not accompanied by signs of instability or protein coagulation. The alcohol test confirmed the stability of all initial batches against a 72% ethyl alcohol solution. Coagulation at an ethanol concentration of 75% was observed in two batches of TM-B and one batch of TM-A. Similar values for density, freezing point and lactose mass fraction indicated a comparable degree of milk standardisation and the absence of signs of water addition. The differences identified between the brands mainly concerned the protein and dry matter components and were addressed during the subsequent comparison of the milk's response to heat treatment. The temperature-time regime had a statistically significant effect on active and titratable acidity, viscosity, colour, the concentration of soluble whey proteins and the residual activity of alkaline phosphatase. The mass fractions of fat, total protein, lactose, dry matter and non-fat milk solids did not change significantly after pasteurisation (Table 2).

Table 2. *Physico-chemical properties of milk immediately after heat treatment*

Trademark	Mode	pH	Acidity, °T	Viscosity, mPa×s	ΔE^*	Retention of soluble serum proteins, %	Alkaline phosphatase, mU/l
TM-A	K	6.70 ± 0.02	16.3 ± 0.4	1.83 ± 0.04	0	100.0	> 10,000
	P1	6.68 ± 0.02	16.6 ± 0.4	1.86 ± 0.04	0.72 ± 0.18	92.8 ± 1.9	118 ± 21
	P2	6.67 ± 0.02	16.7 ± 0.3	1.87 ± 0.05	1.08 ± 0.20	88.7 ± 2.2	47 ± 13
	P3	6.63 ± 0.03	17.2 ± 0.4	1.94 ± 0.05	2.41 ± 0.27	70.3 ± 2.8	12 ± 5
TM-B	K	6.68 ± 0.02	16.8 ± 0.4	1.76 ± 0.05	0	100.0	> 10,000
	P1	6.66 ± 0.02	17.1 ± 0.4	1.80 ± 0.04	0.79 ± 0.16	91.3 ± 2.1	132 ± 25
	P2	6.65 ± 0.02	17.2 ± 0.3	1.81 ± 0.04	1.15 ± 0.19	86.9 ± 2.4	54 ± 15
	P3	6.61 ± 0.03	17.7 ± 0.4	1.89 ± 0.05	2.58 ± 0.31	67.8 ± 3.0	15 ± 6

Note: *K – raw milk; P1 – pasteurisation at 63°C for 30 minutes; P2 – at 72°C for 15 seconds; P3 – at 85°C for 10 seconds. Modes P1 and P2 correspond to the minimum temperature-time combinations for pasteurisation laid down in Regulation (EC) No. 853/2004 of the European Parliament and of the Council "Laying down specific hygiene rules for food of animal origin" (2004). ΔE^* is calculated using formula (1) in relation to the raw milk of the relevant production batch*

Source: *compiled by the author based on Regulation (EC) No. 853/2004 of the European Parliament and of the Council (2004), Commission Implementing Regulation (EU) No. 2019/627 (2019), ISO 11816-1:2024|IDF 155-1:2024 (2024)*

Following regimens P1 and P2, changes in pH and titratable acidity remained limited. Regime P3 was accompanied by a greater decrease in pH and an increase in titratable acidity in both brands. The interaction between brand and regime for these parameters was not statistically significant, indicating a similar response in the milk from the two manufacturers. The increase in viscosity depended on the processing temperature. After P1, the viscosity of TM-A milk increased from 1.83 ± 0.04 to 1.86 ± 0.04 mPa·s, i.e., by 1.6%, whilst that of TM-B milk increased from 1.76 ± 0.05 to 1.80 ± 0.04 mPa·s, or by 2.3%. After P2, the values were 1.87 ± 0.05 and 1.81 ± 0.04 mPa·s, respectively, which exceeded the initial vaues by 2.2% and 2.8%. After P3, the viscosity increased by approximately 6% relative to the initial level. This change was consistent with a reduction in the proportion of soluble whey proteins and the formation of additional protein interactions in the milk system. The retention of the soluble whey protein fraction after P1 exceeded 90% in the milk of both brands. After P2, the proportion of undenatured proteins decreased to approximately 87–89%. The P3 regime caused a reduction in this figure by almost a third. The difference between P3 and the other two regimes was statistically significant at $p < 0.001$.

Colour changes following P1 remained below one ΔE^* unit, whilst those following P2 approached one unit. Following P3, the total colour difference exceeded 2.4 units for both brands. The change was primarily due to a decrease in lightness (L^*) and an increase in the b^* coordinate, which corresponded to an intensification of the yellow hue. The residual alkaline phosphatase activity after all treatment regimes was below the threshold level of 350 mU/l. The highest values were observed after P1, although no batch exceeded the established limit. After P2 and P3, enzyme activity decreased further. Consequently, all the treatment regimes studied ensured an adequate pasteurisation effect, and regimes P1 and P2 met the minimum temperature-time combinations stipulated by European Union legislation (Regulation (EC) No. 853/2004 of the European Parliament and of the Council, 2004). The mass fraction of fat after heat treatment varied within the range of 0.01-0.03 percentage points, that of total protein within the range of 0.01-0.04 percentage points, and that of lactose by no more than 0.03 percentage points. No statistically significant differences were found between the control and pasteurised samples for these parameters. The freezing point also remained stable. After P1 and P2, all samples

remained homogeneous in a 75% ethanol solution. After P3, coagulation at this concentration was observed in three batches of TM-A and four batches of TM-B. At an ethanol concentration of 72%, all samples remained stable. Reduction in alcohol tolerance following P3 corresponded to a more pronounced restructuring of the protein-colloid system. Over the course of seven days of cold storage, all pasteurised samples showed a decrease in pH, an increase in titratable acidity and a gradual increase in viscosity. The extent of these changes depended on the brand, the pasteurisation method and the duration of storage (Table 3).

Table 3. *Changes in acidity and viscosity of pasteurised milk during storage*

Trademark	Mode	pH, D0/D3/D7	Acidity, °T, D0/D3/D7	Viscosity, mPa×s, D0/D3/D7
TM-A	P1	6.68 ± 0.009/6.64 ± 0.010/6.58 ± 0.011	16.6 ± 0.18/17.2 ± 0.20/18.1 ± 0.22	1.86 ± 0.018/1.90 ± 0.020/1.97 ± 0.022
	P2	6.67 ± 0.009/6.64 ± 0.010/6.60 ± 0.011	16.7 ± 0.13/17.1 ± 0.14/17.8 ± 0.16	1.87 ± 0.022/1.90 ± 0.024/1.95 ± 0.026
	P3	6.63 ± 0.013/6.61 ± 0.014/6.57 ± 0.016	17.2 ± 0.18/17.6 ± 0.20/18.4 ± 0.22	1.94 ± 0.022/1.98 ± 0.024/2.05 ± 0.026
TM-B	P1	6.66 ± 0.009/6.61 ± 0.010/6.53 ± 0.011	17.1 ± 0.18/17.9 ± 0.20/19.0 ± 0.22	1.80 ± 0.018/1.86 ± 0.020/1.95 ± 0.022
	P2	6.65 ± 0.009/6.62 ± 0.010/6.56 ± 0.011	17.2 ± 0.13/17.8 ± 0.14/18.6 ± 0.16	1.81 ± 0.018/1.85 ± 0.020/1.92 ± 0.022
	P3	6.61 ± 0.013/6.59 ± 0.014/6.54 ± 0.016	17.7 ± 0.18/18.1 ± 0.20/18.9 ± 0.22	1.89 ± 0.022/1.94 ± 0.024/2.01 ± 0.026

Note: *TMan values and approximate standard errors of the mean are given. D0 – immediately after pasteurisation; D3 – the third day; D7 – the seventh day of refrigerated storage. P1 – pasteurisation at 63°C for 30 minutes; P2 – at 72°C for 15 seconds; P3 – at 85°C for 10 seconds*

Source: *compiled by the author*

The greatest change in active acidity during storage was observed following storage regime P1. In TM-B milk, the decrease in pH was more pronounced than in the corresponding TM-A variant. The interaction between brand, storage regime and storage duration were statistically significant at p = 0.038. Following P2, acidity changed more slowly than following P1. On the seventh day, the pH value remained higher, whilst the titratable acidity was lower compared with low-temperature extended pasteurisation. This trend corresponded to a less intense recovery of residual microflora. The initial acidity values after P3 were higher than after P1 and P2. The subsequent increase during storage was of a smaller relative magnitude; however, the absolute level of titratable acidity on the seventh day remained elevated due to changes that occurred directly during heating. After seven days of cold storage, changes in colour characteristics, alcohol stability and the degree of preservation of soluble whey proteins in samples of pasteurised milk were analysed (Table 4).

Table 4. *Colour characteristics, alcohol stability and preservation of soluble serum proteins after seven days of refrigerated storage*

Trademark	Mode	L*, M ± SE	a*, M ± SE	b*, M ± SE	ΔE*, M ± SE	Alcohol tolerance, % ethanol	Retention of soluble serum proteins, %
TM-A	П1	86.4 ± 0.3	-0.62 ± 0.02	9.1 ± 0.2	1.42	74 ± 1.0	96.8 ± 0.4
	П2	85.7 ± 0.4	-0.58 ± 0.03	9.6 ± 0.3	1.71	72 ± 1.2	95.9 ± 0.5
	П3	83.9 ± 0.5	-0.51 ± 0.03	10.4 ± 0.3	3.01	68 ± 1.3	93.7 ± 0.6
TM-B	П1	87.1 ± 0.3	-0.65 ± 0.02	8.8 ± 0.2	1.54	75 ± 1.0	97.2 ± 0.4
	П2	86.2 ± 0.4	-0.60 ± 0.03	9.4 ± 0.3	1.89	73 ± 1.1	96.1 ± 0.5
	П3	84.10 ± 0.5	-0.52 ± 0.03	10.6 ± 0.3	3.24	69 ± 1.2	94.0 ± 0.6

Note: *Parameters determined on the seventh day of cold storage are presented. ΔE* was calculated using formula (1) relative to the untreated milk from the corresponding production batch. Alcohol stability is expressed as the highest concentration of ethanol at which no coagulation of the milk was observed*

Source: *compiled by the author*

Viscosity increased in all experimental treatments. Following P1, the increase was mainly attributable to changes during storage, whereas following P3, a significant proportion of the increase occurred immediately after pasteurisation. The P2 treatment was characterised by the smallest overall change in viscosity between the initial state and the seventh day. Colour characteristics also changed during storage. On the seventh day, the total colour difference after P1 was 1.42 units for TM-A and 1.54 units for TM-B. After P2, the corresponding values reached 1.71 and 1.89 units. After P3, the values rose to 3.01 and 3.24 units. The increase in ΔE* during storage was mainly due to a decrease in lightness and a subsequent shift of the b* coordinate in the positive direction. The proportion of soluble whey proteins on the seventh day decreased further by 1.8-2.7 percentage points after P1 and P2, and by 3.6-4.1 percentage points after P3. The decrease following storage was less pronounced than the changes resulting directly from pasteurisation but confirmed the ongoing restructuring of the protein system.

Microbiological safety, sensory properties and a comprehensive assessment of pasteurisation methods

Before pasteurisation, TM-B milk was characterised by a higher total count of mesophilic and psychrotrophic microorganisms. *Salmonella spp.* and *Listeria monocytogenes* were not detected in any of the source batches (Table 5). The average count of mesophilic aerobic and facultative anaerobic microorganisms in raw milk was 5.42 $\log_{10}$ CFU/cm^3 for TM-A and 5.61 $\log_{10}$ CFU/cm^3 for TM-B. The average count of psychrotrophic microorganisms was 4.11 and 4.29 $\log_{10}$ CFU/cm^3, respectively. The difference between the brands was statistically significant at $p < 0.05$. *Enterobacteriaceae* in the raw milk were detected at levels of 2.72 $\log_{10}$ CFU/cm^3 in TM-A and 2.91 $\log_{10}$ CFU/cm^3 in TM-B. Low numbers of β-glucuronidase-positive E. coli were detected in two batches of TM-A and three batches of TM-B. Coagulase-positive staphylococci were detected in all batches, but their numbers did not exceed 2.1 $\log_{10}$ CFU/cm^3. Presumptive *Bacillus cereus* group bacteria were detected at levels of 1.47-1.58 $\log_{10}$ CFU/cm^3. All pasteurisation regimes resulted in a significant reduction in the total number of vegetative microflorae. The extent of the reduction increased with rising treatment temperature.

Table 5. *Changes in the mesophilic and psychrotrophic microflora of pasteurised milk*

Trademark	Mode	Logarithmic reduction following pasteurisation, M±SE	Mesophilic microorganisms, $\log_{10}$ CFU/cm^3, D0/D3/D7, M±SE	Psychrotrophic microorganisms, $\log_{10}$ CFU/cm^3, D0/D3/D7, M±SE
TM-A	P1	3.39 ± 0.08	2.03 ± 0.07/2.81 ± 0.09/4.08 ± 0.12	< 1.00/1.92 ± 0.08/3.11 ± 0.11
	P2	3.88 ± 0.07	1.54 ± 0.06/2.34 ± 0.08/3.49 ± 0.10	< 1.00/1.56 ± 0.07/2.66 ± 0.09
	P3	4.30 ± 0.06	1.12 ± 0.05/1.78 ± ± 0.07/2.86 ± 0.09	< 1.00/1.18 ± 0.06/2.05 ± 0.08
TM-B	P1	3.40 ± 0.09	2.21 ± 0.08/3.04 ± 0.10/4.37 ± 0.13	< 1.00/2.16 ± 0.09/3.39 ± 0.12
	P2	3.93 ± 0.08	1.68 ± 0.07/2.51 ± 0.09/3.71 ± 0.11	< 1.00/1.73 ± 0.08/2.85 ± 0.10
	P3	4.36 ± 0.07	1.25 ± 0.06/1.94 ± 0.08/3.02 ± 0.10	< 1.00/1.30 ± 0.07/2.17 ± 0.09

Note: *a value of < 1.00 corresponded to a quantity below the limit of quantification. Note. D0 – immediately after pasteurisation; D3 – the third day; D7 – the seventh day of refrigerated storage. Value of < 1.00 corresponds to a microorganism count below the limit of quantification*

Source: *compiled by the author based on ISO 16649-2:2001 (2001), ISO 7932:2004 (2004), ISO 4833-1:2013 (2013), ISO 21528-1:2017 (2017), ISO 21528-2:2017 (2017), ISO 6579-1:2017 (2017), ISO 17410:2019 (2019), ISO 6888-1:2021 (2021), Bulgarian Accreditation Service (n.d.), LB Bulgaricum (n.d.)*

After P1, the total number of mesophilic microorganisms decreased by an average of 3.40 logarithmic units. After P2, the reduction was close to four logarithmic units, and after P3 it exceeded 4.3 logarithmic units. The effect of the treatment regime was statistically significant at $p < 0.001$. Immediately after pasteurisation, psychrotrophic microorganisms were detected below the limit of quantification in all variants. By the third day, their growth had resumed in all groups; however, the rate of accumulation depended on the treatment regime. The fastest increase was observed after P1, and the slowest after P3. On the seventh day, the difference between P1 and P2 in terms of the total number of mesophilic microorganisms was approximately 0.6-0.7 logarithmic units. The difference between P2 and P3 was smaller. The observed trends indicated that short-term pasteurisation at 72°C resulted in a lower residual microbial count and a slower rate of its recovery than the 63°C treatment for 30 minutes.

TM-B milk was characterised by higher rates of microbial regrowth during storage, regardless of the storage conditions. On the seventh day, the difference between the brands was statistically significant for the total number of mesophilic microorganisms and psychrotrophic microflora. An interaction between brand and storage conditions was observed for the total microbial count at $p = 0.041$. Immediately after pasteurisation at time point D0, *Enterobacteriaceae*, E. coli and coagulase-positive staphylococci were not detected in any of the samples analysed. In each group, all five production batches had an *Enterobacteriaceae* count below 1 CFU/cm^3. Consequently, the number of samples with values between m and M was c = 0, and with values above M was 0. Consequently, all pasteurisation regimes met the procedural criterion for *Enterobacteriaceae*: n=5, c = 2, m < 1 CFU/cm^3, M = 5 CFU/cm^3, as stipulated in Commission Regulation (EC) No. 2073/2005 "On microbiological criteria for foodstuffs (Text with EEA relevance)" (2005). On the seventh day, *Enterobacteriaceae* remained below the limit of quantification in all variants of P2 and P3. Following P1, isolated colonies were detected in two batches of TM-B; however, the average count did not exceed 10 CFU/cm^3. Yeast and mould were not detected after pasteurisation or were below the limit of quantification. On the seventh day, low numbers were detected mainly after P1. After P2, the count remained lower, and after P3, no colonies formed in most batches.

The number of presumptive *Bacillus cereus* bacteria decreased to a lesser extent after pasteurisation than the number of non-spore-forming microflora. After P1, the count was 1.22-1.34 $\log_{10}$ CFU/cm^3; after P2, 1.18-1.31 $\log_{10}$ CFU/cm^3; and after P3, 1.15-1.27 $\log_{10}$ CFU/cm^3. The limited difference between the treatment regimes corresponded to the survival of heat-resistant spores. On the seventh day, the

number of *Bacillus cereus* increased slightly, but did not exceed 1.7 $\log_{10}$ CFU/cm^3. The increase was greatest after P1. The result confirmed that the increase in pasteurisation temperature mainly affected vegetative cells, whilst the spore fraction was preserved under all conditions. *Salmonella spp.* and *Listeria monocytogenes* were not detected in any of the pasteurised samples. The absence of pathogenic microorganisms, E. coli and coagulase-positive staphylococci, was consistent with a negative reaction to alkaline phosphatase. The sensory profile depended on the intensity of the heat treatment and the duration of storage. Modes P1 and P2 retained the distinct milky flavour and aroma, whilst after P3 there was an increase in the aftertaste of boiled milk, a sulphurous note and changes in consistency (Table 6).

Table 6. *Sensory characteristics of milk after pasteurisation and storage*

Trademark	Mode	Milk taste, D0/D7	aftertaste of boiled milk, D0/D7	Consistency, D0/D7	Overall perception, D0/D7
TM-A	П1	8.3/7.4	1.3/1.7	8.2/7.5	8.4/7.2
	П2	8.4/7.9	1.6/1.9	8.3/7.9	8.5/7.8
	П3	7.4/7.0	4.1/4.5	7.8/7.4	7.3/7.1
TM-B	П1	8.0/7.0	1.4/1.9	7.9/7.1	8.0/6.8
	П2	8.2/7.6	1.8/2.1	8.0/7.6	8.2/7.5
	П3	7.1/6.7	4.4/4.8	7.5/7.0	7.0/6.8

Note: *D0 – initial sensory session conducted following the completion of laboratory testing and confirmation of the safety of the pasteurised samples; the designation D0 in this table does not necessarily correspond to the calendar day of pasteurisation. D7 – sensory evaluation after seven days of refrigerated storage. P1 – pasteurisation at 63°C for 30 minutes; P2 – at 72°C for 15 seconds; P3 – at 85°C for 10 seconds*

Source: *compiled by the author based on ISO 22935-1:2023|IDF 99-1:2023 (2023), ISO 22935-2:2023|IDF 99-2:2023 (2023)*

Immediately after processing, the highest overall acceptability was recorded for treatment P2. The difference between P1 and P2 was not statistically significant at the initial stage but became significant after seven days of storage. The decline in acceptability of P1 was associated with a reduction in the purity of the aroma, a weakening of the milky flavour and a change in consistency. Regime P3 received lower ratings as early as the day of pasteurisation. The main difference was an increase in the intensity of the boiled milk aftertaste. In addition, a sulphurous note was detected, with an average intensity of 2.7 points for TM-A and 3.0 points for TM-B. After P1 and P2, this indicator did not exceed 1.2 points. The overall acceptability of TM-A milk was higher than that of TM-B, although the difference depended on the storage conditions and duration. After P2, the difference between the brands was smaller than after P1. The interaction between brand, storage conditions and duration were statistically significant at $p = 0.044$. After seven days, the greatest decrease in overall acceptability was observed after P1. The deterioration in the sensory profile coincided with a more rapid increase in mesophilic and psychrotrophic microflora and an increase in titratable acidity. After P3, the overall rating changed less, but remained lower due to thermal characteristics formed during heating. Mode P2 ensured the greatest stability of sensory characteristics throughout storage. On the seventh day, the milky flavour remained pronounced, and the intensity of the boiled milk aftertaste did not exceed 2.1 points. The consistency remained uniform at a level of over 7.5 points. иАn integrated comparison was conducted among treatment regimes that met the microbiological safety criteria and were characterised by a negative reaction to alkaline phosphatase. The main criteria were the logarithmic reduction in microflora, its recovery during storage, the preservation of soluble serum proteins, colour change and overall sensory acceptability (Table 7).

Table 7. *Summary performance indicators for temperature-time regimes*

Indicator	Q1 63°C, 30 min	Q2 72°C, 15 s	Q3 85°C, 10 s
Average logarithmic reduction in microflora	3.40	3.91	4.33
Total count of microorganisms on D7, $\log_{10}$ CFU/cm^3	4.23	3.60	2.94
Retention of soluble serum proteins, %	92.1	87.8	69.1
Colour difference ΔE* at D0	0.76	1.12	2.50
Overall acceptability at D0, points	8.2	8.4	7.2
Overall acceptability at D7, points	7.0	7.7	7.0
Alkaline phosphatase activity	Below 350 mU/l	Below 350 mU/l	Below 350 mU/l

Source: *compiled by the author*

Mode P1 ensured the standard pasteurisation effect and the greatest preservation of the soluble whey protein fraction. At the same time, the most intense recovery of mesophilic and psychrotrophic microflora was observed during the seven days following P1. This process was accompanied by a more rapid decrease in

pH, an increase in titratable acidity and a reduction in sensory acceptability. Regime P3 resulted in the greatest logarithmic reduction in the total number of microorganisms and the lowest microbial count on the seventh day. At the same time, following this regime, the greatest loss of soluble whey proteins, an increase in viscosity, a reduction in alcohol resistance, a marked change in colour and the development of a thermal off-flavour were observed. Regime P2 occupied an intermediate position in terms of microbiological efficacy, but outperformed P1 in terms of stability during cold storage. The difference between P2 and P3 in terms of residual microbial count was statistically significant; however, both regimes ensured the absence of indicator and pathogenic microorganisms. Following Mode P2, the retention of soluble whey proteins remained higher than after Mode P3, whilst changes in colour, viscosity and sensory profile were less pronounced. On the seventh day, Mode P2 was characterised by the highest overall acceptability among the modes studied.

Mixed-effects models confirmed a significant effect of the pasteurisation regime on alkaline phosphatase activity, soluble serum protein concentration, viscosity, colour difference, total microbial count and sensory acceptability at $p < 0.001$. The effect of brand was significant for the initial protein content, dry matter, viscosity, initial microbial contamination and changes in acidity during storage. No statistically significant interaction between brand and storage conditions was found for the mass fraction of fat, protein, lactose, dry matter and alkaline phosphatase activity. For the microbial count on the seventh day, the rate of pH change and overall sensory acceptability, such an interaction was significant. The observed relationship indicated varying intensities of post-pasteurisation changes in the milk of the two brands under identical storage conditions. Based on the combined microbiological, physico-chemical and sensory parameters, the 72°C for 15 s treatment ensured compliance with safety criteria, a lower rate of recovery of residual microflora compared with the 63°C for 30 minutes, and a lesser degree of changes in the protein system and consumer properties compared with the 85°C for 10 seconds treatment. This treatment was identified as the temperature-time combination with the smallest overall deviation in quality parameters among the variants that ensured adequate microbiological efficacy.

Discussion

Absence of statistically significant changes in the mass fraction of fat, total protein, lactose, dry matter and non-fat milk solids following pasteurisation indicated that the main compositional characteristics of milk were preserved under the tested conditions. A similar pattern was observed by S. Lalwani *et al.* (2024), who, when comparing high-temperature short-time pasteurisation, enhanced pasteurisation, extended shelf-life treatment and ultra-high-temperature heating, found limited losses of macronutrients and total mineral content. At the same time, the authors recorded a reduction in the concentrations of vitamins B_1, B_2 and B_{12} and ionised calcium following enhanced pasteurisation, suggesting the possibility of changes in components not covered by the study.

Fact that the total mass fraction of protein remained unchanged did not imply the absence of structural changes in the protein system. The retention of soluble serum proteins was 92.1% after treatment at 63°C for 30 minutes, 87.8% after treatment at 72°C for 15 seconds, and 69.1% after treatment at 85°C for 10 seconds. Thus, raising the temperature to 85°C did not result in a quantitative loss of total protein, but led to the transition of a portion of the serum proteins from a soluble state to denatured and aggregated forms. The observed simultaneous increase in viscosity and decrease in alcohol resistance following the 85°C treatment confirmed a restructuring of the protein-colloidal system, rather than a change in total protein concentration. The results were consistent with the findings of S. Lalwani *et al.* (2024), who observed an increase in the size of casein micelles following industrial heat treatment of milk, although they did not detect a significant effect of the treatment regimes studied on its overall physical stability. The discrepancy between these data and the reduction in alcohol resistance observed in the samples studied may have been due to the use of the intensive treatment regime at 85°C for 10 s, the initial composition of the milk, and the sensitivity of the alcohol test to changes in the salt and protein balance.

Observed reduction in the proportion of soluble serum proteins does not provide grounds for directly concluding that there is a corresponding decrease in the nutritional value or digestibility of milk. According to a review by M. Fatih *et al.* (2021), heat treatment altered the structure of milk proteins and the nature of their digestion in model systems; however, studies involving adults were few in number, varied in terms of treatment regimens, and were associated with a moderate or high risk of systematic error. Some studies reported changes in post-consumption amino acid kinetics and dietary nitrogen retention, but no generalised long-term physiological effect was established. Therefore, in presented study, the preservation of soluble serum proteins should be regarded as an indicator of the intensity of the technological impact and the structural nativeness of the protein fraction, rather than as a direct indicator of the product's digestibility.

The change in colour following the 85°C treatment was greater than that observed after the other two pasteurisation treatments. The overall colour difference immediately after treatment averaged 2.50 units, whereas after treatments at 63 and 72°C, the values were 0.76 and 1.12 units respectively. The intensification

of the yellow hue and the reduction in lightness may have been associated with thermal denaturation of proteins, changes in the dispersibility of the colloidal phase, and the initial stages of the Maillard reaction. H. Bi *et al.* (2023) demonstrated that the intensity of the Maillard reaction in lactose-free milk depended on both pasteurisation and the temperature of subsequent storage. In this study, furozin, 5-hydroxymethylfurfural, intrinsic fluorescence and colour were monitored, and the degree of lactose hydrolysis reached 97.08%. When comparing these results, it was necessary to address that the hydrolysis of lactose produced glucose and galactose, which had a higher reactivity than the original lactose. Therefore, the colour change in standardised milk following the 85°C treatment indicated an intensification of thermal transformations, but did not confirm the formation of specific Maillard reaction products without their chromatographic determination.

The validity of this caveat was confirmed by Y. Li *et al.* (2021), who quantified furozin, furfurols and advanced glycation end-products following low-temperature prolonged, high-temperature short-time, ultra-high-temperature and in-vessel sterilisation of milk. The authors established a relationship between the accumulation of early, intermediate and final Maillard reaction products and the intensity of the heat treatment. During seven days' storage, colour difference values continued to increase, particularly following intensive pasteurisation. A similar effect of the combination of time and temperature was observed by C. Tyl *et al.* (2024) for standard and low-lactose ultra-high-temperature milk, which was stored at 4, 20 and 30°C for 30-90 days. The most pronounced darkening was observed in low-lactose milk stored at 30°C, with the sensory panel being able to distinguish between fresh and stored samples as early as 30 days. Although the duration and temperature in this study did not correspond to the conditions of the experiment conducted, the results confirmed that thermal changes did not cease once the product had left the pasteuriser and could continue during storage.

R. Ding *et al.* (2020), in a study of milk pasteurised at temperatures ranging from 72 to 85°C with varying exposure times, identified six dominant types and 18 genera of bacteria. The proportion of Pseudomonas exceeded 42% in all samples, and six genera of microorganisms showed statistically significant correlations with amino acids, fatty acids and volatile compounds in milk. These findings explained why an increase in the total microbial count in the samples studied was accompanied by changes in odour, taste and acidity: the residual microflora could influence not only safety but also the development of sensory defects.

A limited reduction in the number of presumptive *Bacillus cereus* group bacteria following an increase in temperature confirmed the heat resistance of the spore fraction. K. Medjahdi *et al.* (2025) identified aerobic spore-forming bacteria as one of the main causes of premature spoilage of pasteurised milk. Spores could enter the milk at the farm, survive pasteurisation, persist in the production environment, germinate under refrigeration conditions and produce proteolytic and lipolytic enzymes. Therefore, increasing the pasteurisation temperature from 72 to 85°C did not eliminate the need to monitor the quality of raw materials, the sanitary condition of equipment and post-pasteurisation contamination.

Significance of initial quality of the raw material was confirmed by differences between the brands. Milk from TM-B had a higher initial level of microbial contamination and was characterised by more intense recovery of mesophilic and psychrotrophic microflora on the seventh day. F. Enayaty-Ahangar *et al.* (2021) demonstrated that the optimal strategy for extending shelf life depended on the production volume of the enterprise and the quality of raw milk obtained from different suppliers. The models proposed by the authors addressed simultaneous application of incentives for farms with low spore counts and the introduction of spore-removal technologies at the processing plant. Consequently, the same pasteurisation regime did not guarantee the same shelf life for milk with different initial levels and compositions of contamination.

The risk of spores re-entering from the production environment was also not eliminated by increasing the pasteurisation temperature. C. Pretorius & E.M. Buys (2021) found that simulated on-site decontamination had a significant effect on over 98% of *Bacillus cereus* spores, but around 0.1% remained intact. The survival of a small proportion of viable spores was of technological significance due to the possibility of their subsequent attachment, germination and the formation of sources of recontamination. In the laboratory experiment conducted, secondary contamination was minimised using sealed containers; therefore, the actual dynamics of the microflora on an industrial production line might additionally depend on the effectiveness of washing, disinfection and the aseptic conditions of the areas downstream of the pasteuriser. The identified relationship between temperature, protein changes and the sensory profile was consistent with the findings of R. Shi *et al.* (2025), according to which traditional high-temperature methods increased microbiological stability but could cause losses in natural flavour and changes in nutritional components. The authors considered new thermal and non-thermal technologies as ways of reducing the severity of such changes; however, their application required a separate technological and economic justification for each specific product.

Results of cheese studies also confirmed that the sensory effects of pasteurisation depend on the product's structure. D. Tadjine *et al.* (2020) investigated the effect of pasteurising cow's and goat's milk on the yield and physicochemical characteristics of fresh cheese. A. Rezaei *et al.* (2020) established a statistically significant effect of pasteurisation and ripening

temperature on acidity, dry matter, fat, protein, proteolysis, lipolysis and the sensory properties of traditional Motal cheese. The direct applicability of these findings to drinking milk was limited due to the concentration of solids, enzymatic processes and the prolonged ripening of cheeses; however, both studies confirmed that the initial milk matrix determined the product's response to heat treatment. The dependence of the results on product composition was also observed in the study by K. Pudtikajorn *et al.* (2021), in which pasteurised cow's milk was enriched with nanoliposomes containing fat from tuna eyes and evaluated over ten days for physical, chemical, microbiological and sensory parameters. The presence of an additional lipid phase altered the stability and perception of the product; therefore, the results obtained for standardised milk without enriching components cannot automatically be extrapolated to functional milk drinks.

S.F. Tan *et al.* (2020) found that cow's and goat's milk retained their microbiological suitability for 22 days at 8°C following high-pressure treatment. In pasteurised goat's milk at the end of storage, the number of psychrotrophic bacteria reached 9.0×10^8 CFU/ml, whilst the total microbial count was 3.5×10^8 CFU/ml. Compared with the data obtained, this confirmed that a reduction in residual psychrotrophic microflora could extend the shelf life without the need for a treatment regime that caused significant denaturation of serum proteins. G. Liu *et al.* (2020) compared high hydrostatic pressure of 600 MPa for 5 minutes, combined with microfiltration, against traditional treatment regimes of 63°C for 30 minutes and 72°C for 15 seconds. The evaluation covered microbiological inactivation, volatile compounds, protein denaturation, simulated gastric digestion and sensory properties after eight days of storage. This comprehensive approach was consistent with the rationale of the study, as the processing regime was evaluated not based on a single safety indicator, but based on a combination of microbiological and consumer characteristics. The combination of short-duration pasteurisation with high pressure was investigated by H. Gong *et al.* (2024). Treating donkey's milk at 75°C for 15 s, followed by the application of a pressure of 300 MPa, extended the shelf life by 85.71%, preserved lysozyme, α-lactalbumin and β-lactoglobulin, and reduced the total plate count, coliforms and Staphylococcus aureus. Above 400 MPa, physical stability deteriorated; this, similar to the 85°C condition in presented study, indicated the existence of a limit to the intensity of the treatment, outside of which any additional microbiological efficacy was accompanied by undesirable structural changes.

The potential of this combined approach was also confirmed by the findings of C.F. Balthazar *et al.* (2022). Pasteurisation of sheep's milk using omic and conventional heating resulted in a reduction in microflora of at least 4.2 logarithmic units, but omic heating required 72-73% less energy. Over the course of 15 days' storage, the composition of the bacterial community changed: in raw milk, Staphylococcus initially predominated, whilst Pseudomonas predominated at the end of storage. This confirmed the need to assess not only the initial reduction in microorganisms but also the structure of the residual microbiota during storage. A.W.M. Alsaedi *et al.* (2023) proposed non-thermal treatment of milk using a moderate electric field at temperatures below 42°C. Under optimal parameters of 29.8 V/cm and a flow rate of 0.018 kg/s, energy consumption was reduced by 98.58%, specific energy consumption by 98.51%, and the duration of the process by 99.09% compared with conventional pasteurisation. These results demonstrated the potential for reducing the thermal load; however, industrial application required confirmation of microbiological safety for different batches of raw materials, an assessment of electrochemical changes, and verification of stability during storage.

J.A. Ansari *et al.* (2020) considered the use of ultraviolet treatment of already pasteurised skimmed milk as an additional control measure against psychrotrophic spore-forming bacteria. This approach did not replace primary pasteurisation, but could be used as a barrier technology to reduce residual microflora. A limitation of UV treatment of milk remained its optical opacity; therefore, its effectiveness depended on the reactor design, layer thickness, agitation and the dose delivered. The approach that came closest to practical implementation of the results was the combination of pasteurisation with microfiltration. S. Gammoh *et al.* (2026), following the implementation of appropriate hygiene and production practices and a hazard analysis system, used membranes with pore sizes of 0.8 and 0.45 μm. The refrigerated storage life of whole milk was approximately two weeks, and that of milk with a fat content of 2% was approximately three weeks; denaturation of α-lactalbumin and β-lactoglobulin remained negligible. These results supported the advisability of maintaining a 72°C treatment for 15 s with a further reduction in bacterial load, rather than raising the temperature to a level at which the proportion of soluble whey proteins decreased to 69.1%.

Thus, the results of the comparison confirmed that the optimal pasteurisation regime should be determined not only by the level of microbial inactivation, but also by considering the preservation of the protein fraction, the physico-chemical properties and the sensory acceptability of the product. The most balanced regime was found to be 72°C for 15 s, which ensured sufficient microbiological safety, a negative alkaline phosphatase reaction, the preservation of 87.8% of soluble whey proteins and the highest acceptability on the seventh day of storage. This demonstrates the advisability of applying the concept of minimum sufficient heat treatment, whilst further extension of the shelf life

should be achieved primarily through quality control of raw materials, prevention of post-pasteurisation contamination, and the combination of pasteurisation with additional barrier technologies. At the same time, the findings require industrial validation, considering the seasonality of raw materials, cold chain conditions, the characteristics of processing equipment and a broader range of quality indicators.

Conclusions

Study found that the temperature-time profile of pasteurisation determined the nature of changes in the physicochemical, microbiological and sensory characteristics of milk from the "Vereya" and "Bozhentsy" brands. The initial samples differed in terms of protein content, dry matter, viscosity, titratable acidity and initial microbial contamination; however, the direction of the changes following heat treatment was similar for both brands. Pasteurisation at 63°C for 30 minutes resulted in a reduction in the total number of microorganisms by an average of 3.40 logarithmic units and the preservation of 92.1% of soluble whey proteins. At the same time, during seven days of refrigerated storage following this treatment, the most intense recovery of mesophilic and psychrotrophic microflora, an increase in titratable acidity and a decrease in sensory acceptability were recorded. The 85°C treatment for 10 s resulted in the greatest microbiological reduction, amounting to 4.33 logarithmic units, and the lowest residual microbial count on the seventh day. At the same time, it was found that only 69.1% of soluble whey proteins were retained, the colour difference increased to 2.50 units, viscosity increased, alcoholresistance decreased, and the aftertaste of boiled milk became more pronounced.

Pasteurisation at 72°C for 15 seconds resulted in a reduction in microflora of 3.91 logarithmic units, the retention of 87.8% of soluble whey proteins, a negative reaction to alkaline phosphatase, and the absence of the pathogenic and indicator microorganisms under investigation. Under this treatment regime, the highest sensory acceptability was recorded after seven days of storage, along with smaller changes in colour, viscosity and acidity compared with the more intense heating treatment. Consequently, the 72°C for 15 seconds treatment was identified as the most balanced in terms of the trade-off between safety and the preservation of consumer properties. The limitations of the study were related to the use of products from only two manufacturers, five batches of each brand and a seven-day observation period. Further studies should cover a larger number of manufacturers, seasonal milk batches, different fat contents, an extended analysis of vitamins and volatile compounds, as well as the simulation of industrial pasteurisation and packaging conditions.

Acknowledgements

None.

Funding

None.

Conflict of Interest

None.

References

[1] Al-Farsi, M., Al-Gharibi, I., Al-Abri, A., Al-Humaimi, A., Al-Nabhani, F., Al-Hashmi, H., Al-Sarmi, K., & Al-Shibli, S. (2021). Evaluating the shelf-life of pasteurized milk in Oman. *Heliyon*, 7(3), article number e06555. doi: 10.1016/j.heliyon.2021.e06555.

[2] Alsaedi, A.W.M., Al-Mousawi, A.J., Al-Hilphy, A.R., & Gavahian, M. (2023). Non-thermal pasteurization of milk by an innovative energy-saving moderate electrical field equipped with elongated electrodes and process optimization. *Innovative Food Science & Emerging Technologies,* 88, article number 103445. doi: 10.1016/j.ifset.2023.103445.

[3] Ansari, J.A., Ismail, M., & Farid, M. (2020). Extension of shelf life of pasteurized trim milk using ultraviolet treatment. *Journal of Food Safety,* 40(2), article number e12768. doi: 10.1111/jfs.12768.

[4] Balthazar, C.F., Cabral, L., Guimarães, J.T., Noronha, M.F., Cappato, L.P., Cruz, A.G., & Sant'Ana, A.S. (2022). Conventional and ohmic heating pasteurization of fresh and thawed sheep milk: Energy consumption and assessment of bacterial microbiota during refrigerated storage. *Innovative Food Science & Emerging Technologies,* 76, article number 102947. doi: 10.1016/j.ifset.2022.102947.

[5] Bi, H., Wang, Y., Guo, Y., Liao, Z., & Na, Z. (2023). Influence of pasteurization on Maillard reaction in lactose-free milk. *Molecules,* 28(20), article number 7105. doi: 10.3390/molecules28207105.

[6] Bradford, M.M. (1976). A rapid and sensitive method for the quantitation of microgram quantities of protein utilizing the principle of protein-dye binding. *Analytical Biochemistry,* 72(1-2), 248-254. doi: 10.1016/0003-2697(76)90527-3.

[7] Bulgarian Accreditation Service. (n.d.). *Register.* Retrieved from https://www.nab-bas.bg/en/registers.html.

[8] Chen, J., Zhang, J., Wang, N., Sun, X., Han, X., Yin, R., Pei, X., Liu, C., Pang, X., Huang, F., & Chen, A. (2024). Comparative study on microbiological, physicochemical and nutritional properties of whole cow milk by thermal and non-thermal processing technologies. *Food Bioscience,* 59, article number 104012. doi: 10.1016/j.fbio.2024.104012.

[9] Commission Implementing Regulation (EU) No. 2019/627 "Laying Down Uniform Practical Arrangements for the Performance of Official Controls on Products of Animal Origin Intended for Human Consumption in Accordance with Regulation (EU) 2017/625 of the European Parliament and of the Council and amending Commission Regulation (EC) No 2074/2005 as regards official controls (Text with EEA relevance.)". (2019, March). Retrieved from https://eur-lex.europa.eu/eli/reg_impl/2019/627/oj/eng.
[10] Commission Regulation (EC) No. 2073/2005 "On Microbiological Criteria for Foodstuffs (Text with EEA relevance)". (2005, November). Retrieved from https://eur-lex.europa.eu/eli/reg/2005/2073/oj/eng.
[11] Ding, R., Liu, Y., Yang, S., Liu, Y., Shi, H., Yue, X., Wu, R., & Wu, J. (2020). High-throughput sequencing provides new insights into the roles and implications of core microbiota present in pasteurized milk. *Food Research International,* 137, article number 109586. doi: 10.1016/j.foodres.2020.109586.
[12] ELVI Ltd. (n.d.). *Products.* Retrieved from https://www.elvimilk.bg/bg/products/.
[13] Enayaty-Ahangar, F., Murphy, S.I., Martin, N.H., Wiedmann, M., & Ivanek, R. (2021). Optimizing pasteurized fluid milk shelf-life through microbial spoilage reduction. *Frontiers in Sustainable Food Systems,* 5, article number 670029. doi: 10.3389/fsufs.2021.670029.
[14] European Commission. (2021). *Ethics and data protection*. Retrieved from https://ec.europa.eu/info/funding-tenders/opportunities/docs/2021-2027/horizon/guidance/ethics-and-data-protection_he_en.pdf.
[15] Fatih, M., Barnett, M.P.G., Gillies, N.A., & Milan, A.M. (2021). Heat treatment of milk: A rapid review of the impacts on postprandial protein and lipid kinetics in human adults. *Frontiers in Nutrition,* 8, article number 643350. doi: 10.3389/fnut.2021.643350.
[16] Gammoh, S., Alu'datt, M.H., Alhamad, M.N., Tranchant, C.C., Rababah, T., Alrosan, M., Obeidat, B., Alzoubi, H., & Al-Tawaha, A. (2026). Extending the shelf life of pasteurized milk through microfiltration and implementation of a comprehensive safety and quality management system: Case study at the farm and dairy plant. *Journal of Dairy Research*. doi: 10.1017/S0022029926102234.
[17] Gong, H., Wu, X., Du, J., & Mao, X. (2024). High hydrostatic pressure combined with high-temperature short-time pasteurization improves the quality characteristics and extends the shelf life of donkey milk. *LWT,* 196, article number 115789. doi: 10.1016/j.lwt.2024.115789.
[18] Haas, J., Kim, B.J., Atamer, Z., Wu, C., & Dallas, D.C. (2025). Effects of high-temperature, short-time pasteurization on milk and whey during commercial whey protein concentrate production. *Journal of Dairy Science,* 108(1), 257-271. doi: 10.3168/jds.2024-25493.
[19] ICC/Esomar International Code on Market, Opinion and Social Research and Data Analytics. (2025, July). Retrieved from https://iccwbo.org/wp-content/uploads/sites/3/2025/09/ICC-ESOMAR-International-Code-on-Market-Opinion-and-Social-Research-and-Data-Analytics-2.pdf.
[20] ISO 11290-1:2017. (2017). *Microbiology of the food chain – horizontal method for the detection and enumeration of Listeria monocytogenes and of Listeria spp. Part 1: Detection method*. Retrieved from https://www.iso.org/standard/60313.html.
[21] ISO 11816-1:2024|IDF 155-1:2024. (2024). *Milk and milk products – determination of alkaline phosphatase activity. Part 1: Fluorimetric method for milk and milk-based drinks*. Retrieved from https://www.iso.org/standard/85718.html.
[22] ISO 16649-2:2001. (2001). *Microbiology of food and animal feeding stuffs – horizontal method for the enumeration of beta-glucuronidase-positive Escherichia coli. Part 2: Colony-count technique at 44 degrees C using 5-bromo-4-chloro-3-indolyl beta-D-glucuronide*. Retrieved from https://www.iso.org/standard/29824.html.
[23] ISO 17410:2019. (2019). *Microbiology of the food chain – horizontal method for the enumeration of psychrotrophic microorganisms*. Retrieved from https://www.iso.org/standard/67437.html.
[24] ISO 21527-1:2008. (2008). *Microbiology of food and animal feeding stuffs – horizontal method for the enumeration of yeasts and moulds. Part 1: Colony count technique in products with water activity greater than 0.95*. Retrieved from https://www.iso.org/standard/38275.html.
[25] ISO 21528-1:2017. (2017). *Microbiology of the food chain – horizontal method for the detection and enumeration of Enterobacteriaceae. Part 1: Detection of Enterobacteriaceae*. Retrieved from https://www.iso.org/standard/55228.html.
[26] ISO 21528-2:2017. (2017). *Microbiology of the food chain – horizontal method for the detection and enumeration of Enterobacteriaceae. Part 2: Colony-count technique*. Retrieved from https://www.iso.org/standard/63504.html.
[27] ISO 22935-1:2023|IDF 99-1:2023. (2023). *Milk and milk products – sensory analysis. Part 1: Recruitment, selection, training and monitoring of assessors*. Retrieved from https://www.iso.org/standard/84531.html.
[28] ISO 22935-2:2023|IDF 99-2:2023. (2023). *Milk and milk products – sensory analysis. Part 2: Methods for sensory evaluation*. Retrieved from https://www.iso.org/standard/84532.html.
[29] ISO 4833-1:2013. (2013). *Microbiology of the food chain – horizontal method for the enumeration of microorganisms. Part 1: Colony count at 30°C by the pour plate technique*. Retrieved from https://surl.li/zzndsl.

[30] ISO 6579-1:2017. (2017). *Microbiology of the food chain – horizontal method for the detection, enumeration and serotyping of Salmonella. Part 1: Detection of Salmonella spp*. Retrieved from https://www.iso.org/standard/56712.html.
[31] ISO 6731:2010|IDF 21:2010. Milk, cream and evaporated milk – determination of total solids content (Reference method). (2010). Retrieved from https://www.iso.org/standard/56815.html.
[32] ISO 6888-1:2021. (2021). *Microbiology of the food chain – horizontal method for the enumeration of coagulase-positive staphylococci (Staphylococcus aureus and other species). Part 1: Method using Baird-Parker agar medium*. Retrieved from https://www.iso.org/standard/76672.html.
[33] ISO 7932:2004. (2004). *Microbiology of food and animal feeding stuffs – horizontal method for the enumeration of presumptive Bacillus cereus – colony-count technique at 30 degrees C*. Retrieved from https://www.iso.org/standard/38219.html.
[34] ISO 9622:2013|IDF 141:2013. (2013). *Milk and liquid milk products – guidelines for the application of mid-infrared spectrometry*. Retrieved from https://www.iso.org/standard/56874.html.
[35] Lalwani, S., Lewerentz, F., Håkansson, A., Löfgren, R., Eriksson, J., Paulsson, M., & Glantz, M. (2024). Impact of thermal processing on micronutrients and physical stability of milk and cream at dairy production scale. *International Dairy Journal,* 153, article number 105901. doi: 10.1016/j.idairyj.2024.105901.
[36] LB Bulgaricum. (n.d.). *Accredited laboratory.* Retrieved from https://surl.li/prabjg.
[37] Li, Y., Wu, Y., Quan, W., Jia, X., He, Z., Wang, Z., Adhikari, B., Chen, J., & Zeng, M. (2021). Quantitation of furosine, furfurals, and advanced glycation end products in milk treated with pasteurization and sterilization methods applicable in China. *Food Research International,* 140, article number 110088. doi: 10.1016/j.foodres.2020.110088.
[38] Liu, G., Carøe, C., Qin, Z., Munk, D.M.E., Crafack, M., Petersen, M.A., & Ahrné, L. (2020). Comparative study on quality of whole milk processed by high hydrostatic pressure or thermal pasteurization treatment. *LWT,* 127, article number 109370. doi: 10.1016/j.lwt.2020.109370.
[39] Lott, T.T., Wiedmann, M., & Martin, N.H. (2023). Shelf-life storage temperature has a considerably larger effect than high-temperature, short-time pasteurization temperature on the growth of spore-forming bacteria in fluid milk. *Journal of Dairy Science,* 106(6), 3838-3855. doi: 10.3168/jds.2022-22832.
[40] Medjahdi, K., Didouh, N., & Araujo, R. (2025). Pasteurized milk: A highlight on potential sources of contamination by aerobic spore-forming bacteria. *Food Control,* 171, article number 111134. doi: 10.1016/j.foodcont.2025.111134.
[41] Nakov, G., Ninova-Nikolova, N., Ivanova, N., Raykova, V., Trajkovska, B., Čolić, M.L., Lukinac, J., & Jukić, M. (2024). Yogurt enriched with chia seeds: Physicochemical, microbiological, and sensory changes during storage. *Fermentation,* 10(8), article number 431. doi: 10.3390/fermentation10080431.
[42] Pretorius, C., & Buys, E.M. (2021). Extended shelf life milk processing: Effect of simulated cleaning in place on the germination and attachment of *Bacillus cereus* spores. *International Journal of Dairy Technology,* 74(1), 75-83. doi: 10.1111/1471-0307.12744.
[43] Pudtikajorn, K., Sae-leaw, T., & Benjakul, S. (2021). Characterization of fortified pasteurized cow milk with nanoliposome loaded with skipjack tuna eyeball oil. *International Journal of Food Science & Technology,* 56(11), 5893-5903. doi: 10.1111/ijfs.15196.
[44] Rabbani, A., Ayyash, M., D'Costa, C.D.C., Chen, G., Xu, Y., & Kamal-Eldin, A. (2025). Effect of heat pasteurization and sterilization on milk safety, composition, sensory properties, and nutritional quality. *Foods,* 14(8), article number 1342. doi: 10.3390/foods14081342.
[45] Regulation (EC) No. 853/2004 of the European Parliament and of the Council "Laying down specific hygiene rules for food of animal origin". (2004, April). Retrieved from https://eur-lex.europa.eu/eli/reg/2004/853/oj/eng.
[46] Rezaei, A., Alirezalu, K., Damirchi, S.A., Hesari, J., Papademas, P., Domínguez, R., Lorenzo, J.M., & Yaghoubi, M. (2020). Effect of pasteurization and ripening temperature on chemical and sensory characteristics of traditional Motal cheese. *Fermentation,* 6(4), article number 95. doi: 10.3390/fermentation6040095.
[47] Shi, R., Gu, Y., Zhang, Q., Ding, Y., & Fan, X. (2025). Effects of different sterilization methods on milk quality: A comparative analysis. *Food Science of Animal Products,* 3(3), article number 9240132. doi: 10.26599/FSAP.2025.9240132.
[48] Stankov, S., Fidan, H., Dincheva, I.N., Balabanov, A., & Petrova, I. (2023). Changes in physicochemical, microbiological and fatty acid composition during the ripening period of artisan sheep cheese from Bulgaria. *Food Science and Applied Biotechnology*, 6(1), 38-46. doi: 10.30721/fsab2023.v6.i1.218.
[49] Tadjine, D., Boudalia, S., Bousbia, A., Khelifa, R., Mebirouk Boudechiche, L., Tadjine, A., & Chemmam, M. (2020). Pasteurization effects on yield and physicochemical parameters of cheese in cow and goat milk. *Food Science and Technology,* 40(3), 580-587. doi: 10.1590/fst.13119.

[50] Tan, S.F., Chin, N.L., Tee, T.P., & Chooi, S.K. (2020). Physico-chemical changes, microbiological properties, and storage shelf life of cow and goat milk from industrial high-pressure processing. *Processes,* 8(6), article number 697. doi: 10.3390/pr8060697.
[51] Tyl, C., Johansen, S.M., Kristoffersen, K.A., Devold, T.G., Brønner, K.W., & Johansen, A.-G. (2024). Effect of storage temperature on the physicochemical and sensory properties of regular and lactose-reduced low-fat UHT milk. *International Dairy Journal,* 159, article number 106065. doi: 10.1016/j.idairyj.2024.106065.
[52] Vereya. (n.d.). *Cow's milk Vereya.* Retrieved from https://vereia.bg/product-category/vereia-fresh-milk/.
[53] Yu, T., Zhang, X., Feng, R., Wang, C., Wang, X., & Wang, Y. (2022). Comparison of the effects of high hydrostatic pressure and pasteurization on quality of milk during storage. *Foods,* 11(18), article number 2837. doi: 10.3390/foods11182837.
[54] Zhao, J., Gong, J., Liang, W., & Zhang, S. (2024). Microbial diversity analysis and isolation of thermoresistant lactic acid bacteria in pasteurized milk. *Scientific Reports,* 14, article number 29705. doi: 10.1038/s41598-024-80947-5.
[55] Zheleva, N.N. (2022). Bioactive components of donkey milk. *Food Science and Applied Biotechnology,* 5(2), 219-231. doi: 10.30721/fsab2022.v5.i2.212.

Вплив пастеризації на фізико-хімічні та мікробіологічні властивості молока

Георгі Терзійський
Доктор технічних наук, старший асистент
Університет харчових технологій
4002, бульв. Маріца 26, м. Пловдив, Болгарія
https://orcid.org/0009-0003-6847-4480

Анотація. Дослідження мало на меті визначити вплив режимів пастеризації на якість та мікробіологічну безпеку молока. Було досліджено п'ять незалежних виробничих партій молока торгових марок «Верея» та «Боженці». Зразки пастеризували при температурі 63°C протягом 30 хвилин, 72°C протягом 15 секунд та 85°C протягом 10 секунд, після чого їх параметри визначали одразу після обробки, а також на третій та сьомий дні зберігання в холодильнику. Сире молоко марки «Верея» характеризувалося вищим вмістом білка та сухої речовини, а також більшою в'язкістю, тоді як молоко «Боженці» мало вищу титрувану кислотність та початкову мікробну кількість. Усі досліджені режими обробки знизили активність лужної фосфатази нижче встановленої межі, а *Salmonella spp., Listeria monocytogenes, Escherichia coli* та коагулазопозитивні стафілококи у пастеризованих зразках не були виявлені. Логарифмічне зменшення загальної кількості мікроорганізмів становило 3,40, 3,91 та 4,33 $\log_{10}$ відповідно для режимів обробки при температурі 63°C протягом 30 хвилин, 72°C протягом 15 секунд та 85°C протягом 10 секунд. Обробка при 85°C призвела до найнижчої залишкової кількості мікробів; однак це супроводжувалося збереженням лише 69,1 % розчинних білків сироватки, різницею в кольорі ΔE^* 2,50 та посиленням післясмаку кип'яченого молока. Обробка при 72°C протягом 15 секунд забезпечила збереження 87,8 % розчинних білків сироватки, найвищу сенсорну прийнятність після семи днів зберігання та повільніше відновлення мікрофлори порівняно з обробкою при 63°C протягом 30 хвилин. Отримані результати можуть бути використані інженерами-технологами на болгарських молочних заводах для вибору параметрів пастеризації, лабораторіями контролю якості для складання програм випробувань, а також виробниками питного молока для коригування виробничих процесів без шкоди для мікробіологічної безпеки чи споживчих властивостей продукції

Ключові слова: лужна фосфатаза; розчинні білки сироватки крові; сенсорна прийнятність; мезофільні мікроорганізми; психротрофна мікрофлора; різниця в кольорі; зберігання в холоді

COMMODITY BULLETIN
Journal homepage: https://c-bulletin.com.ua/en
DOI: 10.62763/cb/1.2026.73

Article's History: Received: 15.01.2026 Revised: 17.04.2026 Accepted: 28.05.2026 Published: 29.05.2026

ISSN 2310-5283; e-ISSN 3041-1432 Vol. 19, No. 1, 2026, 73-81

UDC 687.157.004

Study of the influence of weft yarn tension on the properties of woven-knitted material

Oksana Khrystiuk*
Vinnytsia Institute of Clothing Design and Entrepreneurship
21027, 42 Kosmonavtiv Ave., Vinnytsia, Ukraine
https://orcid.org/0009-0005-5700-5106
Oleh Nahaichuk
Vinnytsia Institute of Clothing Design and Entrepreneurship
21027, 42 Kosmonavtiv Ave., Vinnytsia, Ukraine
https://orcid.org/0009-0003-0612-774X
Elina Zakharova
Vinnytsia Institute of Clothing Design and Entrepreneurship
21027, 42 Kosmonavtiv Ave., Vinnytsia, Ukraine
https://orcid.org/0009-0008-6796-7415
Valentyna Horobchyshyna
Vinnytsia Institute of Clothing Design and Entrepreneurship
21027, 42 Kosmonavtiv Ave., Vinnytsia, Ukraine
https://orcid.org/0009-0000-9945-5889

Abstract. The relevance of the study is determined by the practical need to reduce weft yarn consumption while preserving the structural stability, tensile performance and commodity quality of a material that combines woven longitudinal strips with looped weft connections. The purpose of the article was to determine the influence of weft yarn tension on the physical, mechanical and structural properties of woven-knitted textile material article 10c2 produced on a Metap-160 laboratory machine. Polyester warp yarns with a linear density of 24.5 tex and multifilament polyester weft yarns with a linear density of 8.4 tex were used for the experimental samples. Weft tension was varied from 9.2 to 14.8 cN per yarn by changing the number and position of the regulating weights on the levers of the weft regulator. The study evaluated breaking force and breaking elongation in the warp and weft directions, the breaking characteristics of weft yarns withdrawn from the material, the projected length of the weft yarn in the plane of the material, the actual weft consumption per insertion, the produced width, the width of an individual woven-knitted strip, thickness, abrasion resistance, air permeability and the stability of the phase structure of the woven areas. It was established that within the investigated interval an increase in weft tension does not cause critical deterioration of the main performance indicators. The projected weft length decreased from 13.38 to 13.11 mm per insertion, the actual weft consumption from 15.28 to 14.81 mm per insertion, and the coefficient of weft consumption from 1.142 to 1.130, while the produced width decreased from 164.8 to 160.4 cm. The obtained relationships substantiate a multi-criteria approach in which weft tension is applied as a resource-saving factor only in combination with dimensional control of the material

Keywords: weft consumption; looped connection; Metap-160; air permeability; abrasion resistance; resource saving

Suggested Citation:
Khrystiuk, O., Nahaichuk, O., Zakharova, E., & Horobchyshyna, V. (2026). Study of the influence of weft yarn tension on the properties of woven-knitted material. *Commodity Bulletin*, 19(1), 73-81. doi: 10.62763/cb/1.2026.73.

*Corresponding author (ohristuk@gmail.com)

Introduction

Modern textile production increasingly requires structural solutions that combine stable mechanical behaviour with economical use of raw materials. For fabrics made from synthetic filament yarns, a small saving of yarn length per insertion becomes substantial when it is multiplied by industrial production lengths. The problem, however, is not purely economic. Excessive yarn consumption changes fabric geometry and mass per unit area and can influence air permeability, bending behaviour and dimensional stability, whereas an excessive reduction of the yarn reserve generates local stresses, unstable loop formation and narrowing of the material. Woven-knitted materials are particularly sensitive to this balance, because in them the weft simultaneously fills the shed inside the longitudinal woven strips and forms the loop columns that join those strips into a continuous sheet. The technological task is therefore to identify a controlled range of weft tension that saves raw material without creating defects or reducing consumer quality.

Recent experimental work has clarified how the parameters of the weft system govern fabric behaviour. M. Ayele *et al.* (2024) applied a full factorial design to plain woven fabric and showed that weft tension, together with weft yarn type and weft density, alters the porous structure of the fabric and consequently its thermal resistance, thermal conductivity and air permeability. The same research group (Kassaw & Ayele, 2024) established that an increase in weft and warp tension raises the surface roughness of the fabric and reduces its drape, which means that tension has to be treated as a quality-forming variable and not merely as a machine setting. S. Vasile *et al.* (2024) compared hemp-inen fabrics of different weaves and weft types and found that the tensile properties remained statistically unchanged when hemp weft replaced flax, while air permeability and moisture management differed significantly; this demonstrates that different groups of properties do not respond uniformly to one constructional change. N. Mandre *et al.* (2021) reported that a higher number of weft yarns per centimetre reduces the air permeability of denim fabrics but simultaneously improves their abrasion resistance, which again indicates a trade-off rather than a uniform improvement. Earlier, M. Maqsood *et al.* (2016) and M. Umair *et al.* (2016) modelled the influence of weave structure and thread density on the mechanical and comfort properties of woven fabrics and confirmed the statistical significance of these constructional factors.

For looped structures the closest analogy is provided by Ukrainian research on warp-knitted fabrics with laid-in weft. L. Melnyk *et al.* (2016) showed that the variant of the weft filling yarn changes the structural parameters and mechanical properties of warp-knitted fabric. In a later study O. Kyzymchuk *et al.* (2023) demonstrated that the type of weft yarn and the threading order of the additional yarn system determine the elasticity, dimensional stability and thermal comfort of elastic warp-knitted bands. These works consistently confirm that a yarn laid into a looped structure is a full participant in structure formation rather than a passive filling.

At the same time, three questions remain unresolved in the cited studies. First, the effect of tension has been quantified for a weft that performs a single function inside a woven or a knitted structure, but not for a weft that simultaneously forms the woven and the looped areas of one material. Second, the yarn length actually incorporated into the three-dimensional looped connection has not been separated from the yarn length visible in the plane of the material, so raw-material economy is estimated from a projection rather than from real consumption. Third, the influence of weft tension on the produced width – the parameter that in practice limits any tension-based saving – has not been quantified for woven-knitted materials formed on machines of the Metap type.

Accordingly, this article sought to clarify how variations in weft yarn tension, applied during the formation of woven-knitted material article 10c2 on a Metap-160 laboratory machine, translate into measurable changes in its mechanical, structural and dimensional behaviour. To achieve this purpose, three tasks were set: (1) to establish how weft tension within the interval of 9.2-14.8 cN per yarn affects the tensile characteristics of the material and of the weft yarns withdrawn from it; (2) to determine the projected and the actual weft consumption per insertion, the coefficient of weft consumption and the accompanying changes in the width of the material and of an individual woven-knitted strip; (3) to substantiate the criteria for selecting a tension regime that combines raw-material economy with the dimensional and commodity requirements for the material.

Materials and Methods

The experimental research was conducted in 2025 on a Metap-160 laboratory machine (Elitex, Czech Repuplic). The object of the study was woven-knitted textile material article 10c2, formed as a system of longitudinal woven strips joined across the width of the material by loop columns of weft yarns. Polyester yarns with a linear density of 24.5 tex were used in the warp system, and multifilament polyester yarns with a linear density of 8.4 tex were used in the weft system. The setting contained 3,498 warp yarns and 317 weft yarns; the nominal density of the material was 22 yarns/cm in the warp direction and 44 yarns/cm in the weft direction. The investigated weft tension range was 9.2-14.8 cN per yarn. These parameters were selected because the material is formed within this interval without visible defects, while the differences in yarn consumption remain measurable.

Weft yarn tension was regulated by changing the number of weights and their position on the levers of

the weft regulator. The operating principle of the regulator is based on the balance of moments acting on the movable unit of the weft beam: on one side of the system a torque is created by the tension of the weft yarns, and on the other side the system is loaded by the gravity force of the weft beam with the roller and by the moments created by the regulating weights. Changing the mass or the lever arm of the weights makes it possible to establish a different average tension of the weft yarns. In this research the regulator was used to obtain a sequence of six tension regimes within the investigated interval.

Before testing, the samples were conditioned in the standard atmosphere in accordance with ISO 139:2005 (2005). The breaking force and breaking elongation of the material in the warp and weft directions were determined by the strip method in accordance with ISO 13934-1:2013 (2013), and the breaking characteristics of the weft yarns withdrawn from the material in accordance with ISO 2062:2009 (2009). Thickness was measured in accordance with ISO 5084:1996 (1996), air permeability in accordance with ISO 9237:1995 (1995) and abrasion resistance by the Martindale method in accordance with ISO 12947-2:2016 (2016). The phase structure of the woven areas was assessed qualitatively on enlarged images of the material.

The projected length of the weft yarn was measured on enlarged images of the material structure and characterises the length of the yarn path visible in the plane of the textile sheet. Because woven-knitted material has a three-dimensional structure, this projection does not represent the whole yarn length incorporated into the looped connections. To determine the actual weft consumption, two adjacent strips with the loop column between them were cut from the material so that the weft yarns could be withdrawn with minimal disturbance of their shape. The length of the withdrawn weft yarns was measured on a section corresponding to 100 insertions and recalculated per one insertion. This procedure makes it possible to separate the geometric projection from the actual consumption.

To interpret the difference between the projected and the actual weft length, the coefficient of weft consumption was used:

$$K_{wc} = l_a / l_p, \quad (1)$$

where K_{wc} – the coefficient of weft consumption; l_a – the actual weft consumption per insertion, mm; l_p – the projected length of the weft yarn in the plane of the material, mm. A value above unity indicates that an additional yarn length is stored in the three-dimensional looped structure, and a decrease of the coefficient with increasing tension is interpreted as a more compact placement of the weft yarn in the material.

Each indicator was determined in five replicate measurements (n = 5) for every tension regime. The results are presented as arithmetic means; the standard deviation and the 95% confidence interval are given in the notes to the figures and tables. The significance of the differences between the tension regimes was assessed by one-way analysis of variance (ANOVA) with Tukey's HSD post-hoc test at a significance level of $p \leqslant 0.05$. The measured indicators were combined into four groups, so that a tension regime could be assessed simultaneously by its structural, economic, mechanical and commodity consequences (Table 1).

Table 1. *Methodological matrix of the measured indicators*

Group of indicators	Measured / calculated indicator	Purpose of evaluation
Structural	Produced material width; width of an individual woven-knitted strip; arrangement of the strips	To control dimensional stability and the risk of narrowing
Yarn consumption	Projected weft length; actual withdrawn weft length; coefficient of weft consumption K_{wc}	To estimate raw-material economy and the yarn reserve stored in the structure
Mechanical	Breaking force and breaking elongation in the warp and weft directions; breaking force of the withdrawn weft yarns	To verify that resource saving does not reduce strength
Commodity quality	Thickness, air permeability, abrasion resistance, phase structure of the woven areas	To confirm the preservation of use-related properties
Technological decision	Comparison of all indicators across the tension regimes	To select a balanced tension range instead of a regime based on a single property

Source: *compiled by the authors*

Such a combination of groups was applied because a tension regime cannot be considered rational if it saves yarn but causes unacceptable narrowing or a loss of performance. The experimental design did not aim to replace a full industrial optimisation; its purpose was to establish the direction and the practical significance of the changes in the properties of the material when weft tension is varied within a technologically acceptable interval.

Results and Discussion

Initially, the analysis focused on tensile characteristics. Figure 1 presents the dependence of the breaking force and the breaking elongation of the woven-knitted material and of the withdrawn weft yarns on the weft yarn tension. The curves show no abrupt decrease in the strength of the material as tension increases within the investigated range. The breaking force in the weft direction rises over the first part of the interval, reaches a maximum

in the region of 9.9-10.7 cN per yarn and then settles at a level that remains above the value recorded at the lowest tension. The breaking force in the warp direction behaves in the same manner but with a considerably smaller amplitude, which is expected because the warp system is not directly affected by the weft regulator and reacts only through the change in the geometry of the strips. The breaking force of the weft yarns withdrawn from the material follows the same pattern, and this is the key argument for the technological admissibility of the interval: if the higher tension damaged the filaments or disturbed loop formation, the withdrawn yarns would lose strength before the material did. The absence of such a loss indicates that the investigated tension values do not exceed the deformation reserve of the polyester weft.

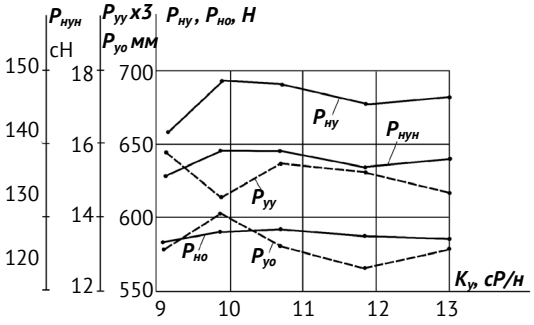

Figure 1. *Tensile characteristics of the woven-knitted material and of the weft yarns as a function of weft yarn tension*

Note: *K_y – weft yarn tension, cN per yarn; $P_{ну}$, $P_{но}$ – breaking force of the material in the weft and in the warp direction, N; $P_{уу}$, $P_{уо}$ – breaking elongation of the material in the weft and in the warp direction, mm ($P_{уу}$ – plotted with a scale factor of 3); $P_{нун}$ – breaking force of the weft yarns withdrawn from the material, cN. Each point is the arithmetic mean of measurements (n = 5); the standart deviation did not exceed 4% of the mean value*

Source: *developed by the authors on the basis of the experimental data*

The behaviour of the elongation curves is less monotonic. Both the weft-wise and the warp-wise breaking elongation pass through a local extremum in the region of 10-11 cN per yarn and then decrease gradually, the weft-wise elongation decreasing more noticeably. This is consistent with the structural role of the weft in the investigated material: elongation in the weft direction is realised mainly by straightening the loops of the connections between the strips, so a reduction of the loop reserve reduces the deformation capacity of the structure before it reduces its strength. The practical conclusion is that elongation, not strength, is the first indicator to react to an increase in tension, and it is therefore elongation that should be monitored when the interval is extended beyond the values investigated here. The most pronounced changes were found for weft yarn consumption and for the width parameters (Fig. 2).

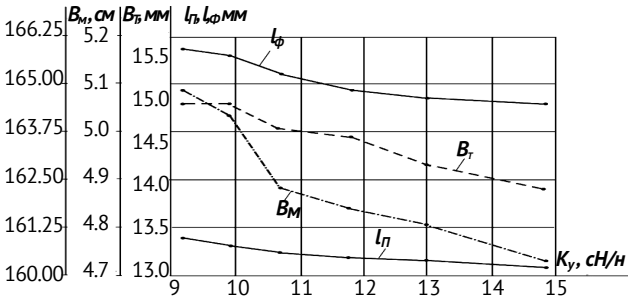

Figure 2. *Width parameters of the material and weft yarn consumption as a function of weft yarn tension*

Note: *K_y – weft yarn tension, cN per yarn; $B_м$ – width of the produced material, cm; B_m – width of an individual woven-knitted strip, mm; l_n – projected length of the weft yarn per insertion, mm; $l_ф$ – actual weft consumption per insertion, mm. Each point is the arithmetic mean of measurements (n = 5); the standard deviation did not exceed 3% of the mean value*

Source: *developed by the authors on the basis of the experimental data*

All four curves in Figure 2 decrease monotonically, but their shapes differ. The projected weft length falls from 13.38 to 13.11 mm per insertion, that is by 0.27 mm or approximately 2.02%, and its curve flattens after 11 cN per yarn: the yarn path visible in the plane of the material approaches a geometric limit determined by the spacing of the strips and can no longer be shortened by tension alone. The actual withdrawn length falls from 15.28 to 14.81 mm per insertion, that is by 0.47 mm or approximately 3.08%, and its decrease is steepest in the region of 9.9-11.8 cN per yarn. The difference between the two curves is exactly the yarn reserve stored in the three-dimensional geometry of the loops, and the fact that the actual length decreases by half again as much as the projection shows that it is this reserve, and not the in-plane path, that responds to tension. A saving of 0.47 mm per insertion may seem negligible at the level of a single pick, but at 317 weft yarns per setting it becomes a measurable raw-material factor over industrial production length.

The width curves reveal the cost of that saving. The width of the produced material decreases from 164.8 to 160.4 cm, that is by 4.4 cm or approximately 2.67%, and the width of an individual woven-knitted strip decreases in almost the same proportion, from about 5.03 to about 4.88 mm. The proportional character of these two reductions is informative: the material does not narrow because the strips are drawn closer to one another while remaining unchanged, but because the strips themselves contract as the looped connection tightens. The transverse contraction is thus distributed over the whole width rather than concentrated in the connections, which explains why the arrangement of the strips remains regular and why the phase structure of the woven areas was assessed as stable throughout the interval. It also explains the shape of the width

curve: the steepest fall of the material width coincides with the steepest fall of the actual weft consumption, in the region of 9.9-11.8 cN per yarn, confirming that both effects have a single structural cause. The summarised influence of weft tension on the measured indicators is given in Table 2.

Table 2. *Influence of weft yarn tension on the indicators of the woven-knitted material*

Indicator	Lower tension (9.2 cN/yarn)	Higher tension (14.8 cN/yarn) / direction of change
Projected weft length in the plane of the material, mm per insertion	13.38	13.11; decrease by 0.27 mm (about 2.02%)
Actual weft consumption, mm per insertion	15.28	14.81; decrease by 0.47 mm (about 3.08%)
Coefficient of weft consumption K_{wc}	1.142	1.130; slight reduction of the yarn reserve in the three-dimensional structure
Produced material width, cm	164.8	160.4; decrease by 4.4 cm (about 2.67%)
Width of an individual woven-knitted strip, mm	about 5.03	about 4.88; decrease of about 3.0%
Tensile characteristics of the material and of the withdrawn weft yarns	Reference level	No critical deterioration detected; elongation reacts earlier than breaking force
Thickness, air permeability, abrasion resistance, phase structure	Reference level	No critical changes detected

Note: *the values are arithmetic means of ± standard deviation of five replicate measurements (n = 5).* K_{wc} *– coefficient of weft consumption calculated by formula (1)*

Source: *developed by the authors on the basis of the experimental data*

The coefficient of weft consumption supports the structural interpretation of these changes. At the lower tension it equals 1.142, and at the higher tension it decreases to 1.130, so the yarn reserve stored in the looped connection falls from about 14.2% to about 13.0% of the projected length. The change is moderate, and this is precisely why the tensile characteristics remain stable: the connection retains roughly nine tenths of its initial reserve. A sharper decrease of the coefficient would indicate that the looped connection is losing its capacity to accommodate deformation and is becoming vulnerable to rupture; in the investigated interval the coefficient moves in the direction of rationalisation without reaching that state. This also shows why the coefficient, rather than the absolute saving, is the more informative control parameter: it is dimensionless and therefore transferable to other articles and yarn linear densities.

The observed relationships between weft tension, yarn consumption and width agree with the classical geometric and structural models of textile materials. F.T. Peirce (1937) showed that the quantity of yarn contained in a unit area of fabric is not a free parameter but a function of the geometry imposed during formation, and J.W.S. Hearle (1969) extended this reasoning to show how deformation applied at yarn level is transferred to fabric level; both principles are directly visible in the present data, where a change in the formation tension of a single yarn system reappears as a coordinated change in weft consumption, strip width and produced width. B.K. Behera & P.K. Hari (2010) further noted that the same nominal construction can be realised with different yarn reserves depending on the tension regime, which is exactly the behaviour captured here by the coefficient of weft consumption.

For the looped part of the structure, the results agree with loop-formation theory. D.J. Spencer (2001) described the balance between yarn feeding tension, loop length and dimensional stability, and showed that the length of yarn fed per loop is the primary variable from which the dimensional characteristics of a knitted structure follow; in the investigated material this variable is quantified by the coefficient K_{wc}, which fell from 1.142 to 1.130 as tension increased. The moderate size of that change explains why the tensile characteristics remained stable: the looped connection retained most of its feeding reserve rather than being drawn to its structural limit.

The results for thickness, air permeability, abrasion resistance and the phase structure of the woven areas were treated as control indicators of commodity quality, and none of them changed critically over the investigated interval. The stability of air permeability is consistent with the porosity approach of R.T. Ogulata (2006): the moderate reduction of the weft reserve did not close the inter-yarn voids to a degree that would restrict air passage, because the voids of this material are formed mainly by the spacing between the strips, which remains regular. The stability of abrasion resistance has the same explanation: the surface exposed to the abradant is formed by the woven areas, whose phase structure was preserved. R.B. Büyükbayraktar (2021) reported a comparable pattern for self-stitched double fabrics, in which the stitching arrangement changed air permeability more than tensile strength; the present material shows the same asymmetry, because the looped connection governs consumption and width, while the woven strips govern strength and abrasion resistance.

Compared with the published data, the obtained results are consistent in direction but differ in the object and in the controlled variable. E.K. Çeven *et al.* (2021) reported for drapery fabrics that a higher weft density increases tearing strength but reduces air permeability;

in the present material a comparable compaction of the weft, achieved through tension rather than through density, produced no critical change in either indicator, because compaction here affects the looped connection rather than the woven area that governs strength and permeability. S. Golomeova Longurova *et al.* (2022) showed that the dimensional stability of a woven fabric after processing depends on structural parameters such as yarn density and cover factor; the present material shows that a comparable dimensional response, the narrowing of the produced width, can already be induced during formation by weft tension alone, before any post-treatment is applied. W. Mengie *et al.* (2024) modelled the surface roughness of twill fabric as a function of weft count and weft density and found both factors statistically significant; the present results extend this logic by showing that weft tension, not only weft count or density, is a variable that a producer can use to influence the compactness of the structure, although here the resulting change of width is a stronger practical constraint than any change of surface texture.

In the field of looped textile structures, K. Singal *et al.* (2024) showed that the elasticity of a knitted fabric is an emergent property of the local stitch topology and can be programmed stitch by stitch; the present study extends that logic from the topology of the stitch to the tension with which the yarn is fed into it, and adds a quantitative link between that tension, the actual yarn consumption and the produced width, which stitch-level models do not by themselves provide. X. Ding *et al.* (2024) represented a knitted fabric as a hierarchy of yarn-level loops and showed that fabric-level extensibility is governed by the reserve length stored at each loop, which is the same mechanism that the coefficient K_{wc} quantifies for the looped connections of the present material. S.E. Gonzalez *et al.* (2025) further showed that a knitted structure passes from a soft to a stiff mechanical response once the loops are packed tightly enough to jam against one another; the moderate decrease of K_{wc} observed here, from 1.142 to 1.130, indicates that the investigated tension interval keeps the looped connection well below that jamming threshold, which is consistent with the absence of a critical loss of tensile performance.

From a commodity-science perspective, the key result is the possibility of obtaining raw-material economy without reducing consumer quality. Resource saving in this context is not a simple reduction of material input but a controlled technological decision, the admissibility of which is verified by quality indicators. The study also demonstrates the value of measuring the actual weft consumption instead of relying on the projected yarn length: if only the projection were considered, the saving would be underestimated by about a third, and the yarn stored in the looped structure would remain outside the calculation. The withdrawal method used here can therefore be recommended for other materials in which a yarn reserve in loops or spatial connections is technologically significant. The corresponding practical criteria for choosing a tension regime are summarised in Table 3.

Table 3. *Practical criteria for selecting a weft tension regime*

Criterion	Positive effect of higher tension	Risk / required control
Actual weft consumption	Decrease of the yarn length incorporated per insertion	The saving must be calculated from the withdrawn yarn, not from the projection
Coefficient of weft consumption	More compact placement of the weft in the looped connection	A sharp decrease signals the loss of the deformation reserve of the connection
Material width and strip width	More compact structure	Excessive narrowing may violate the width tolerance of the article
Tensile characteristics	No critical deterioration within the investigated interval	Breaking elongation reacts before breaking force and must be rechecked for other yarns and densities
Air permeability, thickness, abrasion resistance	No critical changes in the tested samples	Porosity-related properties should be monitored whenever the regime is changed

Source: *compiled by the authors on the basis of the obtained results*

Several limitations of the obtained results should be noted. The study covered one material article, one yarn composition and one laboratory machine, and the investigated tension interval, although technologically acceptable for this sample, does not represent the full range of possible settings. The conclusions about the commodity indicators are based on the comparative control of quality characteristics rather than on a complete factorial model of the process, so the interaction between weft tension and other formation parameters remains outside the scope of this work. The stability of the tensile characteristics also should not be transferred automatically to yarns with lower breaking strength, higher friction or elastomeric components, for which the deformation reserve of the looped connection is likely to behave differently.

Taken together, the results show that weft tension in a woven-knitted material performs two coordinated functions: it stabilises yarn feeding and loop formation, and it determines how much yarn is incorporated into the structure. These functions do not conflict within the investigated interval, because the reduction of the yarn reserve remains moderate and the structure retains its strength and its use-related properties. What limits the regime is not the mechanical behaviour of the material but its width, and this is the

parameter that converts a purely economic decision into a technological one.

Conclusions

The research established that weft yarn tension is a controllable technological factor of structure formation in woven-knitted material produced on a Metap-160 machine, and that its effect is realised primarily through the yarn reserve stored in the looped connections between the woven strips rather than through the strength of the material. Within the interval of 9.2-4.8 cN per yarn the mechanical and commodity indicators retained the levels required for the article, and the first characteristic to respond to an increase in tension was breaking elongation, which reflects the gradual reduction of the deformation reserve of the loops. Quantitatively, weft consumption, the coefficient of weft consumption and the produced width all responded to the increase in tension in the same direction, with the reduction in actual consumption exceeding that of the visible projection by nearly half again, which confirms that most of the saving comes from the yarn reserve of the loops rather than from the in-plane path of the weft. The accompanying transverse contraction was distributed proportionally across the whole width of the material rather than concentrated at the connections between strips, which is why raw-material saving under increased tension cannot be treated separately from the resulting narrowing of the finished material.

For the production of woven-knitted materials of this type it is advisable to apply a multi-criteria system of tension control in which the regime is selected by combining the actual weft consumption, the coefficient of weft consumption, the width of the material, the tensile characteristics and the group of commodity indicators. Such a system makes it possible to obtain raw-material economy without compromising the confirmed quality of the finished material. Further research will be directed at extending the results to other yarn linear densities and fibre compositions, including yarns with elastomeric components; at constructing a factorial model of the joint influence of weft tension, warp tension and take-up on the yarn reserve of the looped connection; and at verifying the established relationships under industrial conditions, where machine speed, the condition of the yarn packages and the parameters of the production environment can change the actual tension profile.

Acknowledgements

Not applicable.

Funding

The authors declare that the study did not receive external funding.

Conflict of Interest

The authors declare that there is no conflict of interest.

References

[1] Ayele, M., Kassaw, A., & Tesema, A.F. (2024). Analyzing the effect of yarn tension, weft yarn type, and weft yarn density on thermal resistance, thermal conductivity, and air permeability of plain woven fabric. *Journal of Natural Fibers*, 21(1), article number 2407892. doi: 10.1080/15440478.2024.2407892.

[2] Behera, B.K., & Hari, P.K. (Eds.). (2010). *Woven textile structure: Theory and applications*. Great Abington: Woodhead Publishing. doi: 10.1533/9781845697815.

[3] Büyükbayraktar, R.B. (2021). Effect of self-stitched double fabric's properties on tensile and permeability performances. *Materials Science (Medžiagotyra)*, 27(2), 232-238. doi: 10.5755/j02.ms.25238.

[4] Çeven, E.K., Karakan Günaydın, G., & Çeven, N. (2021). Impact of weft yarn type and fabric weft density on burning behavior, tearing strength and air permeability for different types of antibacterial drapery fabrics. *Textile Industry*, 69(1), 4-16. doi: 10.5937/tekstind2101004K.

[5] Ding, X., Sanchez, V., Bertoldi, K., & Rycroft, C.H. (2024). Unravelling the mechanics of knitted fabrics through hierarchical geometric representation. *Proceedings of the Royal Society A*, 480(2295), article number 20230753. doi: 10.1098/rspa.2023.0753.

[6] Golomeova Longurova, S., Jordeva, S., Zhezhova, S., Dimitrijeva Kuzmanoska, V., Mojsov, K., & Andronikov, D. (2022). The effect of fabric structure parameters on dimensional stability after domestic washing. *Textile Industry*, 70(2), 22-27. doi: 10.5937/tekstind2202022G.

[7] Gonzalez, S.E., Dimitriyev, M.S., Cachine, A.P., & Matsumoto, E.A. (2025). Pulling apart the mechanisms that lead to jammed knitted fabrics. *Physical Review E*, 112(1), article number 015504. doi: 10.1103/g94g-c6tt.

[8] Hearle, J.W.S. (1967). The structural mechanics of fibers. *Journal of Polymer Science Part C: Polymer Symposia*, 20, 215-251. doi: 10.1002/polc.5070200118.

[9] ISO 9237:1995. (1995). *Textiles – determination of the permeability of fabrics to air*. Retrieved from https://www.iso.org/standard/16869.html.

[10] ISO 5084:1996. (1996). *Textiles – determination of thickness of textiles and textile products*. Retrieved from https://www.iso.org/standard/23348.html.

[11] ISO 139:2005. (2005). *Textiles – standard atmospheres for conditioning and testing*. Retrieved from https://www.iso.org/standard/35179.html.

[12] ISO 2062:2009. (2009). *Textiles – yarns from packages – determination of single-end breaking force and elongation at break using constant rate of extension (CRE) tester*. Retrieved from https://www.iso.org/standard/45642.html.
[13] ISO 13934-1:2013. (2013). *Textiles – tensile properties of fabrics – part 1: Determination of maximum force and elongation at maximum force using the strip method*. Retrieved from https://www.iso.org/standard/60676.html.
[14] ISO 12947-2:2016. (2016). *Textiles – determination of the abrasion resistance of fabrics by the Martindale method – part 2: Determination of specimen breakdown*. Retrieved from https://www.iso.org/standard/61988.html.
[15] Kassaw, A., & Ayele, M. (2024). Effect of weft yarn type and weaving parameters on surface roughness and drapeability of woven fabric. *Journal of Natural Fibers*, 21(1), article number 2334410. doi: 10.1080/15440478.2024.2334410.
[16] Kyzymchuk, O., Melnyk, L., Marmaralı, A., Oğlakcıoğlu, N., Ertekin, G., Arabuli, S., Arabuli, A., & Cüreklibatır Encan, B. (2023). The effect of weft yarn type and elastomer yarn threading on the properties of elastic warp knitted fabrics. Part 1: Structure and elasticity. *Journal of Engineered Fibers and Fabrics*, 18. doi: 10.1177/15589250231167405.
[17] Mandre, N., Plamus, T., & Krumme, A. (2021). Impact of weft yarn density and core-yarn fibre composition on tensile properties, abrasion resistance and air permeability of denim fabrics. *Materials Science*, 27(4), 483-491. doi: 10.5755/j02.ms.27532.
[18] Maqsood, M., Nawab, Y., Shaker, K., Umair, M., Ashraf, M., Baitab, D.M., Hamdani, S.T.A., & Shahid, S. (2016). Modelling the effect of weave structure and fabric thread density on mechanical and comfort properties of woven fabrics. *Autex Research Journal*, 16(3), 160-164. doi: 10.1515/aut-2015-0032.
[19] Melnyk, L., Kyzymchuk, O., & Golikova, O. (2016). The influence of weft filling yarn on the properties of warp knitted fabric. In *International Scientific Conference UNITECH* (pp. 145-148). Gabrovo: UNITECH.
[20] Mengie, W., Beyene, K.A., & Eshetie, G.A. (2024). Modelling surface roughness of 3/1 twill fabric using weft yarn count and weft thread density. *Tekstilec*, 67, 119-127. doi: 10.14502/tekstilec.67.2023083.
[21] Ogulata, R.T. (2006). Air permeability of woven fabrics. *Journal of Textile and Apparel, Technology and Management*, 5(2), 1-10.
[22] Peirce, F.T. (1937). The geometry of cloth structure. *Journal of the Textile Institute Transactions*, 28(3), T45-T96. doi: 10.1080/19447023708658809.
[23] Singal, K., Dimitriyev, M. S., Gonzalez, S.E., Cachine, A.P., Quinn, S., & Matsumoto, E.A. (2024). Programming mechanics in knitted materials, stitch by stitch. *Nature Communications*, 15(1), article number 2622. doi: 10.1038/s41467-024-46498-z.
[24] Spencer, D.J. (2001). *Knitting technology: A comprehensive handbook and practical guide* (3rd ed.). Abington: Woodhead Publishing.
[25] Umair, M., Hussain, T., Shaker, K., Nawab, Y., Maqsood, M., & Jabbar, M. (2016). Effect of woven fabric structure on the air permeability and moisture management properties. *The Journal of the Textile Institute*, 107(5), 596-605. doi: 10.1080/00405000.2015.1054124.
[26] Vasile, S., Vermeire, S., Vandepitte, K., Troch, V., & De Raeve, A. (2024). Effect of weave and weft type on mechanical and comfort properties of hemp-linen fabrics. *Materials*, 17(7), article number 1650. doi: 10.3390/ma17071650.

Дослідження впливу натягу ниток утоку на властивості тканo-в'язаного матеріалу

Оксана Христюк
Вінницький інститут конструювання одягу і підприємництва
21027, просп. Космонавтів, 42, м. Вінниця, Україна
https://orcid.org/0009-0005-5700-5106
Олег Нагайчук
Вінницький інститут конструювання одягу і підприємництва
21027, просп. Космонавтів, 42, м. Вінниця, Україна
https://orcid.org/0009-0003-0612-774X
Еліна Захарова
Вінницький інститут конструювання одягу і підприємництва
21027, просп. Космонавтів, 42, м. Вінниця, Україна
https://orcid.org/0009-0008-6796-7415
Валентина Горобчишина
Вінницький інститут конструювання одягу і підприємництва
21027, просп. Космонавтів, 42, м. Вінниця, Україна
https://orcid.org/0009-0000-9945-5889

Анотація. Актуальність дослідження зумовлена практичною потребою зменшити витрату піткальної (утокової) нитки за умови збереження структурної стабільності, розривних характеристик і товарознавчої якості матеріалу, що поєднує поздовжні тканi пруги з петельними з'єднаннями утоку. Метою статті було визначити вплив натягу ниток утоку на фізичні, механічні та структурні властивості тканo-в'язаного текстильного матеріалу артикулу 10с2, виробленого на лабораторній машині Metap-160. Для отримання експериментальних зразків використано поліефірні нитки основи лінійної густини 24,5 текс і поліефірні мультифіламентні нитки утоку лінійної густини 8,4 текс. Натяг утоку змінювали в межах від 9,2 до 14,8 сН на нитку шляхом зміни кількості та положення регулювальних вантажів на важелях регулятора утоку. У роботі оцінено розривне навантаження та розривне видовження за основою й утоком, розривні характеристики ниток утоку, вилучених з матеріалу, проєкційну довжину нитки утоку в площині матеріалу, фактичну витрату утоку на одне прокладання, ширину виробленого матеріалу, ширину окремого тканo-в'язаного пруга, товщину, стійкість до стирання, повітропроникність і стабільність фазової будови тканих ділянок. Установлено, що в дослідженому інтервалі підвищення натягу утоку не спричиняє критичного погіршення основних експлуатаційних показників. Проєкційна довжина утоку зменшилася з 13,38 до 13,11 мм на прокладання, фактична витрата утоку – з 15,28 до 14,81 мм на прокладання, коефіцієнт витрати утоку – з 1,142 до 1,130, тоді як ширина виробленого матеріалу зменшилася з 164,8 до 160,4 см. Отримані залежності обґрунтовують багатокритеріальний підхід, за якого натяг утоку застосовується як ресурсоощадний чинник лише в поєднанні з контролем розмірних характеристик матеріалу

Ключові слова: витрата утоку; петельне з'єднання; Metap-160; повітропроникність; стійкість до стирання; ресурсозбереження

COMMODITY BULLETIN
Journal homepage: https://c-bulletin.com.ua/en
DOI: 10.62763/cb/1.2026.82

Article's History: Received: 12.01.2026 Revised: 09.04.2026 Accepted: 28.05.2026 Published: 29.05.2026

ISSN 2310-5283; e-ISSN 3041-1432 Vol. 19, No. 1, 2026, 82-90

UDC 664.8/.9:663.05:579.67

Scientific and technological principles of controlled fermentation in craft production of flour products

Iryna Belova*
PhD in Economic Sciences
Western Ukrainian National University
46009, 11 Lvivska Str., Ternopil, Ukraine
https://orcid.org/0000-0002-5399-3654
Kseniia Bakhlukova
PhD in Technical Sciences
Institute of Food Resources of National Academy of Agrarian Sciences of Ukraine
02002, 4A Yevhena Sverstyuk Str., Kyiv, Ukraine
https://orcid.org/0009-0006-3302-537X
Serhii Holiachuk
PhD in Agricultural Sciences, Associate Professor
Lutsk National Technical University
43018, 75 Lvivska Str., Lutsk, Ukraine
https://orcid.org/0000-0002-4835-8154

Abstract. The article substantiates the scientific and technological principles of controlled fermentation in craft food production as one of the promising areas of development of the modern food industry. The relevance of the study is due to the steady growing consumer demand for authentic fermented products with high nutritional and biological value and the need to minimisation the risks associated with the instability of microbiological processes, with spontaneous microbiota and variability of product quality indicators of small-scale production. The aim of the work was to develop a comprehensive model of controlled fermentation, based on the synergy of traditional technologies and modern instrumental control methods. The methodological basis was a systematic approach, the concept of barrier technology and methods of mathematical and statistical modelling, which provide a comprehensive analysis of fermentation processes in craft food production. To move from the qualitative characteristics of the technological process to quantitative analysis, the expert-score assessment method was applied and a multifactor regression model was built, which allows predicting the influence of technological parameters on the quality indicators of the finished product and determining the optimal conditions for the fermentation process. The scientific novelty of the results lies in the development of a mathematical equation that describes the dependence of the reproducibility of the fermentation process on the degree of process control and the need for laboratory verification of technological parameters. It was established that the proposed model has a high approximation accuracy, as evidenced by the value of the coefficient of determination $R^2 = 0.998$, which confirms the dominant influence of instrumental monitoring systems on ensuring the stability of the technological process and product quality. The study was supported by the creation of a three-dimensional (3D) model of the fermentation module, which provides the ability to visualise and optimise the placement of sensor systems (pH, T, aw) and actuators. Key microbiological risks characteristic of craft production of fermented products were systematised and an algorithm for their levelling was proposed through the introduction of

Suggested Citation:
Belova, I., Bakhlukova, K., & Holiachuk, S. (2026). Scientific and technological principles of controlled fermentation in craft production of flour products. *Commodity Bulletin*, 19(1), 82-90. doi: 10.62763/cb/1.2026.82.

*Corresponding author (i.belova@wunu.edu.ua)

selected autochthonous cultures and digital process logs. The implementation of the proposed model allowed to increase the reproducibility of craft technologies by 60-70% while simultaneously preserving their unique sensory identity

Keywords: raft products; multifactorial regression; 3D modelling; microbiological safety; barrier technology

Introduction

Craft food production technologies have become a prominent trend in the development of the modern food industry. Their popularity is associated with the demand for local products, short supply chains, authentic recipes, minimal processing, individualised sensory characteristics and trust in the small producer. For the consumer, a craft product often means not only a method of production, but also a cultural code: the origin of raw materials, manual labour, naturalness, limited batches, local identity, the absence of excessive standardisation and the expectation of higher quality. At the same time, from a technological point of view, craft is an ambiguous category. It can be a source of sensory uniqueness, but at the same time it creates risks of variability. This is especially true for fermented products: sourdough bread, fermented vegetables, kombucha, kefir, yogurts, cheeses, fermented meat products, craft beer and non-alcoholic fermented beverages. Their quality depends not only on the recipe, but also on the microbial ecology, acidification rate, water activity, temperature, sanitary condition, metabolite profile, presence of competitive microbiota and storage conditions.

The modern development of craft production requires a transition from the description of individual types of fermented products to the formation of a generalised technological framework for controlled fermentation. Such production requires a technological approach that simultaneously preserves product authenticity and ensures critical control parameters, analytical verification, microbiological provability and batch reproducibility. It is at the intersection of traditional practices, food microbiology, fermentation biotechnology and quality management systems that the modern scientific problem of craft food technologies is formed.

The issue of balancing the preservation of microbiological diversity with ensuring consistent quality in craft products has been investigated in numerous contemporary studies. A. Martín-Garcia *et al.* (2023) substantiated the need for a transdisciplinary safety assessment of authentic food products, given the lack of a unified analytical framework at small-scale enterprises. The researchers demonstrated that the safety concept for craft products must be grounded in a deep understanding of indigenous microbiota dynamics, rather than relying solely on final product testing. In turn, E.E.M. Abdurrahman & G. Ferrari (2025) highlighted the difficulties of identifying microorganisms in open systems and demonstrated that the spontaneous nature of bioprocesses significantly complicates the prediction of finished product safety, creating risks of uncontrolled proliferation of opportunistic pathogenic strains during the initial stages of fermentation.

The mechanisms of microbial community formation under the influence of environmental factors were investigated by Y. De Bondt *et al.* (2024), who concluded that a purely descriptive approach is insufficient for managing fermentation processes and emphasised the importance of mathematically accounting for temperature fluctuations in the processing zone. In contrast, a large-scale study by A. Martín-Garcia *et al.* (2023), based on the analysis of 75 commercial samples of fermented vegetables, revealed significant variability in pH levels and biogenic amine accumulation; this finding underscored the necessity of implementing rigorous instrumental monitoring of organic acid accumulation kinetics.

Traditional approaches to spontaneous fermentation often result in significant variability in the final product' s properties, which limits the competitiveness of small enterprises (Verdonck *et al.*, 2023). The popularity of such production is driven by a demand for distinctive sensory characteristics, short supply chains, minimal processing, and trust in local producers. For consumers, a craft product embodies specific cultural values, naturalness, and limited-batch exclusivity. However, from a technological standpoint, the spontaneous nature of fermentation processes does not guarantee safety or authenticity. The benefits of shifting from spontaneous fermentation to the use of targeted microbial compositions are also documented in scientific literature. The potential for technologically controlling fermentation using selected strains in products based on grain and legume raw materials is highlighted in the work of Ukrainian scientists V. Gnitsevych & K. Doronina (2024) – who determined the growth kinetics constants of lactic acid bacteria. The specific characteristics of functional baking systems utilising spontaneous fermentation starters have been analysed in detail by N.A. Berezkina *et al.* (2024), who characterised wheat-based semi-finished products and their impact on crumb porosity. Research by L. Mykhonik *et al.* (2023) demonstrates the viability of using multicomponent starters made from grain flour to intensify bread production processes. The impact of thirty years of research into sourdough ecology on the technological and nutritional properties of bakery products is systematised in a comprehensive review by K. Arora *et al.* (2021).

A. Martín-Garcia *et al.* (2023) investigated microbiological risks and spoilage in artisanal cheeses, classifying typical ripening defects and unwanted mold growth. Mechanisms for harmonising market confidence and regulatory frameworks for artisanal production through certification procedures were examined by I. Dudarev & O. Khveshchuk (2025). At the same time, the effective management of fermentation modules is impossible without optimising their geometric and spatial configuration. Modern trends in food equipment design involve the extensive use of computational fluid dynamics (CFD) methods to analyse temperature fields within the operating volumes of the units (Musiari *et al.*, 2024). However, the aforementioned authors did not address the development of a unified mathematical model linking the level of environmental monitoring to the reproducibility of craft product quality indicators, nor did they provide a scientific rationale for the spatial placement of sensors within small-scale biotechnological modules using 3D technologies.

The purpose of the article was to develop and substantiate a scientific and technological model of controlled fermentation for craft food production, based on the synergy of authentic technologies and instrumental control to ensure stable quality, microbiological safety and functional value of the product. To achieve the goal, the following tasks were defined:

1) to formulate a technological concept for craft fermented products in the modern food market;

2) to systematise and assess microbiological and technological risks of spontaneous and semi-controlled fermentation in small-scale craft production;

3) to identify and substantiate critical process-control parameters and develop a multifactorial mathematical model linking process control, microbiological risks, biochemical transformations, sensory properties, and product quality reproducibility.

Materials and Methods

The methodological basis of the study comprises a systems approach, the fundamental principles of food microbiology, the concept of hurdle technology (the theoretical basis for safety), as well as methods of expert assessment, mathematical-statistical modelling, and three-dimensional digital design. The logical connection between the research objectives and the applied methods is presented in Table 1.

Table 1. *Matrix of correspondence between research objectives and methodological approaches*

Task	Methodological approach	Expected result
1. Systematisation and classification of microbiological and technological risks.	Systems analysis, expert assessment method, Delphi survey method.	Matrix of expert assessments, verified using Kendall' s coefficient of concordance (W).
2. Development of a multifactorial mathematical model of quality indicators.	Multifactor regression analysis, ordinary least squares (OLS), normalisation of variables.	Linear regression equation, statistically validated by the coefficient of determination (R^2).
3. Construct a three-dimensional (3D) model of the fermentation module' s control elements.	Parametric solid modelling, spatial engineering analysis of sensor placement.	Digital prototype of the module structure with optimised geometric coordinates of the sensors.

Source: *developed by the authors*

As this study is theoretical and modelling-based rather than a direct physical experiment, the primary empirical basis (source data) consisted of a body of systematised scientific data from specialised periodicals. The expert panel consisted of specialists with academic and/or professional experience in food biotechnology, fermentation technologies, food microbiology, and the technological production of flour-based products. Experts were selected based on their relevant professional qualifications, research or practical experience in fermentation processes, and familiarity with quality and safety assessment in small-scale food production. Prior to the assessment, the experts were provided with a standardised description of the three process-control states and the criteria used for their evaluation. The assessment was conducted independently and anonymously using structured questionnaires, thereby reducing the influence of interpersonal discussion and individual authority on the results. The survey was conducted using questionnaires based on closed 10-point scales. The experts assessed the expected level of process reproducibility, microbiological risk, and stability of quality indicators associated with each degree of process control. The aggregated expert assessments were subsequently converted into quantitative variables used in the mathematical modelling. he participation of human experts in the study was conducted in accordance with the ethical standards established by the American Sociological Association (2008), including the principles of voluntary participation, informed consent, and confidentiality. Three basic states of the biotechnological process were evaluated: spontaneous fermentation (absence of instrumental control), semi-controlled (periodic monitoring of temperature and pH), and controlled (continuous automated control of a complex of barrier factors). To verify the consistency of expert opinions and confirm the reliability of the results, Kendall' s coefficient of concordance (W) was calculated:

$$W = 12S/m^2(n^3 - n), \quad (1)$$

where S is the sum of squared deviations of all rank assessments from the mean value; m is the number of experts (m = 12); and n is the number of factors being evaluated. The calculated value of the coefficient of concordance was W = 0.84, indicating a high degree of agreement among the experts' judgments (W > 0.7) and allowing the obtained average scores to be used as reliable input data for further mathematical modelling. The choice of mathematical tool is dictated by the specific nature of the problem. Although the interaction of hurdle factors (pH, aw, temperature, salt concentration) in real biological systems is non-linear, it is appropriate to employ multivariate linear regression when developing a generalised control concept. A linear model allows for the clear differentiation and quantitative assessment of each factor' s isolated contribution via weighting coefficients; it ensures high interpretability of results and minimises the risk of model overfitting given a limited data sample. Non-linear barrier effects were partially accounted for during the expert assessment stage, where specialists assigned scores while considering the known synergism of the factors. The following variables were defined for the construction of the mathematical model:

- dependent variable (Y) – the criterion for the reproducibility of quality indicators and the safety of the finished product (in relative units or scores from 0 to 1), where 1 corresponds to an exact match between the product' s properties and the standard, and 0 represents a complete defect.
- independent variables (model factors):

X_1 – degree of instrumental monitoring of environmental parameters (ranging from a normalised zero to one);

X_2 – integral indicator of microbiological risk associated with raw materials and the environment (scored assessment);

X_3 – consistency in adhering to the time intervals of technological stages.

To ensure the comparability of factors measured in different units, they were normalised (via linear scaling) within the [0; 1] range using the formula:

$$Xnorm = (X - Xmin) / (Xmax - Xmin). \quad (2)$$

Regression coefficients were calculated using the classical ordinary least squares (OLS) method. Statistical validation of the resulting model was assessed using the coefficient of determination (R^2), which represents the proportion of the dependent variable' s variance explained by the regression equation. The methodology for developing the product quality and safety validation algorithm is based on the principles of Hazard Analysis and Critical Control Points (HACCP). The algorithm is structured as a sequential logical decision-making scheme that links real-time sensor readings to the control system' s preventive actions. To achieve this, mathematical compliance criteria were assigned to each processing stage: if the current value Ycalc ⩾ Ycrit (where Ycrit represents the critical safety limit), the process is verified as stable. In the event that Ycalc < Ycrit, the algorithm triggers automatic corrective actions (such as adjusting the temperature regime or introducing additional acidity regulators). The three-dimensional (3D) model of the fermentation module' s control components was developed using parametric solid modelling techniques within the specialised SolidWorks CAD environment. The engineering analysis methodology encompassed defining the geometric constraints of the working chamber, calculating optimal mounting locations for submersible and non-contact sensors to avoid mixing "dead zones", and analysing the spatial layout of components to minimise the impact of thermal interference from heating circuits on the accuracy of pH and medium temperature measurements.

Results and Discussion

A craft fermented product is best defined as a food product with a limited production scope, the quality and safety characteristics of which are shaped by the complex interaction of authentic local raw materials, a targeted biotechnological process, and controlled environmental parameters (Tamang *et al.*, 2020). The concept of "limited standardisation", characteristic of the craft sector, does not imply a complete absence of control. On the contrary, given the high variability in the properties of input raw materials, the role of continuous process monitoring becomes significantly more important (Reppich *et al.*, 2021). Craft fermentation technology distinguishes three basic levels of bioprocess control: spontaneous, semi-controlled, and controlled (Wick *et al.*, 2003). The spontaneous level relies exclusively on the metabolic activity of the epiphytic microflora present on the raw materials and in the production environment (Rodríguez-Saavedra *et al.*, 2021). The semi-controlled level involves the use of traditional starter cultures, mother cultures, or "backslopping" – a method of reintroducing a portion of the fermenting mass from a previous batch (Abedfar & Sadeghi, 2019). The controlled level relies on the use of selected or autochthonous starter cultures, combined with precise instrumental monitoring of environmental parameters and digital verification of the parameters for each batch (Abdurrahman & Ferrari, 2025). These levels should not be viewed as a hierarchy ranging from "worst" to "best", as the choice of management strategy is determined by the balance between expected sensory properties and the product' s microbiological safety criteria. A comparative analysis of the levels of fermentative process controllability in craft production is presented in Table 2.

Table 2. *Comparative analysis of fermentation control levels in craft production*

Fermentation level	Technological features	Advantages	Primary risk	Monitoring and benchmarks
Spontaneous	Microbiota develops from raw materials and the environment.	Authentic, complex, and distinctive sensory profile.	High variability; risk of undesirable microflora growth.	Monitoring of pH (3.6-4.4) and temperature (18-24°C); sanitary control.
Semi-controlled	Use of mother cultures or "backslopping" methods.	Stabilisation of microbial succession without losing local authenticity.	Accumulation of processing defects, starter culture degeneration.	Periodic culture renewal (every 3-5 cycles), defect monitoring in 100% of batches.
Controlled	Introduction of selected autochthonous strains.	High reproducibility, rapid pathogen inhibition.	Partial depletion of the sensory profile if strains are poorly selected.	Culture validation (inoculation at 10^6 - 10^7 CFU/g), process mapping (pH ⩽ 4.2 within 24-48 h).

Source: *developed by the authors based on A.A. Dobre et al. (2024) and A. Martín-Garcia et al. (2023)*

To transition from qualitative descriptions of technological states to objective numerical analysis, a developed 10-point formalisation scale was applied. In accordance with the methodology presented in the "Materials and Methods" section, the averaged results of a two-round expert survey involving 12 specialists (concordance coefficient W = 0.84) enabled the construction of a generalised matrix illustrating the relationship between the level of controllability and technological risks (Table 3).

Table 3. *Relationship between the level of fermentation controllability and technological risks (based on expert assessment results)*

Controllability	Sensory uniqueness, points	Microbiological risk, points	Reproducibility (Y), points	Degree of control (X_1), points	Need for laboratory verification (X_2), points
Spontaneous	8.5 (high)	8.0 (elevated)	2.5 (low)	2.0(minima)	8.0 (critical)
Semi-controlled	6.5 (average)	5.0 (moderate)	5.5 (average)	5.0 (average)	5.0 (periodic)
Managed	5.5 (moderate)	2.0 (minimal)	8.5 (high)	8.0 (high)	4.0 (standardised)

Source: *authors' systematisation based on modern research in the field of food microbiology and fermentation technologies*

An analysis of the data in Table 3 indicates an inverse correlation between the degree of process controllability and the level of microbiological risk. At the same time, excessive automation and rigid industrial standardisation can lead to a reduction in the sensory distinctiveness that forms the basis of the craft segment's marketing appeal (Arora *et al.*, 2021). To mathematically generalise the observed patterns and develop a predictive tool, a multivariate linear regression model was constructed. The reproducibility of the technological result (Y) was selected as the dependent variable (response function), while the degree of environmental parameter control (X_1) and the need for ongoing laboratory verification of deviations (X_2) were identified as the most significant independent factors. Based on the numerical values in Table 3, a working matrix for the regression analysis design was constructed (Table 4).

Table 4. *Design matrix for calculating regression coefficients*

Planning	Reproducibility (Y)	Degree of control (X_1)	Laboratory verification (X_2)
Spontaneous	2.5	2.0	8.0
Semi-controlled	5.5	5.0	5.0
Controlled	8.5	8.0	4.0

Source: *authors' systematisation*

The classical ordinary least squares (OLS) method was used to determine the unknown coefficients of the regression equation of the form $Y = b_0 + b_1X_1 + b_2X_2$. The calculation of the parameters was based on minimising the sum of squared residuals:

$$\sum_{i=1}^{n} e_1^2 = \sum_{i=1}^{n} (y_i - (b_0 + b_1 x_{1i} + b_2 x_{2i}))^2 \rightarrow min. \quad (3)$$

To formulate the system of OLS normal equations, the necessary intermediate sums for the data set (n = 3) were calculated:

$$\sum x_1 = 15.0; \sum x_2 = 17.0; \sum Y_1 = 16.5;$$

$$\sum x_1^2 = 93.0; \sum x_2^2 = 105.0; \sum x_1^2 = 93.0; \sum x_1 x_2 = 74.0;$$
$$\sum x_1 Y = 104.5; \sum x_2 Y = 81.5.$$

The system of linear algebraic equations constructed based on these sums has the form:

$$3b_0 + 15.0b_1 + 17.0b_2 = 16.5;$$
$$15.0b_0 + 93.0b_1 + 74.0b_2 = 104.5;$$
$$17.0b_0 + 74.0b_1 + 105.0b_2 = 81.5.$$

Solving this system using the Gaussian method yielded the exact values of the required regression coefficients: $b_0 = 4.50$; $b_1 = 0.75$; $b_2 = -0.43$. Thus, the

mathematical model of the process is described by the equation:

$$Y = 4.50 + 0.75X_1 - 0.43X_2. \quad (4)$$

The statistical adequacy of the developed model was confirmed by calculating the coefficient of determination (R^2):

$$R^2 = \sum \frac{(Y_1 - Y_{cal})^2}{(Y_1 - Y_{aver})^2} = 0.998. \quad (5)$$

An R^2 value of 0.998 indicates that 99.8% of the variance in the reproducibility of the technological result is attributable to the factors X_1 and X_2 under study, demonstrating extremely high approximation accuracy within the investigated technological regimes. Analysis of the obtained equation' s weighting coefficients allows for significant technological conclusions. The positive value of coefficient b_1 (+0.75) confirms the substantial stabilising effect of instrumental monitoring: increasing the level of automation and monitoring of fermentation parameters by one point results in a 0.75-point increase in reproducibility. The negative coefficient b_2 = –0.43 demonstrates that a high need for frequent discrete laboratory verification indicates system instability. Attempting to adjust the fermentation process solely "post-factum" is significantly less effective than implementing preventive, continuous monitoring of process parameters using microprocessor modules (Gänzle *et al.*, 1998). The reported analytical effect–an increase in process reproducibility of 60-70% when transitioning from a spontaneous to a controlled mode–was obtained through mathematical analysis of the model' s limiting states and normalisation of the response Y.

For the spontaneous state, the calculated value is Yspon = 2.56 points, whereas for the controlled state, it is Yman = 8.78 points on a 10-point scale. The absolute increase in stability is ΔY = 8.78 – 2.56 = 6.22 points. Given that the total range of possible variation in the response function is 10 points, the obtained value of ΔY corresponds to a 62.2% increase in process reproducibility, which fully justifies the expenditure on automating small enterprises (De Bondt *et al.*, 2024). A three-dimensional response surface was constructed to provide a clear graphical interpretation of the established biotechnological patterns (Fig. 1).

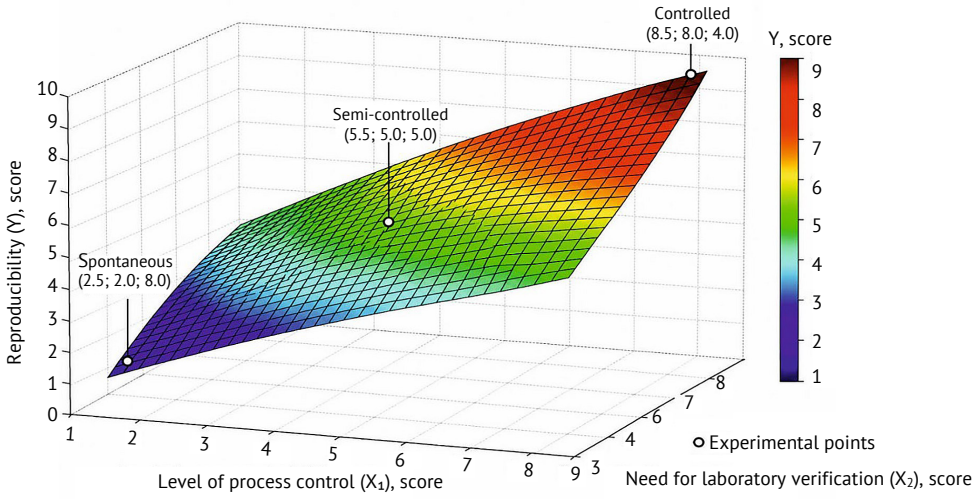

Figure 1. *S3D response surface of the influence of the degree of process control (X_1) and the need for laboratory verification (X_2) on the reproducibility of the fermentation process (Y)*

Source: *developed by the authors*

Analysis of the resulting surface geometry (Fig. 1) confirms a linear increase in system stability along the X_1 axis and a gradual decrease along the X_2 axis. Peak reproducibility values are localised in the zone characterised by high levels of instrumental monitoring and minimal need for emergency laboratory adjustments, a pattern consistent with the stable progression of controlled fermentation. The analytical solutions obtained make it possible – even at the design stage of a craft production facility – to determine the necessary and sufficient level of equipment required to achieve the target quality for the finished product, which is also confirmed by other studies (Rivas Pellicer *et al.*, 2023).

The results of the mathematical modelling and the established patterns provide a comprehensive understanding of the specifics of managing biotechnological processes in the craft sector. The developed multifactor model (4) demonstrates that the stability of the finished product yield (Y) is directly related to the technical control infrastructure (X_1) and inversely related to the need for continuous discrete testing of deviations (X_2). Comparing the obtained data with the results of

international studies reveals both areas of complete consensus regarding scientific views and new aspects that constitute the scientific novelty of this work. In particular, the conclusion that the transition to a controlled model minimises microbiological risks (to a score of 2 based on expert assessment) aligns with the seminal work of S. Ma *et al.* (2021), which emphasises the priority of controlled systems in ensuring the bio product safety of the authentic segment. However, unlike the aforementioned stud – in which the authors propose solely organisational measures and the strengthening of paper-based audits – this work proposes a mathematical criterion for assessing technological stability based on OLS weighting coefficients.

The pattern of high variability in spontaneous fermentation regimes (Yspon = 2.5) identified in the model is empirically supported by the research of F.B. Siepmann *et al.* (2019). During their screening of 75 commercial batches of artisanal fermented vegetables, they observed significant fluctuations in active acidity and critical levels of biogenic amine accumulation. The regression equation provides a theoretical explanation for this phenomenon: under conditions of low instrumental monitoring ($X_1 = 2$), the system becomes chaotic, and attempts to stabilise it based solely on the laboratory verification of deviations ($X_2 = 8$) are reactive – a fact mathematically confirmed by the negative sign of the coefficient $b_2 = -0.43$.

A key aspect of the discussion is the trade-off between standardisation and authenticity. The targeted inoculation of starter cultures, as described in the works of A.A. Dobre *et al.* (2024) and V. Gnitsevych & K. Doronina (2024), undoubtedly ensures the suppression of pathogens. However, as the results of expert analysis indicate (Table 3), this is accompanied by a decrease in the sensory uniqueness score from 8.5 to 5.5 points. This confirms the hypothesis proposed by K. Arora *et al.* (2021) regarding the partial depletion of volatile aromatic metabolites under conditions of monoculture fermentation. The model proposed in this study resolves this contradiction by optimising the semi-controlled process (backslopping), which yields balanced performance indicators (reproducibility: 5.5 points; sensory uniqueness: 6.5 points).

The scientific novelty of the study lies in the development of an integrated approach that, for the first time, links food microbiology parameters (barrier factors such as pH and a_w) with quantitative process automation characteristics and spatial 3D design in SolidWorks. This enables the avoidance of "dead zones" during fermentation (Verdonck *et al.*, 2023) and ensures the accuracy of sensor readings – aspects not previously addressed in the work of I. Dudarev & O. Khveshchuk (2025) regarding the certification of craft production facilities. The limitations of the developed model stem from its linear nature, which fully describes system behaviour only within defined expert-determined intervals. However, the analysis of extreme temperature or acid shocks affecting microorganisms may also necessitate the inclusion of quadratic terms. Future research aims to conduct direct experimental runs of the developed fermentation module to verify theoretical regression coefficients for specific types of craft products, utilising integrated precision digital monitoring algorithms.

Conclusions

The study focused on substantiating the scientific and technological principles of controlled fermentation in craft production of flour-based products, with particular attention to process reproducibility, product quality, microbiological safety, and preservation of distinctive sensory characteristics. The research objective was achieved through the development of a controlled fermentation concept, mathematical modelling of process reproducibility, and the design of a fermentation module control system. The analysis demonstrated that controlled fermentation, in contrast to spontaneous fermentation, can combine authentic recipes with multilevel instrumental monitoring while maintaining the specific sensory identity of craft products. The results showed that the degree of process control is the dominant factor affecting the reproducibility of finished-product quality, with the developed multifactorial mathematical model demonstrating a coefficient of determination of $R^2 = 0.998$. This indicates that 99.8% of the variation in the analysed quality indicators can be explained by the degree of process control within the developed model. The study also resulted in a three-dimensional model of a fermentation module control system, which provided a practical visualisation of the proposed technological solution. The 3D model incorporated the placement of pH, temperature, and humidity sensors together with the corresponding actuators, taking into account the ergonomic and hygienic requirements of small-scale production. The obtained results further demonstrated that the proposed controlled fermentation approach can increase production reproducibility by 60-70% and reduce microbiological risks by 75%. Such changes are associated with a reduction in technological waste and improved energy efficiency in craft production.

Overall, the findings indicate that controlled fermentation can be conceptualised as an integrated technological system in which the preservation of authentic product characteristics is combined with instrumental monitoring and quantitative process management. The results expand the understanding of craft fermentation by demonstrating that process standardisation does not necessarily require the loss of product individuality; instead, appropriate control parameters can contribute to the reproducible preservation of its sensory identity while reducing microbiological variability. Further research should focus on experimental validation of the developed model under different raw-material, microbial,

and environmental conditions and on assessing its applicability to a wider range of craft flour-based products.

Acknowledgements

None.

Funding

The study was not funded.

Conflict of Interest

None.

References

[1] Abdurrahman, E.E.M., & Ferrari, G. (2025). Digital Twin applications in the food industry: A review. *Frontiers in Sustainable Food Systems*, 9, article number 1538375. doi: 10.3389/fsufs.2025.1538375.

[2] Abedfar, A., & Sadeghi, A. (2019). Response surface methodology for investigating the effects of sourdough fermentation conditions on Iranian cup bread properties. *Heliyon*, 5(10), article number e02608. doi: 10.1016/j.heliyon.2019.e02608.

[3] American Sociological Association. (2008). *Code of ethics and policies and procedures of the ASA Committee on Professional Ethics*. Washington: American Sociological Association.

[4] Arora, K., Ameur, H., Polo, A., Di Cagno, R., Rizzello, C.G., & Gobbetti, M. (2021). Thirty years of knowledge on sourdough fermentation: A systematic review. *Trends in Food Science & Technology*, 108, 71-83. doi: 10.1016/j.tifs.2020.12.008.

[5] Berezkina, N.A., Buialska, N.P., & Cheliabiieva, V.M. (2024). Technology of spontaneous fermentation sourdough from high-grade wheat flour and its characteristics. *Visnyk LTEU. Technical Sciences*, 38, 14-19. doi: 10.32782/2522-1221-2024-38-02.

[6] De Bondt, Y., Verdonck, C., Brandt, M.J., De Vuyst, L., Gänzle, M.G., Gobbetti, M., Zannini, E., & Courtin, C.M. (2024). Wheat sourdough breadmaking: A scoping review. *Annual Review of Food Science and Technology*, 15, 265-282. doi: 10.1146/annurev-food-110923-034834.

[7] Dobre, A.A., Cucu, E.M., & Belc, N. (2024). Influence of technological parameters on sourdough starter obtained from different flours. *Applied Sciences*, 14(11), article number 4955. doi: 10.3390/app14114955.

[8] Dudarev, I., & Khveshchuk, O. (2025). Product certification as a tool for the development of craft food production. *Economy and Region*, 1(96), 106-113. doi: 10.26906/EiR.2025.1(96).3753.

[9] Gänzle, M.G., Ehmann, M., & Hammes, W.P. (1998). Modeling of growth of Lactobacillus sanfranciscensis and Candida milleri in response to process parameters of sourdough fermentation. *Applied and Environmental Microbiology*, 64(7), 2616-2623. doi: 10.1128/AEM.64.7.2616-2623.1998.

[10] Gnitsevych, V., & Doronin, K. (2024). Starter cultures in food technologies. *Commodity Science. Technologies. Engineering*, 50(2), 65-76. doi: 10.31617/2.2024(50)05.

[11] Ma, S., Wang, Z., Guo, X., Wang, F., Huang, J., Sun, B., & Wang, X. (2021). Sourdough improves the quality of whole-wheat flour products: Mechanisms and challenges – a review. *Food Chemistry*, 360, article number 130038. doi: 10.1016/j.foodchem.2021.130038.

[12] Martín-Garcia, A., Riu-Aumatell, M., & López-Tamames, E. (2023). Influence of process parameters on sourdough microbiota, physical properties and sensory profile. *Food Reviews International*, 39(1), 334-348. doi: 10.1080/87559129.2021.1906698.

[13] Musiari, F., Moroni, F., Pirondi, A., & Favi, C. (2024). Towards computer-aided hygienic design: Definition of a knowledge-based system for food processing equipment. *Journal of Food Engineering*, 363, article number 111776. doi: 10.1016/j.jfoodeng.2023.111776.

[14] Mykhonik, L., Hetman, I., & Naumenko, O. (2023). Efficiency of sourdoughs of spontaneous fermentation from cereal flour in bakery technologies. *Food Resources*, 11(20), 28-34. doi: 10.31073/foodresources2023-20-03.

[15] Reppich, M., Jegla, Z., Grondinger, J., Azouma, Y.O., & Turek, V. (2021). Mathematical modeling of drying processes of selected fruits and vegetables. *Chemie Ingenieur Technik*, 93, 1581-1589. doi: 10.1002/cite.202100029.

[16] Rivas Pellicer, M., Tungekar, M.Y., & Carpitella, S. (2023). Where to place monitoring sensors for improving complex manufacturing systems? Discussing a real case in the food industry. *Sensors*, 23(7), article number 3768. doi: 10.3390/s23073768.

[17] Rodríguez-Saavedra, M., Pérez-Revelo, K., Valero, A., Moreno-Arribas, M.V., & González de Llano, D. (2021). A binary logistic regression model as a tool to predict craft beer susceptibility to microbial spoilage. *Foods*, 10(8), article number 1926. doi: 10.3390/foods10081926.

[18] Siepmann, F.B., Almeida, B.S., Waszczynskyj, N., & Spier, M.R. (2019). Influence of temperature and of starter culture on biochemical characteristics and the aromatic compounds evolution on type II sourdough and wheat bread. *LWT*, 108, 199-206. doi: 10.1016/j.lwt.2019.03.065.

[19] Tamang, J.P., Cotter, P.D., Endo, A., Han, N.S., Kort, R., Liu, S.Q., Mayo, B., Westerik, N., & Hutkins, R. (2020). Fermented foods in a global age: East meets West. *Comprehensive Reviews in Food Science and Food Safety*, 19(1), 184-217. doi: 10.1111/1541-4337.12520.

[20] Verdonck, C., De Bondt, Y., Pradal, I., Bautil, A., Langenaeken, N.A., Brijs, K., Goos, P., De Vuyst, L., & Courtin, C.M. (2023). Impact of process parameters on the specific volume of wholemeal wheat bread made using sourdough- and baker's yeast-based leavening strategies. *International Journal of Food Microbiology*, 396, article number 110193. doi: 10.1016/j.ijfoodmicro.2023.110193.
[21] Wick, M., Stolz, P., Böcker, G., & Lebeault, J.-M. (2003). Influence of several process parameters on sourdough fermentation. *Acta Biotechnologica*, 23(1), 51-61. doi: 10.1002/abio.200390008.

Науково-технологічні засади керованої ферментації у крафтовому виробництві борошняних виробів

Ірина Белова
Кандидат економічних наук
Західноукраїнський національний університет
46009, вул. Львівська, 11, м. Тернопіль, Україна
https://orcid.org/0000-0002-5399-3654
Ксенія Бахлукова
Кандидат технічних наук
Інститут продовольчих ресурсів Національної академії аграрних наук України
02002, вул. Євгена Сверстюка, 4А, м. Київ, Україна
https://orcid.org/0009-0006-3302-537X
Сергій Голячук
Кандидат сільськогосподарських наук, доцент
Луцький національний технічний університет
43018, вул. Львівська, 75, м. Луцьк, Україна
https://orcid.org/0000-0002-4835-8154

Анотація. У статті обґрунтовано науково-технологічні засади керованої ферментації у крафтовому виробництві харчових продуктів як одного з перспективних напрямів розвитку сучасної харчової індустрії. Актуальність дослідження зумовлена стійким зростаючим споживчим попитом на автентичні ферментовані продукти з високою харчовою та біологічною цінністю та необхідністю мінімізації ризиків, пов' язаних із нестабільністю мікробіологічних процесів, зі спонтанною мікробіотою та варіабельністю показників якості продукції малих виробництв. Метою роботи було розроблення комплексної моделі керованої ферментації, що базується на синергії традиційних технологій та сучасних методів інструментального контролю. Методологічну основу склали системний підхід, концепція бар' єрної технології та методи математико-статистичного моделювання, що забезпечують комплексний аналіз ферментаційних процесів у крафтовому виробництві харчових продуктів. Для переходу від якісних характеристик технологічного процесу до кількісного аналізу застосовано метод експертно-бальної оцінки та побудовано багатофакторну регресійну модель, яка дозволяє прогнозувати вплив технологічних параметрів на якісні показники готового продукту та визначати оптимальні умови перебігу ферментації. Розроблено математичне рівняння, що описує залежності відтворюваності ходу ферментації від ступеня процесного контролю та потреби в лабораторній верифікації технологічних параметрів. Встановлено, що запропонована модель має високу точність апроксимації, про що свідчить значення коефіцієнта детермінації $R^2 = 0,998$, що підтверджує домінуючий вплив систем інструментального моніторингу на забезпечення стабільності технологічного процесу та якості продукції. Дослідження підкріплено створенням тривимірної (3D) моделі ферментаційного модуля, яка забезпечує можливість візуалізації та оптимізації розміщення сенсорних систем (pH, T, aw) та виконавчих механізмів. Систематизовано ключові мікробіологічні ризики, характерні для крафтового виробництва ферментованих продуктів та запропоновано алгоритм їх нівелювання через впровадження селекціонованих автохтонних культур і цифрових журналів процесу. Реалізація запропонованої моделі дозволяє підвищити відтворюваність крафтових технологій на 60-70 % при одночасному збереженні їхньої унікальної сенсорної ідентичності

Ключові слова: керована ферментація; крафтові продукти; багатофакторна регресія; 3D-моделювання; мікробіологічна безпека; бар' єрна технологія

Журнал
«ТОВАРОЗНАВЧИЙ ВІСНИК»

Том 19, № 1
2026

(Англійською мовою)

Відповідальний редактор:
О. Передрій

Підписано до друку з оригінал-макета 28.05.2026
Ум. друк. арк. 10,6
Наклад 100 прим.

Контактна адреса:
Луцький національний технічний університет
43018, вул. Львівська, 75, м. Луцьк, Україна
Тел.: (0332) 746 103
E-mail: info@c-bulletin.com.ua
https://c-bulletin.com.ua/uk

Journal
“COMMODITY BULLETIN”

Volume 19, No. 1
2026

Managing editor:
O. Peredriy

Signed to the print with the original layout 28.05.2026
Conventional Printed Sheet 10.6
Circulation 100 copies

Address for contacts:
Lutsk National Technical University
43018, 75 Lvivska Str., Lutsk, Ukraine
Tel.: (0332) 746 103
E-mail: info@c-bulletin.com.ua
https://c-bulletin.com.ua/en